CENTRO DE INVESTIGACIÓN Y DE ESTUDIOS AVANZADOS DEL INSTITUTO POLITÉCNICO NACIONAL

UNIDAD ZACATENCO

DEPARTAMENTO DE BIOMEDICINA MOLECULAR

“El papel de la miosina 1e en la regulación de las funciones efectoras de neutrófilos”

T E S I S

Que presenta

Iliana Itzel León Vega

Para obtener el grado de

Maestra en Ciencias

En la especialidad de

Biomedicina Molecular

Directores de tesis

Dr. Michael Schnoor y Dr. Eduardo Vadillo

Ciudad de México **Agosto, 2021**

CENTER RESEARCH AND ADVANCED STUDIES OF THE NATIONAL POLYTECHNIC INSTITUTE

ZACATENCO UNIT

DEPARTMENT FOR MOLECULAR BIOMEDICINE

“The role of myosin 1e in the regulation of neutrophil effector functions”

T H E S I S

Presents

Iliana Itzel León Vega

To obtain the degree

Master of Science

In the specialty

Molecular Biomedicine

Thesis directors

Dr. Michael Schnoor y Dr. Eduardo Vadillo

Mexico City **August, 2021**

To my family for their unconditional love and support

To my brother and my mom, the light of my life

AGRADECIMIENTOS

Al Dr. Michael Schnoor, por permitirme llevar a cabo mi proyecto de maestría en su laboratorio. Agradezco su apoyo, dedicación, paciencia y excelente asesoría.

Al Dr. Eduardo Vadillo por guiarme y apoyarme para poder realizar el trabajo experimental en su laboratorio. Gracias por la confianza, la maravillosa asesoría y por transmitirme tanta pasión por la ciencia.

A Idaira Guerrero, por enseñarme toda la práctica experimental. Gracias por tu paciencia, sabiduría y enorme ayuda.

A la Dra. Hilda Vargas, nuestra auxiliar de laboratorio, por su disposición para ayudarme siempre que lo requería.

A todos los profesores del departamento de Biomedicina Molecular quienes me compartieron todo su conocimiento y sabiduría durante los cursos, clases y asesorías. En especial, al Dr. Vianney Ortiz y el Dr. Leopoldo Santos, por inspirarme a continuar en el área de la inmunología.

Al CINVESTAV por permitirme formar parte de una de las mejores instituciones de investigación en México y brindarme las herramientas para continuar en el área de investigación. Al Consejo Nacional de Ciencia y Tecnología (CONACyT) por la beca recibida durante el periodo 2019-2021 que me permitió realizar mis estudios de maestría.

AGRADECIMEINTOS PERSONALES

A mis padres, cuyo apoyo y amor incondicional durante toda mi vida han forjado las bases de la persona que soy hoy en día. Gracias por confiar en mí, y por permitirme cumplir mis sueños. Papá, gracias por enseñarme a ser más fuerte y no darme por vencida. Mamá, gracias por ser mi pilar, mi gran inspiración y por siempre motivarme a seguir adelante en los momentos que quería claudicar, gracias a ti, este trabajo se pudo completar.

A mi hermano, Erny, quien representa mi mayor tesoro. Gracias por estar a mi lado, por siempre motivarme a seguir adelante y no darme por vencida; por acompañarme durante todos estos años y por confiar siempre en mí, te adoro.

A Irene y Alejandra Vega, quienes, a pesar de la distancia, me motivaron y ayudaron en los momentos más difíciles. Gracias por sus palabras y amor, las quiero muchísimo.

A los amigos que hice durante la maestría, en especial Alejandra Parra. Juntas empezamos y juntas terminamos, fuertes y más sabias. Gracias por brindarme tu amistad, por compartirme tu conocimiento, por acompañarme, inspirarme y ayudarme siempre. Te quiero montones

A la familia que escogí, Diego Ramírez, Fernanda Noreña, Luis David Díaz, Valeria y Natalia Corona, Diana Velasco y Diana Trillanes. Gracias por siempre estar en las buenas y en las malas, por aconsejarme, por apoyarme, por darme la gran dicha de ser su amiga y por mostrarme lo importante que es disfrutar cada momento en esta vida. Los quiero a todos.

INDEX

ABBREVIATIONS

ABP	Actin binding proteins
ACTB	Actin
AF488	Alexa Fluor 488
Arg	Arginine
Arp 2/3	Actin-Related Proteins 2/3
ARPC4	Actin-related protein 2/3 complex subunit 4
BM	Bone marrow
BMDN	Bone marrow derived neutrophils
Cdc42	Cell Division Cycle 42
CK2	Casein kinase
CR3	Complement receptor 3
DAMPs	Damage-associated molecular patterns
DC	Dendritic cells
DHR-123	Dihydrorhodamine-123
DNA	Desoxyribonucleic acid
EC	Endothelial Cell
EDTA	Ethylenediaminetetraacetic acid
E-selectin	Endothelial selectin
F-actin	Filamentous actin
FAK	Focal adhesion kinase
FBS	Fetal Bovine Serum
FcγR	Fcγ Receptor
fMLP	N-Formyl-methionine-leucyl-phenylalanine
FNBP1	Formin-binding protein 1
FSC	Forward scatter
G-CSF	Granulocyte colony-stimulating factor
GEFs	Guanine Exchange Factors
GM-CSF	Granulocyte-Macrophage colony-stimulating factor
H_2O_2	Hydrogen peroxide
HBSS	Hank's Balanced Salt Solution

Hck	Hematopoietic cell kinase
HOCl	Hypochlorous acid
ICAM	Intracellular Adhesion Molecules
ICAM-1	Intracellular adhesion molecule -1
ICAM-2	Intracellular adhesion molecule - 2
IgG	Immunoglobulin G
IL-17	Interleukin-17
IL-1β	Interleukin-1-beta
IL-23	Interleukin-23
IL-6	Interleukin-6
iNOS	Inducible nitric oxide synthase
ITAM	Immunoreceptor tyrosine-based activation motifs
KO	Knockout
Lck	Lymphocyte-specific protein tyrosine kinase
LFA-1	Lymphocyte-function associated antigen 1
LncRNA	Long-noncoding RNA
LPS	Lipopolysaccharide
LTB4	Leukotriene B4
Lys	Lysine
Mac-1	Macrophage antigen 1
MOV-10	Putative helicase MOV10
MPO	Myeloperoxidase
MYH9	Myosin-9
MYH11	Myosin-11
MYO1E	Myosin 1e gene
Myo1e	Class I myosin 1e (protein)
MYO5C	Unconventional myosin-Vc
NADPH	Nicotinamide Adenine Dinucleotide Phosphate-Oxidase
NE	Neutrophil Elastase
NETs	Neutrophils Extracellular Traps
NLR	NOD-like receptors

NO	Nitric oxide
NPFs	Nucleation-promoting factors
PAD4	Protein-arginine deiminase 4
PAMPs	Pathogen-associated molecular patterns
PBS	Phosphate-buffered saline
PECAM1	Platelet endothelial cell adhesion molecule
PFA	Paraformaldehyde
Phox	Phagocyte oxidase
PI (3,4) P2	Phosphatidylinositol-4,5-bisphosphate
PI (3,4,5) P3	Phosphatidylinositol- 3,4,5-trisphosphate
PI3K	Phosphatidylinositol 3-kinase
PKC	Protein cinase C
PMA	Phorbol-myristate-acetate
PMN	Polymorphonuclear cells
PRRs	Pattern recognition receptors
P-selectin	Platelet-Selectin
PSGL1	P-selectin glycoprotein ligand-1
RLR	RIG-like receptors
RNS	Reactive nitrogen species
R-123	Rhodamine-123
RNA	Ribonucleic acid
RNF20	E3 ubiquitin-protein ligase BRE1A
ROS	Reactive Oxygen Species
Rpm	Revolutions per minute
RT	Room Temperature
SFK	Src family of protein tyrosine kinases
Src	Proto-oncogene tyrosine-protein kinase Src (sarcoma)
SSC	Side Scatter
Syk	Spleen tyrosine kinase
TEM	Transedothelial Migration
TLR	Toll-like receptors

TNFα Tumor Necrosis Factor-α

VCAM-1 Vascular cell adhesion protein 1

VE-cadherin Vascular endothelial-cadherin

VLA-4 Very Late Antigen-4

WASp Wiskott-Aldrich Syndrome protein

WAVE WASP-family verprolin-homologous protein 2

WT Wild type

FIGURES

TABLES

RESUMEN

Los neutrófilos son células complejas que representan un pilar fundamental de los procesos inflamatorios, ya que son las primeras células en ser reclutadas a sitios de inflamación o de infección. Estas células llevan a cabo una vasta cantidad de funciones especializadas que contribuyen a la promoción de la inflamación o a su resolución. Algunas de las funciones incluyen la eliminación de patógenos mediante la fagocitosis, la liberación de contenido granular, la generación de trampas extracelulares de neutrófilos y la producción de especies reactivas de oxígeno. Estas funciones dependen de la dinámica del citoesqueleto de actina y de moléculas involucradas en su reorganización debido a la necesidad de la célula de movilizarse, extender y modificar su estructura para llevar a cabo dichos procesos correctamente. La miosina-1e (Myo1e) es una proteína de unión a actina que utiliza ATP para promover trabajo mecánico sobre filamentos de actina, por ejemplo, durante el tráfico vesicular, la formación de extensiones membranales, la adhesión y migración celular.

Recientemente, se demostró que la Myo1e se expresa en neutrófilos y promueve la polimerización de actina, la quimiotaxis, la activación de integrinas y la extravasación de neutrófilos. No obstante, su participación durante las funciones efectoras de los neutrófilos no se ha estudiado. Además, tampoco se conoce cómo las modificaciones postraduccionales de la Myo1e afectan su función durante estos procesos. Por ende, en este estudio, se evaluó el papel de la Myo1e en las funciones efectoras del neutrófilo, así como las posibles modificaciones e interacciones proteicas que pueden contribuir a su función.

Los análisis *in-silico* mostraron que la Myo1e puede ser fosforilada en diversos residuos de tirosina, serina y treonina. Estas modificaciones generan posibles motivos de unión para proteínas como las cinasas Syk y PI3K y por factores activadores de las GTPasas pequeñas Rap1 y Rac1. Además, el análisis de redes de interacción con proteínas, mostró la asociación de Myo1e con proteínas involucradas en la remodelación del citoesqueleto de actina como forminas y el complejo Arp2/3. Por otro lado, usando partículas de zymosan opsonizadas, demostramos que la ausencia de Myo1e reduce significativamente la eficiencia de fagocitosis. Además, los neutrófilos deficientes de

Myo1e muestran una reducción significativa en su capacidad de producir especies reactivas de oxígeno en comparación con los neutrófilos silvestres en respuesta a PMA.

En conjunto, estos resultados sugieren que la Myo1e regula la eficacia de la fagocitosis mediada por receptores opsónicos, así como la producción de especies reactivas de oxígeno en neutrófilos, posiblemente por una interacción con moléculas responsables de dichos procesos. En el futuro investigaremos los mecanismos por los cuales la Myo1e regula las funciones efectoras de los neutrófilos.

ABSTRACT

Neutrophils are complex cells that represent a fundamental pillar of inflammatory processes because they are the first immune cells to be recruited to sites of inflammation or infection. Neutrophils carry out a vast number of specialized functions that contribute either to the promotion of inflammation or to its resolution. Some of the functions include the elimination of pathogens by phagocytosis, the release of granular contents, the generation of neutrophil extracellular traps (NETs), and the production of reactive oxygen species (ROS). These functions depend on the dynamic remodeling of the actin cytoskeleton and the molecules involved in its reorganization due to the need for the cell to move, extend and modify its structure in order to carry out these processes efficiently. Myosin 1e is an actin-binding protein that uses ATP to promote mechanical work on actin filaments to enable cellular processes such as vesicular trafficking, membrane extension formation, and cell adhesion and migration.

Recently, it was shown that Myo1e is expressed in neutrophils and that it promotes actin polymerization, chemotaxis, integrin activation, and neutrophil extravasation. However, its role in neutrophil effector functions has not been studied. Moreover, the posttranslational modifications of Myo1e that may affect its functions remain elusive. Thus, in this study, we investigated the role of Myo1e during neutrophil effector functions and the possible modifications and protein interactions that may contribute to its functions.

In-silico analyses showed that Myo1e can be phosphorylated at various tyrosine, serine and threonine residues. These modifications can potentially generate binding motifs recognized by proteins such as the kinases Syk and PI3K and activators of the small GTPases Rap1 and Rac1. Furthermore, analyses of protein interaction networks showed that Myo1e can associate with proteins involved in the remodeling of the actin cytoskeleton such as formins and the Arp2/3 complex. On the other hand, using opsonized zymosan particles, we showed that the absence of Myo1e reduced the efficiency of phagocytosis. In addition, Myo1e-deficient neutrophils showed a significant reduction in their ability to produce ROS compared to wild-type neutrophils in response to PMA.

Taken together, these results suggest that Myo1e regulates the efficiency of opsonic receptor-mediated phagocytosis in neutrophils, as well as ROS production, possibly through an interaction with molecules responsible for these processes. In the future, we will investigate the molecular mechanisms by which Myo1e regulates neutrophil effector functions.

1. INTRODUCTION

1.1. Inflammation: An innate immune response

Inflammation is a fundamental and critical mechanism ensuring the survival of an organism since it is the first immune response to infection, injury, cell damage or irradiation. However, mechanisms of inflammation are not only a protective attempt by the organism to fight infections, or injuries, but also to remove injurious stimuli, to reestablish homeostasis and to repair tissue damage during the healing process.

Inflammation is a critical innate immune response that induces changes to the local vasculature. These changes start with an increase of the vascular diameter that leads to a local increase in blood flow and a reduction in blood flow velocity (Murphy et. al, 2008). Then, the secretion of proinflammatory mediators such as cytokines and chemoattractants by tissue-resident immune cells induces the activation of endothelial cells (EC) in postcapillary venules and vascular leakage to allow the passage of different bioactive molecules present in the blood to the site of active inflammation leading to an accumulation of liquid and plasma proteins in the inflamed tissue known as edema (Murphy et. al, 2008; Schnoor, 2015). The activated endothelium expresses adhesion molecules that, together with the decrease in blood flow velocity, promote the adhesion of leukocytes to the endothelium and subsequent transendothelial migration (TEM). Extravasated leukocytes work together with blood proteins to prevent spreading of pathogens and excessive tissue damage. Within the inflamed tissues, several cells, including tissue-resident cells such as macrophages, dendritic cells (DCs), innate lymphoid cells, endothelial cells, fibroblasts, and mast cells, as well as recruited immune cells including monocytes, eosinophils and neutrophils, work together to induce the proper changes in the inflamed tissue to orchestrate the inflammatory process.

These changes to the inflamed tissue are induced by various inflammatory mediators released as a consequence of the recognition of pathogenic molecules by receptors present in both resident and recruited immune cells. These pattern recognition receptors (PRRs) such as Toll-like receptors (TLRs), NOD-like receptors (NLRs), phagocytic receptors, and RIG-like receptors (RLR) detect a variety of pathogen-associated molecular patterns (PAMPs) as well as damage-associated molecular patterns (DAMPs)

that in turn activate all cells within the inflammatory environment, allowing for the release of inflammatory mediators. These include lipid mediators of inflammation such as prostaglandins, leukotrienes, platelet activating factor (PAF), among others. Their actions are followed by those of chemokines and cytokines including tumor necrosis factor-α (TNF-α), interleukin-1β (IL-1β), interleukin-6 (IL-6), interleukin-12 (IL-12), and CXCL8, among others. Even though an array of innate immune cells contributes to the promotion of the inflammatory process, neutrophils are generally among the first leukocytes to be recruited into inflamed tissues. Once recruited, these cells mediate the onset of the effector response, i.e. the elimination of pathogens and release of granules, thus contributing to a second wave of inflammation that shapes the immune landscape in the inflamed tissue (Murphy et. al, 2008).

By the release of its granular content, neutrophils facilitate recruitment of monocytes into the inflamed tissue (Soehnlein et al., 2008; Soehnlein & Lindbom, 2009). Extravasated monocytes differentiate into tissue macrophages and dendritic cells in order to present antigens, perform phagocytosis, and further modulate the immune response by producing cytokines and growth factors (Mantovani et. al., 2011). Neutrophils are also able to program antigen-presenting cells to activate T cells and release localized factors to attract more immune cells such as natural killer cells, T and B lymphocytes and mast cells. Mast cells contribute greatly to inflammation by the release of a variety of inflammatory mediators, including cytokines, chemokines, histamine, proteases, prostaglandins, leukotrienes, and proteoglycans (Chen et. al., 2018).

However, to prevent progression from acute to chronic inflammation, the inflammatory response must be terminated after removal of the inflammatory cue to prevent host tissue damage, a process known as resolution of inflammation. This process can be divided into anti-inflammatory and pro-resolving phases. The first involves the release of anti-inflammatory mediators, such as interleukin 10 (IL-10) and Tumor growth Factor-β (TGF-β), the downregulation of nuclear factor-κB- (NF-κB) dependent pro-inflammatory gene activity, and the participation of cytokine and chemokine receptor antagonists such as the IL-1 receptor antagonist (IL-1Ra). These anti-inflammatory factors limit neutrophil recruitment into inflamed tissues, and together with endogenously produced

glucocorticoids, induce annexin 1 production to inhibit neutrophil adhesion and TEM (Perretti & Dalli, 2009). The pro-resolving phase is spatially and temporally controlled: proinflammatory gradients are diluted over time and a lipid switch occurs, where cells in the inflamed tissue start to produce pro-resolving lipid mediators such as lipoxin A4 (LXA4), resolvins and protectins (Serhan, 2010). The increase in pro-resolving mediators initiates the recruitment of monocytes and their differentiation into macrophages of an anti-inflammatory phenotype, therefore promoting the phagocytosis of apoptotic neutrophils and the initiation of tissue repair and wound healing (Kolaczkowska & Kubes, 2013). Although neutrophils may also exhibit anti-inflammatory or healing characteristics to contribute during the resolution of inflammation, they have also emerged as important players in the pathogenesis of numerous disorders involving excessive recruitment and pro-inflammatory responses. Therefore, the understanding of their regulation is crucial for the identification of potential therapeutic targets in infectious diseases, autoimmunity, chronic inflammation, or cancer.

1.2. Neutrophils

As mentioned before, neutrophils are among the first cells to be recruited to inflamed tissues and are therefore considered part of the first line of defense against a wide variety of infectious pathogens including bacteria, fungi, and protozoa (Mayadas, 2014). Neutrophils are a population of short-lived polymorphonuclear myeloid cells that represent 50% to 70% of all circulating leukocytes in humans, with 2,3-8,7 x 10^9 cells/L being the normal range of total neutrophils in the blood (Rodak, 2014); whereas in mice, neutrophils represent 10 to 25% of circulating leukocytes (Rosales, 2020). When fully matured, neutrophils reach around 7 to 10 µm in diameter and are characterized by presenting a multilobed irregular segmented nucleus and a high content of cytoplasmic granules and secretory vesicles (Rosales, 2020). Moreover, neutrophils express a variety of cell surface receptors that are able to recognize microbial structures, inflammatory signals within the environment and to respond to adaptive immune signals such as antibodies (**Table 1**). Activation of these receptors leads to neutrophil activation and induction of effector functions such as phagocytosis, degranulation, production of ROS,

NETs, as well as additional responses like chemotactic migration or chemokine and cytokine release (Futosi et. al., 2013).

Table 1. Important cell surface receptors expressed on neutrophils. (Adapted from Futosi et. al., 2013).

G-protein-coupled receptors (GPCRs)	Fc-receptors	Adhesion receptors	Cytokine receptors	Innate immune receptors
Formyl-peptide receptors	***Fcγ-receptors***	***Selectins and selectin ligands***	***Type I cytokine receptors***	***Toll-like receptors***
• FPR1 (FPR)	• FcγRI	• L-selectin	• IL-4R	• TLR1
• FPR2 (FPRL1)	• FcγRIIA (human)	• PSGL-1	• IL-6R	• TLR2
• FPR3 (FPRL2)	• FcγRIIB (inhibitory)	***Integrins***	• IL-12R	• TLR4
Classical chemoattractant receptors	• FcγRIII (mouse)	• LFA-1 (αLβ2)	• IL-15R	• TLR5
• BLT1 (LTB4-rec.)	• FcγRIIIB (human)	• Mac-1 (αMβ2)	• G-CSFR	• TLR6
• BLT2 (LTB4-rec.)	• FcγRIV (mouse)	• VLA-4 (α4β1)	• GM-CSFR	• TLR7 (?)
• PAFR				• TLR8
• C5aR	***Fcα-receptors***		***Type II cytokine receptors***	• TLR9
	• FcαRI (human)		• IFNAR (IFNα/β-rec.)	
Chemokine receptors			• IFNGR	***C-type lectins***
• CXCR1 (human)	***Fcε-receptors***		• IL-10R	• Dectin-1
• CXCR2	• FcεRI			• Mincle
• CCR1	• FcεRII		***IL-1R family***	• MDL-1
• CCR2			• IL-1RI	• Mcl
			• IL1RII (decoy)	• CLEC-2
			• IL-18R	
				NOD-like receptors
			TNFR family	• NOD2
			• TNFR1 (p55)	• NLRP3
			• TNFR2 (p75)	
			• Fas	***RIG-like receptors***
			• LTβR	• RIG-I
			• RANK	• MDA5
			• TRAIL-R2	
			• TRAIL-R3	

Due to a lifespan of only around 5 days in humans and a half-life of approximately 6.5 h in the blood (Pillay, 2010), more than half of the bone marrow is dedicated to constant production and release of neutrophils (Mayadas, 2014; Schnoor, 2015). Neutrophil production in the bone marrow occurs during granulopoiesis, a process driven by a set of transcription factors and cytokines such as granulocyte colony stimulating factor (G-CSF), stem cell factor (SCF), interleukin-1 (IL-1), IL-3, IL-6 and IL-11, with G-CSF and IL-3 being key molecules that start the process and regulate its progression towards differentiation, maturation, and activation of neutrophils (Rodak, 2014). However, this production must be counterbalanced by the clearance of the same number of cells from the system through apoptosis and removal by efferocytosis to prevent overpopulation (Greenlee-Wacker, 2016; Tak, 2013). Neutrophils also undergo apoptosis during an inflammatory

response, after they have accomplished their effector functions, which will be discussed below. Macrophages and DCs are then responsible for clearing dead neutrophils locally (Rosales, 2020).

1.2.1. Neutrophil extravasation

Neutrophils reach sites of tissue inflammation via the vasculature by following a process referred to as the neutrophil recruitment cascade (Ley, 2007), which is orchestrated by a gradient of chemokines guiding neutrophils to the site of inflammation (**Figure 1**). Secretion of proinflammatory mediators by resident immune cells such as histamine, platelet-activating factor (PAF), G-CSF, IL1-β and TNF-α, promote the activation of EC (Fusté, 2004; Petrache, 2002; Pober, 1986). Endothelial activation involves the expression of different surface adhesion molecules on the endothelium and actin remodeling that enable neutrophil adhesion onto the endothelium and subsequent transmigration.

Neutrophils in the blood are separated from the endothelium by a network of negatively charged proteoglycans, glycosaminoglycans and glycoproteins on the apical surface of endothelial cells, also known as glycocalyx. This thick layer must go through several alterations to expose the cellular adhesion molecules involved in neutrophil recruitment (Kolárova, 2014; Schnoor, 2015). The glycocalyx is degraded by enzymes such as heparinase, metalloproteinases released by neutrophils and other activated leukocytes, enabling neutrophil contact with adhesion molecules expressed on the endothelial surface (van Golen, 2012) (Schnoor, 2015). Activated EC express adhesion molecules such as ICAM-1, ICAM-2, and VCAM-1 and a variety of glycoproteins including P- and E-selectin (Vestweber D., 2015). During activation, calcium signaling is induced in EC leading to the activation of motor proteins such as myosins that induce the rapid mobilization of Weibel-Palade bodies (WPBs) that constitutively store P-selectin, and *de novo* expression of E-selectin (Birch, 1994). Subsequently, weak interactions of P/E-selectins with PSGL1 on the neutrophil surface allow for tethering and rolling of neutrophils along the endothelium even under high shear stress within blood vessels (Moore, 1995; Schnoor, 2015; Sundd, 2012; Vestweber D., 2015).

The second step of the recruitment cascade is slow rolling of the neutrophil that is dependent on the activation of the neutrophil β2-integrin LFA-1 (αLβ2 or CD11a/CD18), allowing its interaction with ligands present on the surface of EC such as ICAM-1 and ICAM-2. Other types of integrins present in neutrophils include the β2-integrin Mac-1 (αMβ2 or CD11b/CD18), p150, p95 and the β1 integrin VLA-4 (Sumagin, 2010) (Schnoor, 2015). In addition to selectin-mediated rolling that primes integrin activation (Kuwano, 2010), integrin activation is induced by chemokine receptors that recognize chemokines presented on the EC surface. Chemokine binding then induces inside-out signaling pathways including the PLCγ2, p38 MAPK and PI3Kγ pathways, and activation of small GTPases such as Rac1 and Rap1 to induce the necessary conformational changes of β2 integrins into their high-affinity form (Mueller, 2010). The intermediate-affinity form is crucial for slow rolling because the anchoring of the neutrophil to the EC apical surface allows the neutrophil to correctly execute the next steps of the recruitment cascade. Thus, tethering of high affinity β2 integrins in neutrophils promotes the necessary rearrangements of the membrane and actin cytoskeleton to assure that the neutrophil can firmly adhere (arrest) to the surface of the endothelium. Following arrest, neutrophils spread by reorganizing their actin cytoskeleton to generate protrusive leading edges and contractile uropods (Hyun, 2012) to crawl along the endothelium in an ICAM-1/Mac1-dependent manner towards chemotactic or haptotactic gradients until they reach permissive sites for transmigration (Massena, 2010; Phillipson, 2006; Schnoor, 2015).

Transendothelial migration (TEM), also known as diapedesis, can occur through junctions between adjacent endothelial cells (paracellular TEM) or through the body of an EC (transcellular TEM) (Burns AR, 2000; Feng, 1998; Johnson-Leger, 2000). *In vivo*, approximately 90% of all transmigration events occur paracellularly (Woodfin, 2011). Paracellular TEM depends on the reversible and transient opening of interendothelial junctions, and adhesive interactions between neutrophil receptors and receptors present at the lateral region of EC such as junctional adhesion molecules (JAMs), platelet/endothelial cell adhesion molecule 1 (PECAM1), CD99, ICAM-2, and ESAM (endothelial cell-selective adhesion molecule) (Muller, 2011). ICAM-1 engagement and clustering causes activation of different tyrosine kinases that phosphorylate the intracellular tail of VE-cadherin promoting its internalization, thus enabling the temporary

opening of endothelial cell contacts, and neutrophil TEM (Broermann, 2011; Vockel, 2013) (**Figure 1**). Subsequently, neutrophils must also pass through the continuous basement membrane, achieved by partially digesting it by the release of proteases and moving through membrane regions with low expression of extracellular matrix components. Finally, neutrophils migrate through gaps between pericytes by actively crawling along the cells in a Mac-1/LFA-1/ICAM-1 manner, allowing them to finally leave the vasculature and arrive in the inflamed tissue (Kolaczkowska & Kubes, 2013).

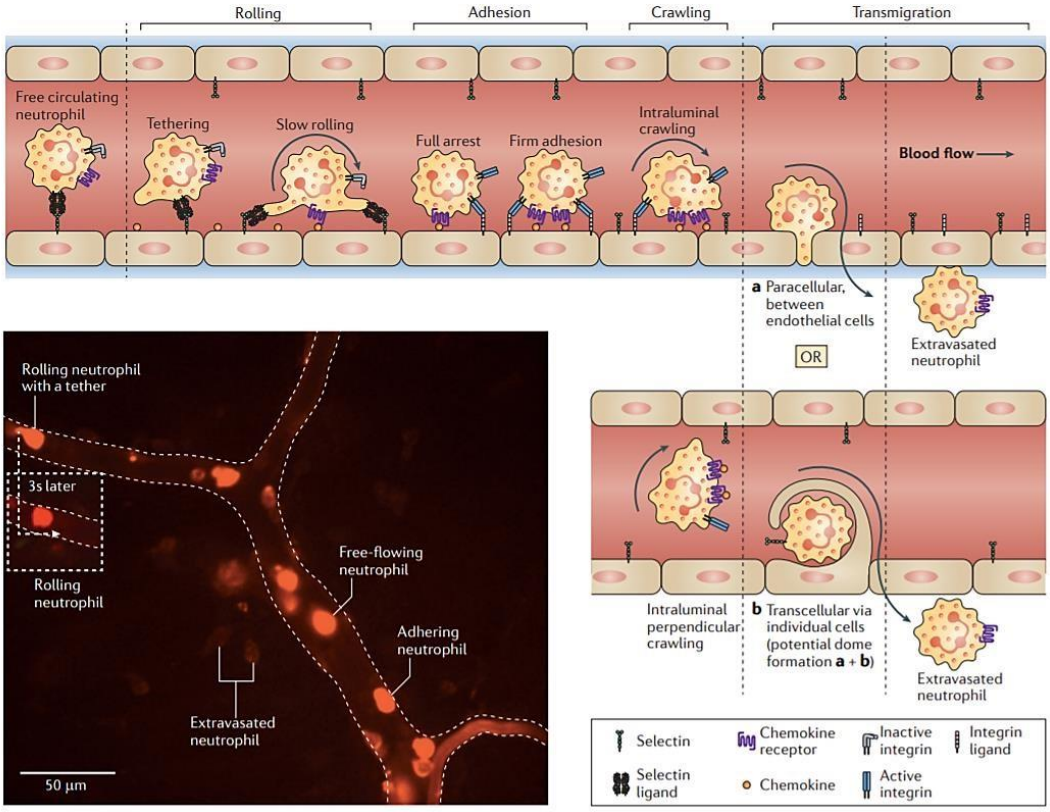

Figure 1. Scheme of the neutrophil extravasation cascade. The scheme shows the sequential steps of neutrophil recruitment from the blood stream to the damaged tissue during inflammation. Extravasation involves tethering, rolling, slow rolling, firm arrest, adhesion strengthening, and crawling mediated by the indicated endothelial cell adhesion molecules and their respective ligands on neutrophils. Subsequent transmigration of neutrophils out of the blood vasculature through the endothelium can be achieved via para or transcellular migration. The image on the lower left shows an intravital microscopy image of a mouse skin postcapillary venule, whose skin was infected with Staphylococcus aureus. The image shows neutrophils (labelled in red with a phycoerythrin antibody conjugate against Ly6G) at different stages of migration two hours post infection (Kolaczkowska & Kubes, 2013).

After transmigration, neutrophils become functionally activated by several stimuli derived from either resident immune cells in the injured or infected tissue, pathogens, or the damaged tissue in the form of PAMPs or DAMPs (Zhang, 2010). Extravasated neutrophils also engage in a bidirectional crosstalk with immune and non-immune cells in the inflamed tissue through receptors that detect cytokines such as IL-1β, TNF-α, IFN-γ, GM-CSF and chemoattractants such as C5a, LTB4, CXCL1/2, and CCL20 to promote antimicrobial activity in macrophages, increase maturation and activation of dendritic cells; increase differentiation, activation and proliferation of T and B cells, as well as cytokine production by NK cells, that in turn also promote further neutrophil activation and survival (**Figure 2**). (Brandau, 2010; Costantini, 2011; Ethuin, 2004; Kolaczkowska, 2013).

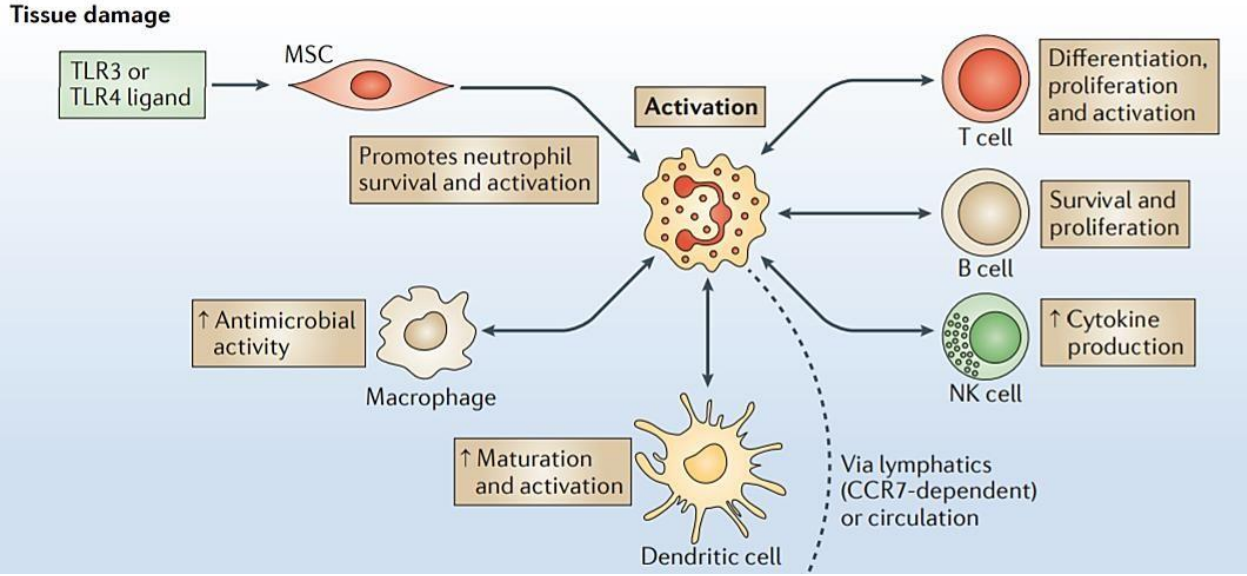

Figure 2. Neutrophil crosstalk with immune and non-immune cells in inflamed tissues. The scheme shows the interaction of resident and recruited immune cells with neutrophils within inflamed tissues through cytokines that promote the activation of neutrophils and the main functions. (Mantovani, 2011).

1.2.2. Neutrophil effector functions

After full activation within the inflammatory environment, neutrophils can fulfill different effector functions to fight pathogens such as phagocytosis, production of ROS (respiratory burst), release of granular content to the extracellular environment (degranulation), and formation of NETs (Rosales, 2020). These effector functions are

critical for the immune response, so that it is important to better understand the underlying mechanisms, which are discussed below.

1.2.2.1. Phagocytosis

Phagocytosis is a critical process in development, tissue homeostasis, and immunity that involves the recognition and ingestion of particles larger than 0.5 μm ranging from pathogens to apoptotic cells into membrane-bound vacuoles known as phagosomes (Freeman, 2014). Neutrophils are professional phagocytes that take up opsonized particles and microbes through opsonic receptors, receptors characterized by detecting host-derived proteins bound to target particles, also known as opsonins (Uribe-Querol & Rosales, 2020). These receptors include antibody receptors (FcRs) and complement receptors such as CR3 (β2 integrin also known as Mac-1 or CD11b/CD18) or CR4 (p150/95 or CD11c/CD18), that recognize fragments of C3 such as iC3b (Dupuy, 2008). Also, non-opsonic receptors including lectin-like recognition molecules, such as CD169, CD33, and related receptors for sialylated residues (Klaas, 2012), Dectin-1 and a group of receptors that bind and internalize a wide array of structurally diverse ligands which can be either endogenous or exogenous in nature, known as scavenger receptors (Dambuza, 2015; Patten & Shetty, 2018), can induce phagocytosis and help enclose the pathogen within the phagosome (Mayadas, 2014; Rabinovitch, 1995). Other receptors, such as TLRs, although not responsible for the internalization during phagocytosis, collaborate with other opsonic or non-opsonic receptors to stimulate the process by inducing neutrophil priming, thus participating as a link between phagocytosis and inflammatory responses by triggering the production of cytokines (Rosales, 2020; van Kessel et. al., 2014) (**Figure 3**).

When neutrophils survey their environment by projecting membrane ruffles and filopodia, they can recognize their phagocytic targets through diverse phagocytic receptors. During FcRγ or CR3-dependent uptake, the F-actin network is disrupted at the phagocytic cup by debranching proteins such as coronins and severing proteins such as cofilin and gelsolin (**Figure 3B**). However, depending on the receptor governing phagocytosis, different signaling pathways are activated (Rosales, 2017). In the case of Fc receptors, as more receptors get engaged around the particle, their cytoplasmic tails

get phosphorylated at immunoreceptor tyrosine-based activation motifs (ITAMs) leading to recruitment of secondary tyrosine kinases such as Syk, and adapter proteins such as NcK, Gab2, and Grb2 via their SH2 domains (Freeman & Grinsteain, 2014). These adaptor proteins ensure the phagocytosis process by recruiting WASp/N-WASp and WAVE nucleation-promoting factors (NPFs) to sites of Fc receptor clustering, through their SH3 domains that bind proline-rich regions present in NPFs. The force applied by the actin cytoskeleton on the plasma membrane is transferred by these adapter proteins to drive the propulsion of the membrane around the target (Gu et. al., 2003; Wachsstock et al, 1994). Once WASp/N-WASp or WAVE are recruited, they get activated via conformational changes that expose their N-terminal VCA domain (verprolin-homology, central, acidic). This VCA exposure is mediated by the binding of the small GTPase Cdc42 in the case of WASp, and the small GTPase Rac1 in the case of WAVE (Park et al. 2014; Prehoda et. al., 2000). Finally, activated WASp/N-WASp and WAVE complexes, induce the activation of a protein complex consisting of seven proteins (Arp2, Arp3, and ARPC1-5), the actin-related protein 2/3 (Arp2/3) complex that nucleates branched actin filaments from an existing mother filament. This is followed by the binding of Ena/VASP proteins that recruit profilins leading to actin filament elongation (Bear & Gertler, 2009; Goley & Welch, 2006), and the formation of local pseudopods and membrane ruffles that engulf the particles (**Figure 3C**) (Allen, 1996; Guerrero, 2018).

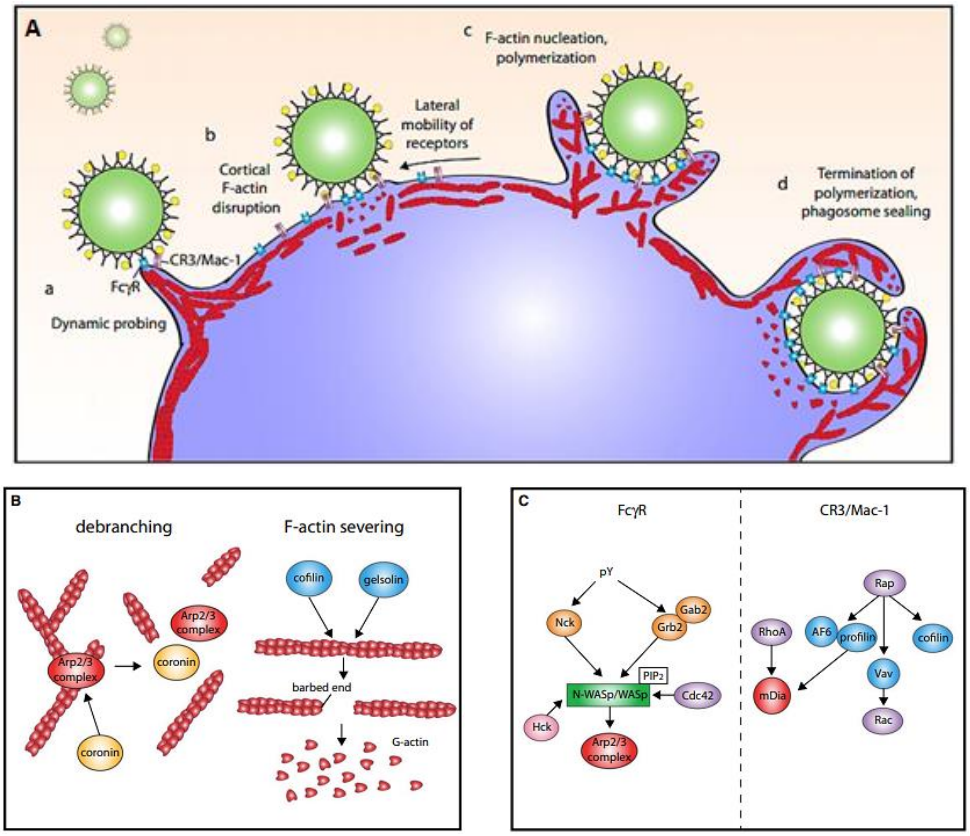

Figure 3. Actin cytoskeleton remodeling during phagocytosis. A) Phagocytes sense their surroundings for phagocytic targets by the extension of ruffles and filopodia. Once a particle is recognized either by Fc receptors (FcR) and/or complement receptors (CR3/Mac1), the cortical F-actin is disrupted at the phagocytic cup by debranching and F-actin severing proteins. This allows the lateral mobility of receptors and as more phagocytic receptors get engaged around the particle, F-actin nucleation and polymerization are promoted to allow the cell to extend pseudopodia that engulf the particle. **B)** F-actin debranching proteins such as coronins, and severing proteins including cofilin and gelsolin are the proteins responsible for the disruption of the actin cytoskeleton. **C)** Depending on the receptor governing phagocytosis, phosphorylation of the cytoplasmic tails of FcRs leads to the recruitment of adaptor proteins (Nck, Gab2, and Grb2) and secondary tyrosine kinases (Syk) that in turn recruit WAVE and WASp/N-WASp complexes. These complexes are activated by Cdc42, PtdIns(4,5)P2, and by Hck-mediated phosphorylation. The clustering of CR3/Mac-1 by C3bi activates RhoA and Rap1, stimulating mDia and Vav1/3 mediated polymerization, respectively, to induce actin polymerization and pseudopodia formation for efficient particle internalization. (Modified from Freeman & Grinstein 2014).

On the other hand, CR3/Mac-1-dependent phagocytosis leads to the formation of adhesion complexes primarily by the activation of RhoA and Rap1 through inside-out and outside-in signaling (Fan & Ley, 2015). First, these integrins undergo inside-out activation in response to chemokine receptors like GPCR and TLRs, that induces activation of Rap1. When GPCRs are stimulated, the second messengers DAG (diacyl glycerol) and

cAMP (cyclic AMP), activate the Rap GEFs, CalDAG (calcium and diacylglycerol-regulated guanine nucleotide exchange factor I) and Epac (exchange proteins directly activated by cAMP), respectively (Freeman & Grinsteain, 2014). Once the Rap GEFs activate the GTPase Rap1, it recruits both RapL and RIAM (Rap1-GTP interacting adapter molecule) which in turn recruit Talin to the cytoplasmic tails of integrins, leading to the disruption of the interactions between the α and β subunits. This in turn induces integrins to change from a bent to an extended intermediate affinity conformation that allows the exposure of the binding domain and thus binding to iC3b and other ligands (Fan & Ley, 2015) (**Figure 4**).

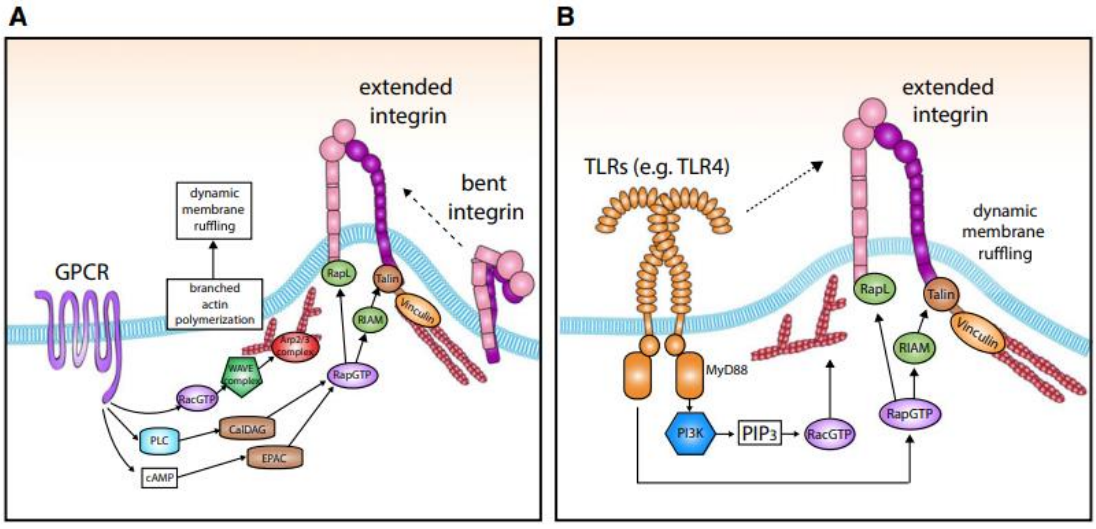

Figure 4. Inside-out activation of β2 integrins. A) GPCR-dependent phagocytosis starts with the external stimuli that promote inside-out signaling via Rap GEFs—CalDAG and Epac—that are activated by the second messengers DAG and cAMP, respectively. This induces activation of Rap1, which recruits the effectors RapL, RIAM and Talin that induce a conformational change of αMβ2 into its extended conformation. **B)** Another inside-out activation pathway of β2 integrins involves the engagement of TLR by its ligands, which induces the production of PIP_3 that activates Rac1 to induce actin polymerization, and Rap1 to induce the extended integrin conformation (Freeman & Grinstein, 2014).

The extended integrin is able to engage its ligand and therefore, in response to CR3/Mac-1 engagement by iC3b, outside-in signaling is promoted, leading to conformational changes that induce headpiece-opening and thus full activation of CR3 (Fan & Ley, 2015). Moreover, the clustering of CR3 during phagocytosis coincides with the formation of adhesion complexes (adhesomes) with talin being a prominent

component of these adhesomes. Thus, bound talin is required for firm binding of active β2 integrins and subsequent internalization of C3b-opsonized targets. This process also involves recruitment other proteins to the cytoplasmic tails of active integrins, which are needed during CR3-mediated phagocytosis including paxillin, vinculin, and α-actinin (Abram & Lowell, 2009; Freeman & Grinsteain, 2014). Following adhesome recruitment, RhoA and Rap1 are recruited to the site of phagocytosis by activation of two specific effector molecules, the formin-related elongating factor, mDia (mammalian diaphanous related formin 1), and the serine/threonine kinase ROCK1. Activation of ROCK1 promotes the local recruitment of the Arp2/3 complex to induce actin polymerization that together with active myosin IIA pulls the particles inside the cell to compartmentalize them into a vacuole; a process supported also by mDia (**Figure 5**) (Colucci-Guyon, 2005; Haas A., 2007; Wiedemann, 2006). Also, during CR3-mediated phagocytosis, Rap1 is activated and sufficient to induce actin remodeling in the absence of RhoA, acting through different effectors such as profilins, cofilins and the guanine nucleotide exchange factor (GEF) Vav1/3. The participation of Vav1/3 may also be crucial for CR3-mediated phagocytosis due to its ability to activate Rac1, which in turn activates Rap1, thus inducing a positive feedback loop (Dupuy & Caron, 2008). Rac1 is involved in the activation of the Arp2/3 complex to drive the formation of branched actin networks that in turn form the pseudopods required for phagocytic cup formation (**Figure 3c**) (Hall et al., 2006). Integrin-dependent actin polymerization during phagocytosis is highly regulated by motor proteins such as myosins that help support the extension of the plasma membrane and fusion of the edges of the cup into the phagosome (Herant, 2006) (**Figure 5**).

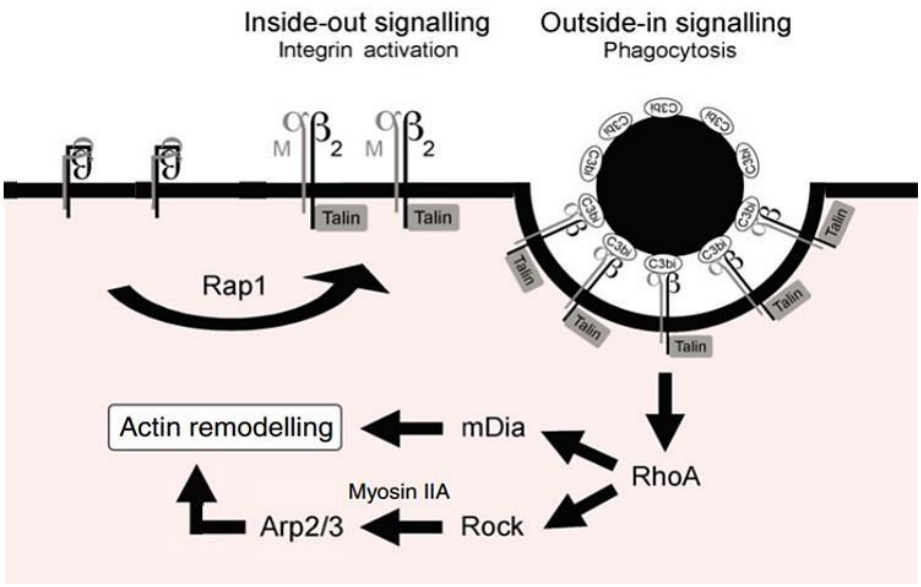

Figure 5. Outside-in signaling during CR3-dependent phagocytosis. Upon CR3 binding to the particle, a force generated via RhoA-dependent actin polymerization and actomyosin contractility pulls the particle inside the cell. During this outside-in signaling pathway, proteins such as Rock, Arp2/3, and mDia are required for proper actin remodeling and phagosome formation (Dupuy & Caron, 2008).

Following internalization, the phagocytic vacuole becomes a mature phagosome after fusion with preformed granules that contain hydrolytic enzymes and the Nicotinamide Adenine Dinucleotide Phosphate-oxidase (NADPH) subunits that initiate killing mechanisms such as ROS production, pH acidification and influx of K^+ to mediate the release of serine proteases and conversion of H_2O_2 into HOCl, leading to the development of a toxic environment that promotes oxidative reactions, electron oxidations, sequestration of biological anions (I-, Br-, Cl-, SCN-, NO-), and inhibition of DNA synthesis, among others (Hurst, 2012; Rosales, 2020); processes discussed in more detail in the following paragraph.

1.2.2.2. Respiratory Burst: Production of Reactive Oxygen Species

Oxygen consumption increases during neutrophil effector functions due to the production of inducible ROS in response to NADPH-oxidase complex activation. ROS can be released extracellularly into the environment at the site of infection or damage, or intracellularly in the phagolysosome following phagocytosis of pathogens (Nguyen et. al., 2017). ROS can cross the membranes of pathogenic microorganisms and damage their

nucleic acids, proteins, and cell membranes (Nguyen et. al., 2017; Winterbourn et. al., 2016). The NADPH enzyme complex, also known as phagocyte oxidase (phox) or NOX2, must be assembled through the translocation of its components from the cytosol to the plasma membrane. These components include the cytosolic heterotrimer regulatory complex made up of the subunits $p47^{phox}$, $p67^{phox}$, and $p40^{phox}$ that interact with the membrane-bound subunits $gp91^{phox}$ (NOX2 or CYBB) and $gp22^{phox}$ (CYBA); together, they make up the heteromeric subunit known as flavocytochrome-b558 ($cytb_{558}$), which constitutes the catalytic core of the NADPH oxidase usually found in the secondary granules, tertiary granules, and secretory vesicles of resting neutrophils (Lambeth, 2004; Mayadas, 2014; Nguyen et. al., 2017). A key component for the assembly and function of the NADPH oxidase complex is active GTP-bound Rac2 (El-Benna et. al., 2016).

Depending on the activation state of neutrophils, the NADPH oxidase complex can be partially or completely activated. If the neutrophil is in a "primed" state, induced by ligand engagement of receptors such as GPCRs, cytokine receptors and TLRs, the NADPH oxidase complex is more susceptible to robust activation by secondary stimuli, thus it becomes partially activated due to conformational changes in the $p47^{phox}$/$p40^{phox}$/$p67^{phox}$ complex including the partial phosphorylation of $p47^{phox}$ and the translocation of $cytb_{558}$ from secondary granules to the plasma membrane or the phagosome (El-Benna et. al., 2016). When Fc receptors, integrins and N-Formylmethionine-leucyl-phenylalanine (fMLP) receptors are engaged, the NADPH oxidase complex gets fully activated (El-Benna et. al., 2016) (**Figure 6**).

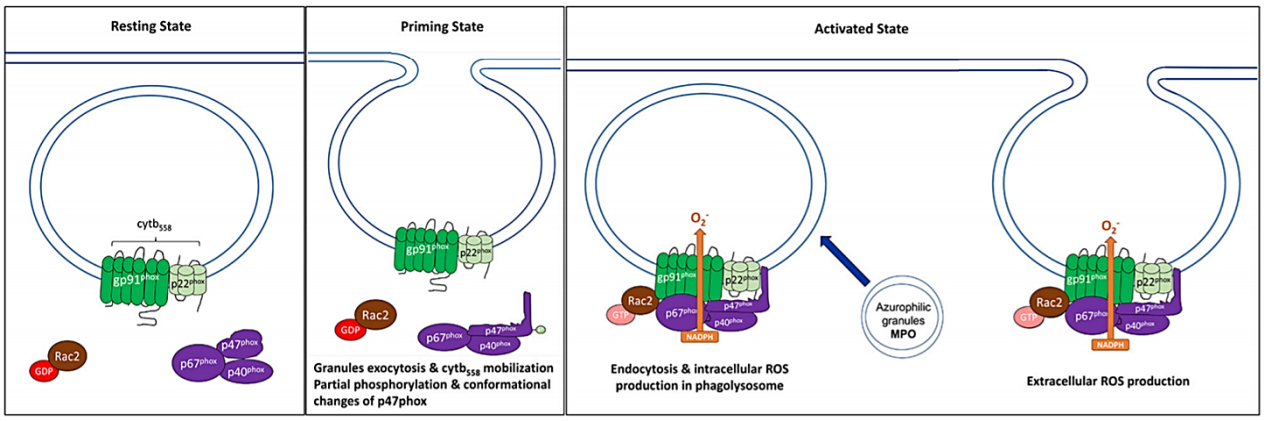

Figure 6. Assembly of the NADPH oxidase upon neutrophil priming and activation. The NADPH oxidase complex consists of five subunits and Rac2. The regulatory subunits $p47^{phox}$, $p67^{phox}$, and $p40^{phox}$ stay dormant in the cytosol at resting state and the flavocytochrome b558 ($gp91^{phox}$ and $gp22^{phox}$) is bound to the membranes of secondary granules. However, when neutrophils are in a "primed" state, cytb558, is translocated to phagosomes and plasma membrane, while $p47^{phox}$ becomes partially phosphorylated. Finally, when neutrophils are fully activated, the regulatory complex is recruited to sites where cytb558 is located, as well as GTP-bound Rac2, allowing the transfer of electrons from NADPH to molecular oxygen generating superoxide anions (O^{-2}) (Nguyen et. al., 2017).

NADPH oxidase complex formation is initiated by the phosphorylation of $p47^{phox}$ via downstream kinases such as phosphoinositide 3-kinase (PI3K), protein kinase C isoforms and A (PKCα, β, δ, ζ, and PKA, respectively), and MAPKs such as ERK1/2 and p38. The kinase mediating phosphorylation depends on the engaged surface receptor governing activation (Nguyen et. al., 2017). Once phosphorylated at multiple serine-threonine residues, $p47^{phox}$ suffers a conformational change allowing the exposure of its SH3-binding pocket and PX domain that interact with the proline-rich region of $gp22^{phox}$ and PtdIns(3,4)P2, respectively (Meijles et. al., 2014). This way, $p47^{phox}$ translocates to the sites where $cytb_{558}$ is located, bringing along $p67^{phox}$ and $p40^{phox}$ to the membrane (**Figure 6**) (El-Benna et. al. 2009). Both $p40^{phox}$ and $p67^{phox}$, interact with each other through the PB1 domain of $p40^{phox}$. Simultaneously, but independently from the regulatory subunits, GTP-bound Rac2 is also recruited to the membrane when signaling proteins such as PIP3 and Gβγ subunits activate Rac2 GEFs to promote the exchange of GDP for GTP, allowing for Rac2 dissociation from Rho-GDI and translocation from the cytosol to the site of NADPH oxidase complex assembly where it then interacts with $p67^{phox}$ (**Figure 6**) (Hawkins et. al., 2010; Hodge & Ridley, 2016). The participation of Rac2 is essential because it induces conformational changes in $p67^{phox}$ that allow it to bind to $gp91^{phox}$, which is required for the oxidative burst (Nguyen et. al., 2017).

Once the NADPH oxidase complex is assembled, the cytosolic domain of $gp22^{phox}$ (the electron transferase), catalyzes the transfer of electrons from NADPH across the membrane to molecular oxygen (O_2) generating superoxide radicals (O^{-2}) that damage nucleic acids, proteins, and cell membranes (Panday et. al., 2015). Next, by a dismutation reaction catalyzed by superoxide dismutase (SOD), O^{-2} radicals are converted into hydrogen peroxide (H_2O_2) and further into water. Also, the fusion of granules carrying

myeloperoxidase (MPO) with the phagosome allows this enzyme to convert H_2O_2 to hypochlorous acid (HOCl) (a very potent microbicidal substance) or to directly convert O^{-2} into singlet oxygen ($^1O_2$) (**Figure 7**).

Another important enzyme is the inducible nitric oxide synthase (iNOS), which is responsible for the production of nitric oxide (NO), a highly reactive and short-lived molecule that, other than antimicrobial activity, has effects on vasculature tone, neurotransmission, and inflammation. NO complements ROS activity by the production of cytotoxic species such as $ONOO^-$ (Fang, 2004). Altogether, within the activated neutrophil, the action of the NADPH oxidase complex generates a toxic environment which promotes antimicrobial activity via peroxidation of proteins and lipids, and by increasing efficient pathogen destruction and clearance (Nguyen et. al., 2017; Rosales, 2020; Williams, 2006).

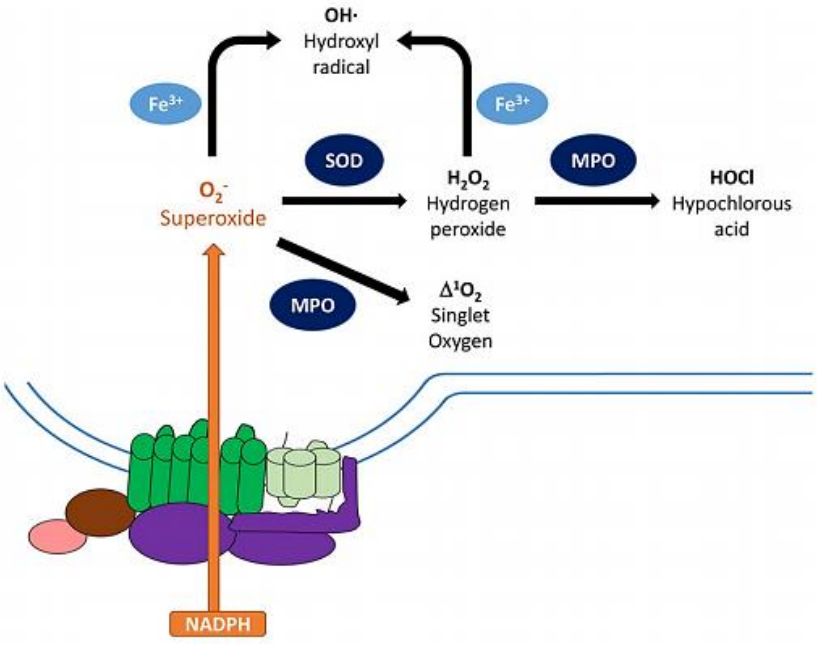

Figure 7. Production of reactive oxygen species by the NADPH oxidase complex. The assembled NADPH oxidase complex transfers electrons from NADPH to molecular oxygen generating O^{-2} radicals. These are further converted into H_2O_2 and water by SOD. H_2O_2 can also be converted into HOCl and O^{-2} radicals into $^1O_2$ by the activity of MPO. NADPH oxidase components: $gp91^{phox}$ (green), $gp22^{phox}$ (light green), regulatory subunits (purple), GTP-Rac2 (pink and brown, respectively) (Adapted from Nguyen et. al., 2017).

1.2.2.3. Degranulation

Neutrophils contain a variety of cytoplasmic granules that represent fundamental microbicidal weapons. These cytoplasmic granules are formed in sequential order during neutrophil development in the bone marrow and can be categorized into three types according to the pro-inflammatory proteins that they contain: Primary or azurophilic granules, which contain myeloperoxidase (MPO), defensins, inducible nitric oxide synthase (iNOS) and elastase; secondary or specific granules, which contain lactoferrin, cathelicidin, olfactomedin-4, lipocalin-2 and metalloproteinases; and tertiary or gelatinase granules, which contain matrix metalloproteinase 9 (MMP9; also known as gelatinase B), arginase 1 and lysozyme (Faurschou, 2002; Häger, 2010) (**Figure 8**). Additionally, neutrophils also contain secretory vesicles that are formed during the final maturation step. They are mobilized to the cell surface upon neutrophil activation due to the need of various adhesion and chemotactic receptors to be rapidly transported and exposed on the cell surface (Borregaard, 1990). The content of secretory vesicles is made up of cytokines, membrane receptors, adhesion molecules, NADPH oxidase and albumin. Antimicrobial peptides such as α-defensins and cathelicidins provide microbicidal activity when interacting with negatively charged membrane components leading to the formation of pores, enabling membrane permeabilization to disrupt biosynthesis of nucleic acids, proteins, and lipids in pathogens (Choi, 2012). Moreover, these peptides have an immunomodulatory function in both neutrophils and cells in the inflamed tissue, where antimicrobial peptides such as LL-37 up-regulate the expression of genes encoding chemokine receptors such as IL-8RB, CXCR4 and CCR2. Also, these peptides can induce the expression of the anti-apoptotic protein BcL-XL and inhibition of caspase-3 activity in neutrophils, and thus promote the survival signals that prevent neutrophil apoptosis (Rosales, 2020; Scott, 2002).

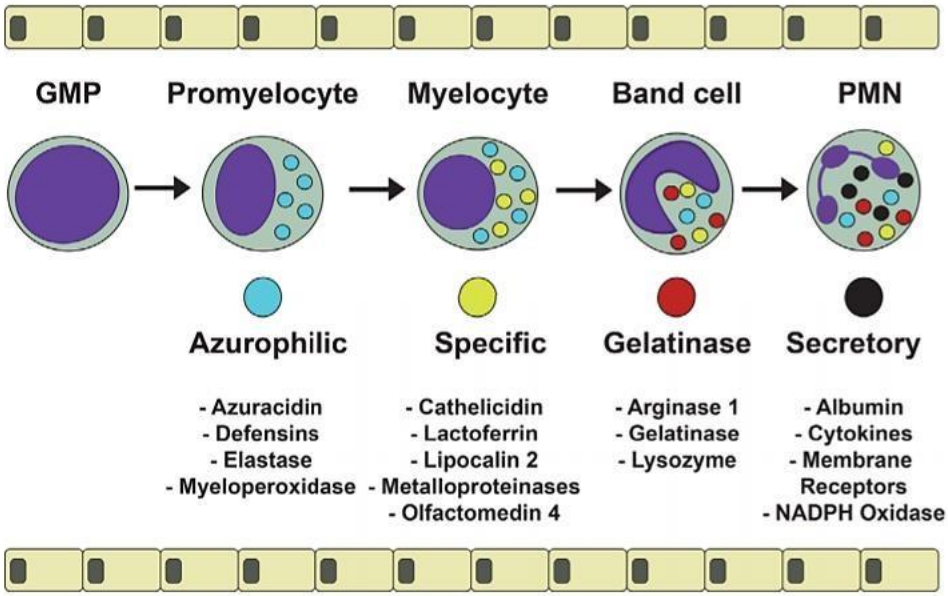

Figure 8. Neutrophil granule formation and composition. During granulopoiesis in the bone marrow, granules are sequentially formed according to the stage of maturation. The first granules to be formed are primary (azurophilic) granules, followed by secondary (specific) and tertiary (gelatinase) granules. In mature neutrophils, secretory vesicles are the last to develop (Rosales, 2020).

The release of the contents from the granules depends on different mechanisms beginning with chemokine receptor stimulation or activation of integrins, culminating in the exocytosis of the components. First, actin cytoskeletal remodeling and microtubule assembly takes place to recruit granules from the cytoplasm to the plasma membrane and allow for vesicle tethering and docking. Chemoattractant exposure causes polarization of the neutrophil to form a leading edge with lamellipodia, in which active actin reorganization takes place, and a trailing edge with uropod formation (Félix, et. al., 2018). This is driven by an increase in the levels of intracellular Ca^{2+}, the hydrolysis of adenosine triphosphate (ATP) and guanosine triphosphate (GTP), and also, by the activation of GEFs to activate the small GTPase Rac2, which regulates actin remodeling at the leading edge, as well as granule movement. During this process, many proteins play an important role such as annexins, calmodulin, GTP-binding proteins, and small monomeric proteins such as vesicle-associated membrane protein 1 (VAMP-1) and VAMP-2, VAMP-7 and SNAP-23 that allow for the formation of the SNARE complex. These proteins act as markers that lead granules to the correct degranulation sites by

following the “actin tracks” and directing granule movement to the plasma membrane for polarized exocytosis (Félix, et. al., 2018). After activation of these effector molecules, the actin cytoskeleton must undergo another reorganization step, involving the disassembly of actin filaments at the cell periphery to allow translocation of the granules to the plasma membrane, therefore, actin depolymerization of the cortical actin network allows the granules to locate near the membrane (Mitchell, 2008). This is followed by the contact of the lipid bilayer surrounding the granule with that of the target plasma membrane, which in turn enables the rapid formation of a fusion pore due to the association of a vesicle-associated SNARE protein that binds to a Q-SNARE protein (named for expression of a glutamine residue in the SNARE domain) on the target membrane to form a SNARE complex that mediates interactions between the vesicle and the plasma membrane (Félix, et. al., 2018). This in turn leads to the fusion of both membranes and the release of the granular contents (Burgoyne, 2003; Sengelov, 1993). Actin remodeling is an important aspect of the mobilization of granules and vesicles to the plasma membrane of neutrophils. Myosins are key motor proteins involved in the movement of vesicles throughout the cell as discussed below, but their specific functions for actin remodeling during degranulation remain elusive.

The granular content of primary granules can also be fused with the phagocytic vacuole to induce its maturation into a phagosome during phagocytosis. The release of cationic antimicrobial peptides and cathelicidines induces pore formation in the membrane of bacteria and inhibition of DNA/RNA synthesis, thus killing the pathogen (Benarafa, 2017). Also, other antimicrobial proteins derived from secondary granules such as lactoferrin can chelate essential metals for bacteria growth and metabolism, thus preventing their survival within the phagosome (Benarafa, 2017). The release of granules into the extracellular space can also occur during neutrophil transmigration through the interaction of selectins and integrins with their respective ligands. This in turn enables the release of proteases within the granules that facilitate the degradation of adhesion molecules, collagen and other matrix-related proteins that may act as a physical barrier and therefore allow efficient neutrophil migration in an inflamed environment (Lacy, 2006).

1.2.2.4. Formation of Neutrophil Extracellular Traps

NETs are extracellular strands of decondensed DNA in complex with histones and decorated with neutrophil granule-derived proteins and enzymes such as elastase, cathepsin G, lactoferrin, defensins, proteinase 3, gelatinase, and myeloperoxidase (Brinkmann, 2004; Kaplan, 2012; Sørensen, 2016). These structures were discovered as an important neutrophil strategy to immobilize invading microorganisms, impede their dissemination, and facilitate phagocytosis. Induction of NET formation occurs in response to a variety of stimuli including microorganisms such as bacteria, fungi, and their products, as well as during sterile inflammation in response to DAMPs, antibodies, MPO, elastase, and gasdermin D, among others. It has been reported that toxins secreted by *S. aureus* induce nuclear swelling in neutrophils and rapid release of their DNA content into the cytoplasm followed by the disintegration of the plasma membrane and release into the extracellular space (Kobayashi, 2010). During exacerbated or chronic inflammation and autoimmune diseases, NET release can also be triggered by proinflammatory cytokines such as TNF-α and IL-8, platelets, activated endothelial cells, nitric oxide, monosodium urate crystals, and various autoantibodies (Clark SR, 2007; Kaplan, 2012; Mitroulis, 2011).

NETs consist of extruded meshworks of chromatin fibers, usually between 15 and 17 nm in diameter (Kaplan, 2012) that are decondensed by peptidyl arginine deaminase 4 (PAD4), which catalyzes the conversion of histone arginines to citrullines, thus reducing the strong positive charge of histones and consequently weakening histone-DNA binding leading to the unwrapping of nucleosomes (Sørensen, 2016). In addition, neutrophil elastase also helps cleave histones after translocating to the nucleus (Papayannopoulos, 2010). As a result, the nuclear membrane disintegrates and the decondensed chromatin is released into the cytoplasm, where it interacts with the granular proteins mentioned before, generating a complex that is released as NETs (Fuchs, 2007; Kaplan, 2012). Finally, the rupture of the plasma membrane, following the destabilization of the cortical actin network, allows the release of NETs culminating in a type of cell death known as NETosis (**Figure 9**) (Mantovani et. al, 2011).

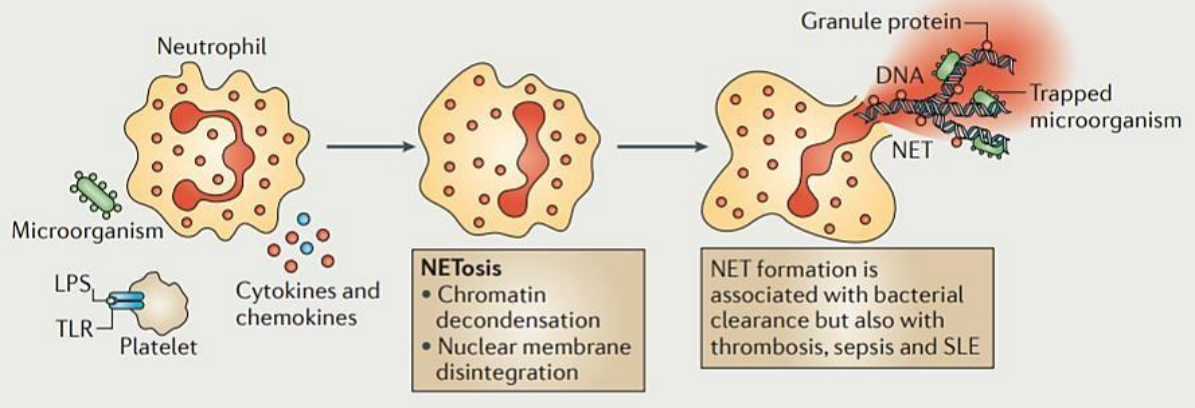

Figure 9. Neutrophil Extracellular Traps (NETs) formation. Several stimuli such as microbes and their products, cytokines, chemokines, immune complexes and even autoantibodies can induce NET formation. When these molecules bind to surface receptors, they induce chromatin decondensation and nuclear membrane disintegration. DNA is released into the cytoplasm and is decorated with proteins from neutrophil granules, to finally be released into the extracellular space. NETs act as a mesh that traps microorganisms and, in turn, facilitate their interaction with neutrophil-derived effector molecules (Mantovani et. al., 2011).

It has been described that the cellular mechanics driving NET expulsion depend on PAD4-mediated chromatin decondensation (Thiam et. al., 2020). Neutrophils exhibit rapid actin cytoskeleton disassembly, followed by the shedding of plasma membrane vesicles, and the disassembly and remodeling of the microtubule and vimentin cytoskeletons. Moreover, the ER forms vesicles, the nucleus becomes rounded, and chromatin decondensation occurs. Subsequently, the nuclear lamin meshwork destabilizes and the plasma membrane and nuclear envelope (NE) progressively permeabilize leading to NE rupture that allows the DNA to be released into the cytoplasm. Finally, the plasma membrane ruptures leading to the discharge of extracellular DNA traps (Thiam et. al., 2020). However, despite the evidence of actin cytoskeletal involvement during NETosis, myosin motor proteins have not been investigated in this context. There is evidence that the class I myosin, Myo1f, is needed for dynamic neutrophil nucleus deformation during extravasation (Salvermoser, 2018), suggesting that during NETosis-derived nuclear changes, class I myosins may also play a key role.

1.3. Myosins: cytoskeletal motors

Many neutrophil functions depend on actin dynamics controlled by a variety of actin-binding proteins (ABP). Together they regulate many of the necessary morphological

changes of neutrophil movements during inflammation. One of the ABP recently studied by our group, the cortactin homolog HS1 in neutrophils, was found to be involved in the regulation of neutrophil extravasation by controlling the activation of small GTPases and integrins (Latasiewicz, 2017). Moreover, in neutrophils, absence of HS1 resulted in a significant reduction of phagocytosis and of the number of phagocytosed opsonized particles per cell demonstrating the importance of HS1 for migration and neutrophil effector functions (Guerrero, 2018). Another example is the ABP Skap2, which is involved in actin remodeling and integrin activation due to regulation of actin polymerization via WASP (Boras, 2017). However, actin-binding motor proteins including class I myosins have not been well studied in the context of neutrophil extravasation and effector functions.

Myosins are motor proteins that bind actin filaments (F-actin) in an adenosine triphosphate (ATP)-regulated manner. When binding to F-actin, myosins hydrolyze ATP that powers the movement of actomyosin filaments along each other. Structurally, these proteins are composed of an N-terminal “head” or motor domain, a middle “neck” region, and a C-terminal “tail” region (Navinés-Ferrer & Martín, 2020). The motor domain contains the ATP-binding site and the actin-binding site that provide the actin-based molecular motor function. Following, the “neck” region consists of a variable amount of isoleucine and glutamine (IQ) motifs, that allow the binding of light chains and serve as a lever arm that permits motor domain movements (Coluccio et. al., 2008). Finally, the tail region has various lengths and functions which depend on the motifs included in its sequence, such as coiled-coil dimerization regions, FERM, MyTH4, or SH3 domains for protein–protein interactions and PH domains for lipid interactions, among others (Coluccio et. al., 2008; Maravillas-Montero & Santos-Argumedo, 2012).

The myosin superfamily consists of 35 proteins, classified into 18 groups based on the structural similarity of the heavy-chain head domains. Some of them are exclusively expressed in plants or vertebrates; however, the majority of myosins are found in eukaryotes (**Figure 10)** (Foth, 2006; Maravillas-Montero & Santos-Argumedo, 2012).

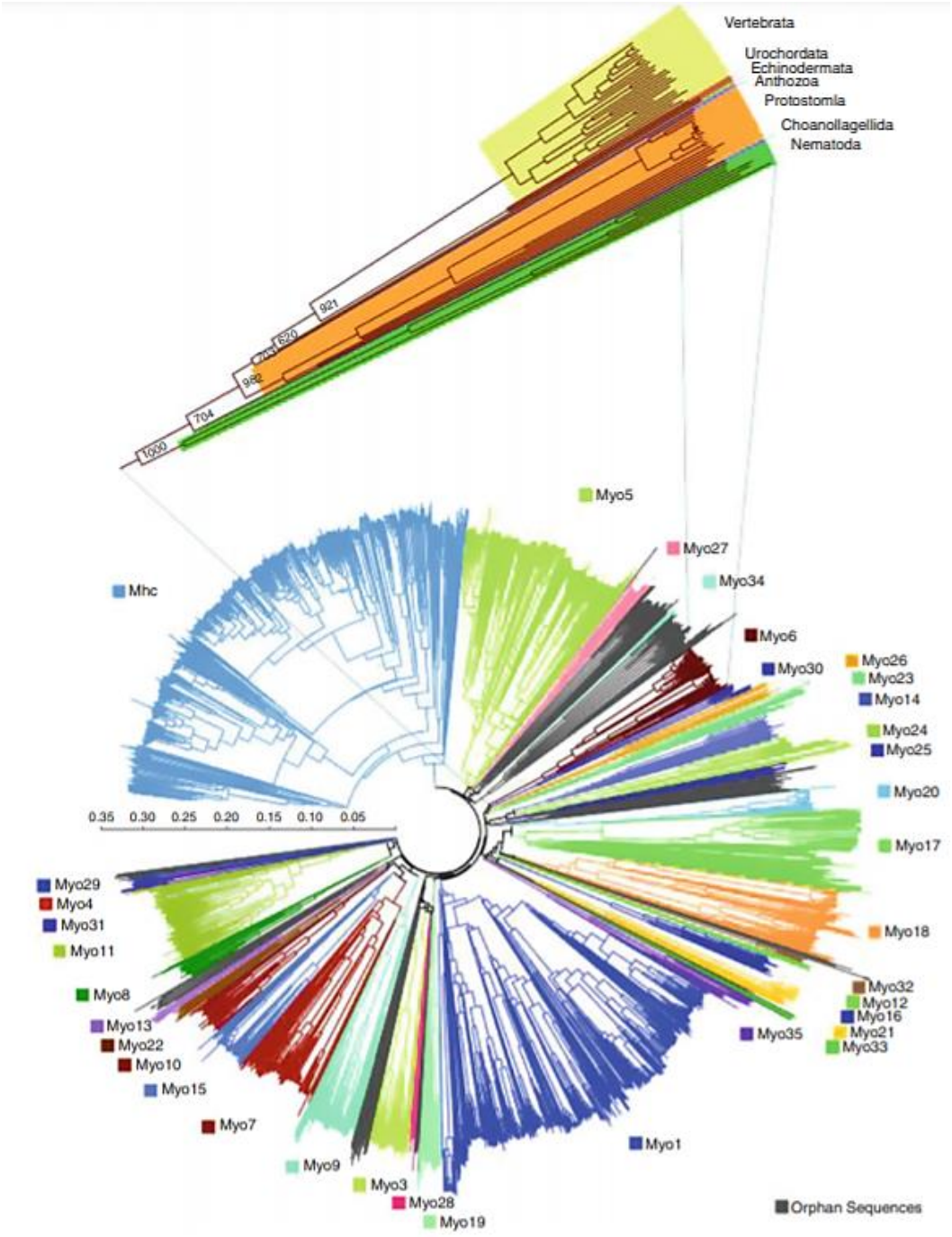

Figure 10. The myosin superfamily. Phylogenetic tree of myosins constructed from multiple sequence alignment of 1984 myosin motor domains. The expanded view shows the myosin sequences of class-VI and their distribution. The bar corresponds to estimated amino-acid substitutions per site (Diagram from Minozzo & Rassier, 2013).

This superfamily is further divided into two classes: Class II are the conventional myosins which include the skeletal, cardiac, and smooth muscle myosins and the non-

muscle myosin II; and class I are the unconventional myosins consisting of myosins responsible for the regulation of membrane tension, formation of cell adhesions and changes in the actin architecture (Fili & Toseland, 2020). The classification of both classes into diverse groups or sub-classes is based on the phylogenetic analysis of the conserved motor domain. This is achieved by delineating the first branches emanating from the center of an unrooted myosin phylogeny. If more than 90% of the branches are observed when the phylogenetic reconstruction is applied on a re-sample set of data, myosins can then be assigned a separate class according to their motor domain similarity (**Figure 11**) (Foth et. al., 2006).

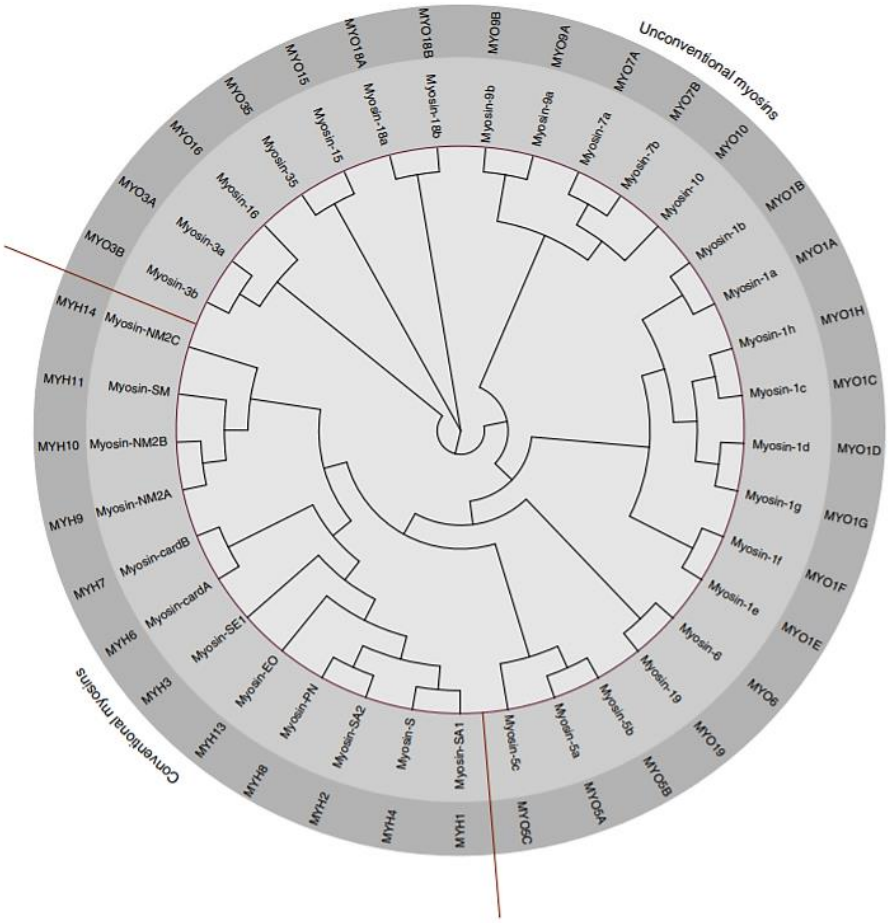

Figure 11. Conventional and unconventional myosins in humans. The human myosome is split into 13 structurally and functionally distinct classes, which are defined by 39 genes encoding the myosin heavy chain genes, including pseudogenes. Class-II myosins are referred to as conventional myosins; all other myosin classes are referred to as unconventional. Abbreviations used for myosins from class-II: cardA, cardiac alpha; cardB, cardiac beta; EO, extra-ocular muscle; NM, nonmuscle; S, skeletal muscle; SA, skeletal muscle adult; SE, skeletal muscle embryonic; SM, smooth muscle; PN, perinatal muscle. Gene

symbols are in uppercase letters, whereas in the corresponding gene products only the first letter is capitalized (Heissler & Sellers, 2016).

In contrast to the conventional class II myosins that form large bipolar chains via tail-directed homo-oligomerization (Maravillas-Montero & Santos-Argumedo, 2012; Woolner & Bement, 2009), unconventional myosins do not form filaments, and instead, their tails allow membrane binding and interaction with other proteins (Woolner & Bement, 2009). In addition, about two-thirds of myosin-coding genes in humans encode genes of the unconventional myosin group (**Figure 11**), and some studies have shown that unconventional myosins perform key roles in a broad range of fundamental cellular processes such as the maintenance of cell morphology (Dippold et. al., 2009; Yumura & Uyeda, 2003), intracellular trafficking (Vale, 2003), endocytosis, exocytosis, cell adhesions, cell motility, signal transduction, and transcription (Fili & Toseland, 2020; Hartman et. al., 2011; Kim et al., 2006).

Although both classes are important, we still know much less about the biochemical characteristics, the different levels of regulation, the molecular association, and the impact on different cellular functions of unconventional myosins compared to conventional myosins. Within the unconventional myosins subfamily (**Figure 11**), class I myosins, represent the largest and most evolutionary ancient group of myosins (Thompson & Langford, 2002). Class I myosins have been implicated in increasingly complex cellular phenomena, yet how every class-I myosin accomplishes multiple types of molecular functions, especially in immunological settings, is still an active area of investigation. Therefore, it is essential to understand the underlying physiology of these myosins, in order to improve different approaches of biological investigation.

Class I myosins are composed of a single-headed monomeric heavy chain of 110-140 kDa that can bind directly to the plasma membrane and cytosolic proteins including actin filaments (Maravillas-Montero & Santos-Argumedo, 2012; Navinés-Ferrer & Martín, 2020). They also contain an N-terminal motor domain and the IQ region characterized by the IQXXXRGXXXR sequence implicated in the binding of calmodulins. However, in class I myosins, the C-terminal “tail” region can be divided into three regions referred to as tail-homology (TH) regions, TH1, TH2 and TH3 (Foth et. al., 2006). According to the number of TH domains, class I myosins can be sub-classified into “short-tailed” myosins that only

contain the TH1 domain, and “long-tailed” myosins that contain three TH domains (Maravillas-Montero & Santos-Argumedo, 2012). In vertebrates, eight different genes exist encoding the class I myosins. These myosins include the short-tailed Myo1a, Myo1b, Myo1c, Myo1d, Myo1g and Myo1h, and the long-tailed Myo1e and Myo1f (**Figure 11**) (Berg, 2001). Myo1e and Myo1f remain the least well studied myosins, and given their additional TH2 and TH3 domains, it is intriguing to investigate how these proteins are functionally different from the short-tailed class I myosins.

1.3.1. Long-tailed Class I myosins: Myo1f and Myo1e

Of the eight class I myosin genes, two encode long-tailed forms: myosin 1e (Myo1e) (**Figure 12**) and myosin 1f (Myo1f). These long-tailed myosins bind to actin in an ATP-dependent manner through their head domain and can associate with calmodulins through their IQ domains that serve as “cervical collars” to maintain the rigidity of the heavy chain. However, changes to the IQ region, can result in rigidity and changes in mechanochemical properties to allow cytoskeletal rearrangements (Wolenski, 1995). The TH1 domain is enriched in basic residues, which allow for membrane interactions by binding to phosphoinositides (Yamamoto, 2016). In addition, long-tailed myosins also contain the TH2 domain which is rich in glycine, proline, and alanine/glutamine amino acids, suitable for binding membrane phospholipids. In addition, the TH2 domain is thought to provide an ATP-insensitive actin-binding site (Feeser, 2010). Finally, these myosins contain the TH3 region which is a Src homology 3 (SH3) scaffold domain that binds proline-rich regions of other proteins (Kurochkina, 2013).

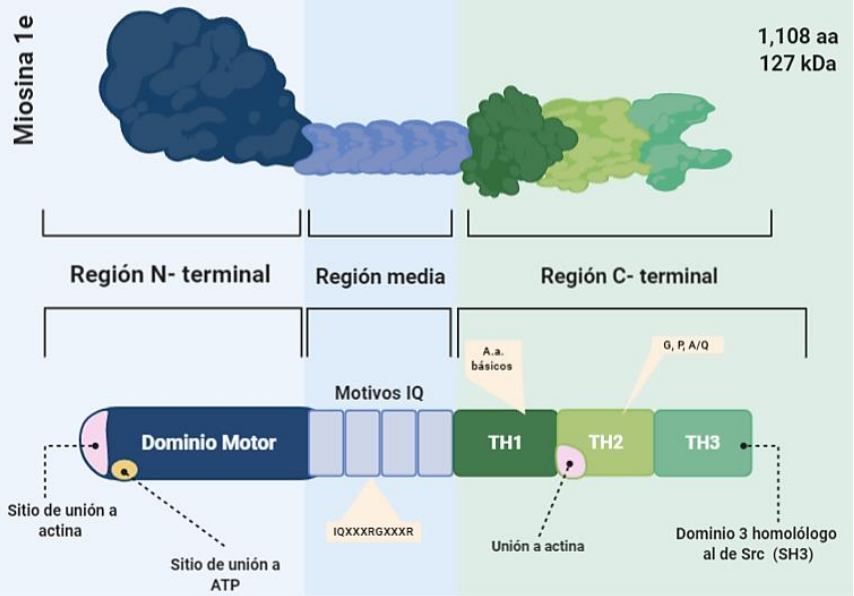

Figure 12. Structure of the long-tailed myosin 1e. This myosin consists of the indicated regions represented in colored boxes. The motor domain (dark blue) contains the actin binding domain as well as the ATP binding domain; IQ-motifs (light blue) bind calmodulin to stabilize and give Myo1e the correct stiffness to permit motor domain movements; the tail region is comprised of three domains: Tail-Homology 1 domain (TH1) (dark green) composed of basic residues that bind phosphoinositides in membranes, TH2 (sage) that contains an ATP-independent actin binding site and proline-rich regions to bind to bind SH3 domain-containing proteins; TH3 (light green) contains a Src homology 3 (SH3) binding site that allows myo1e to bind proline-rich domain-containing proteins. (Image generated using the online drawing tool Biorender https://biorender.com/).

Long-tailed class I myosins perform similar functions such as intracellular transport, the formation of cell-surface projections, the regulation of the cytoskeleton, and the regulation of membrane-related events (Kim & Flavell, 2008; Maravillas-Montero & Santos-Argumedo, 2012). Even though their functions have not been investigated in detail in immunological cells, a recent study demonstrated essential evidence for important roles of Myo1f during neutrophil migration by demonstrating that Myo1f was required only for 3-dimensional neutrophil migration by regulating nucleus deformation. This study highlighted the importance of these motor proteins for neutrophil migration (Salvermoser et. al., 2018).

1.3.1.1. The long-tailed myosin 1e

Out of both long-tailed class-I myosins, *in-silico* analyses and recent literature have shown that Myo1e is more ubiquitously expressed than Myo1f, as it is highly present in

the digestive tract, immune system cells, lung, mesenteric lymph nodes and kidneys (**Figure 13**) (Navinés-Ferrer & Martín, 2020). Even though the *MYO1E* mRNA expression varies depending on the analyzed tissue (**Figure 13A**), the presence of Myo1e protein does not seem to depend on the expression levels of its transcript (**Figure 13B**).

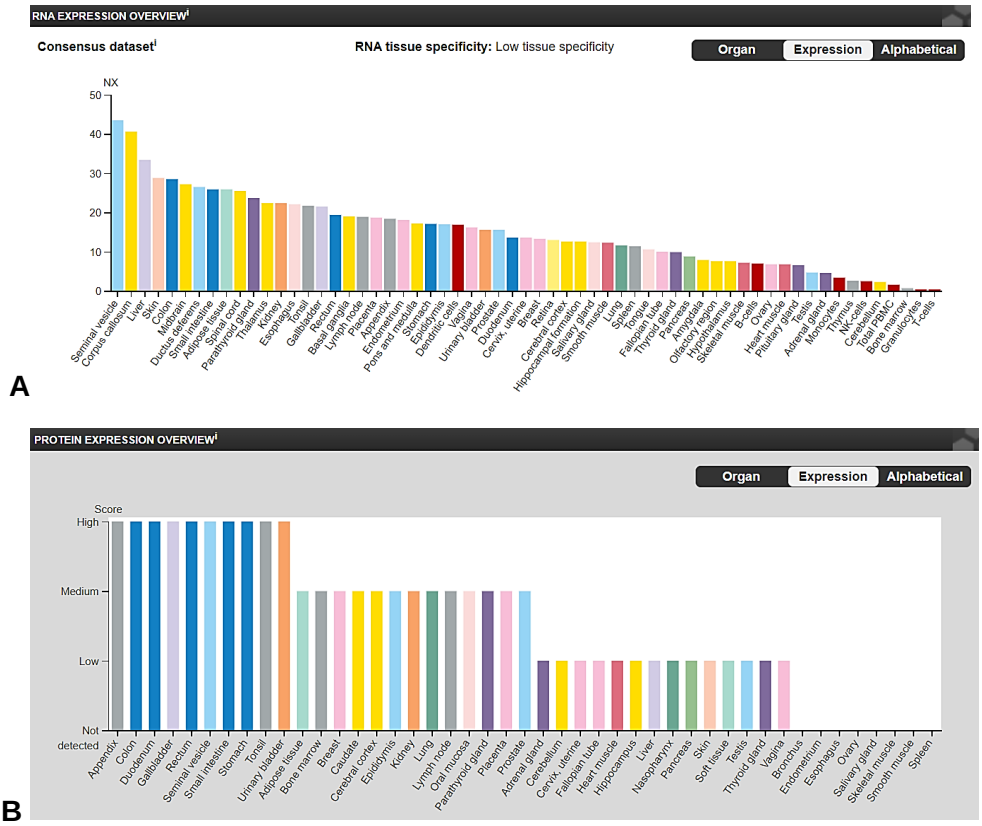

Figure 13. Myosin 1e expression in different human organs. *In-silico* analysis of myosin 1e A) RNA and B) protein expression profiles in different human organs using the human protein atlas database. Myosin 1e is ubiquitously expressed in a variety of organs and tissues although at different levels. The digestive system expresses most Myo1e followed by kidney, breast, lung, and bone marrow, among others. Even though the mRNA expression varies from tissue to tissue, the presence of Myo1e protein in these tissues does not follow the same pattern of expression (**https://v19.proteinatlas.org/ENSG00000157483-MYO1E/tissue**).

The role of Myo1e in neutrophils was until recently unknown because, unlike other immune cells such as B lymphocytes and macrophages, Myo1e has been thought to be absent or expressed at very low levels in neutrophils (**Figure 13**) (Sangwon et. al., 2006). Nonetheless, our group recently showed that Myo1e protein is present in neutrophils (**Figure 14A**), thus opening a new field of research on its role in this cell type. Using

intravital microscopy (IVM) of TNF-α inflamed cremaster venules, absence of Myo1e has been shown to induce an irregular and aberrant slow rolling in neutrophils, in which they detached from the endothelial surface, simulating a “jump”, and then reattached to continue rolling, a defect defined as intermittent slow rolling (**Figure 14B**) (Vadillo et. al., 2019). Moreover, Myo1e-KO neutrophils showed defective arrest and crawling leading to reduced TEM of neutrophils (**Figure 14E and F**). Furthermore, using β2-integrin blocking antibodies, intermittent slow rolling of Myo1e-KO neutrophils was shown to be mediated by defective LFA1/Mac1-mediated neutrophil interactions with the endothelium (**Figure 14C**). Absence of Myo1e in neutrophils also reduced actin polymerization, uropod formation, and chemotaxis (**Figure 14G, H and I**). These data show that Myo1e has important functions in 2-dimensional (2D) as well as 3D neutrophil migration.

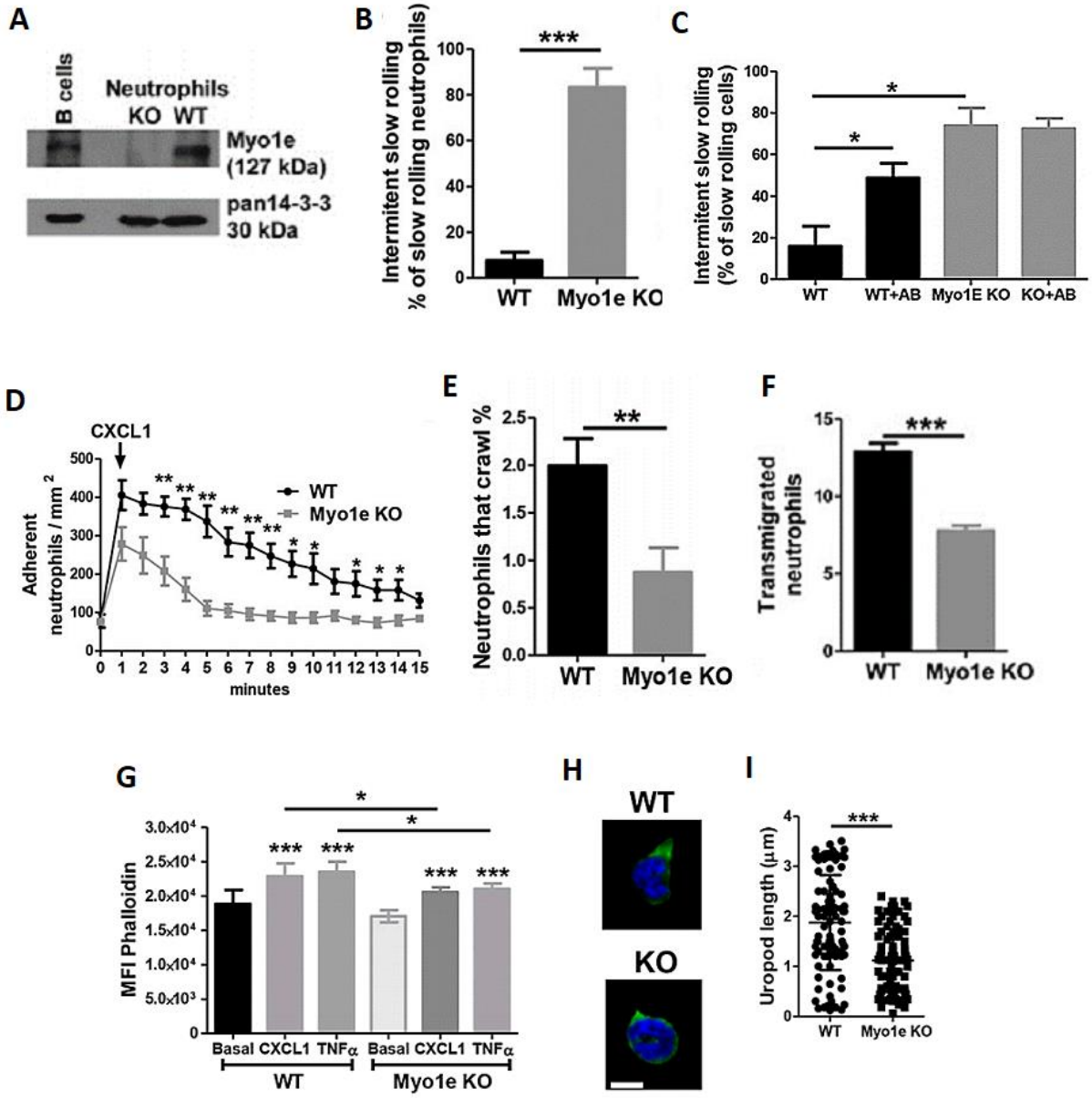

Figure 14. Myosin 1e regulates adhesive interactions of neutrophils during extravasation. A) Western blot showing myosin 1e expression in neutrophils. **B)** Percentage of WT and Myo1e-KO neutrophils exhibiting intermittent slow rolling. **C)** Percentage of intermittent slow rolling after injection of LFA-1 and Mac1 blocking antibodies. **D)** Neutrophil adhesion dynamics within cremaster venules over time after injection of CXCL1. **E)** Percentage of crawling WT and Myo1e-KO neutrophils within an inflamed cremaster vessel. **F)** Number of transmigrated neutrophils in TNF-α-inflamed cremaster muscles. **G)** Mean Fluorescence Intensity of phalloidin staining in unstimulated WT and Myo1e KO neutrophils or after stimulation with TNF-α or CXCL1. **H)** Uropod formation of CXCL-1-treated neutrophils analyzed through phalloidin staining and **I)** quantification of uropod length. (Adapted from Vadillo et. al. 2019).

In macrophages, Myo1e is strongly expressed and gets serine phosphorylated in the tail domain in response to TLR4 activation leading to robust cytoskeletal remodeling (Wenzel, et. al., 2015) (Navinés-Ferrer & Martín, 2020). Moreover, Myo1e regulates antigen presentation of macrophages by controlling the exocytosis of cytoplasmic vesicles that contain the major histocompatibility complex class II through interaction with the small GTPase Arf7 (Wenzel, et. al., 2015). Furthermore, Myo1e is recruited to the phagocytic cups of macrophages, where it is required for efficient actin remodeling and FcR-mediated phagocytosis (**Figure 15**).

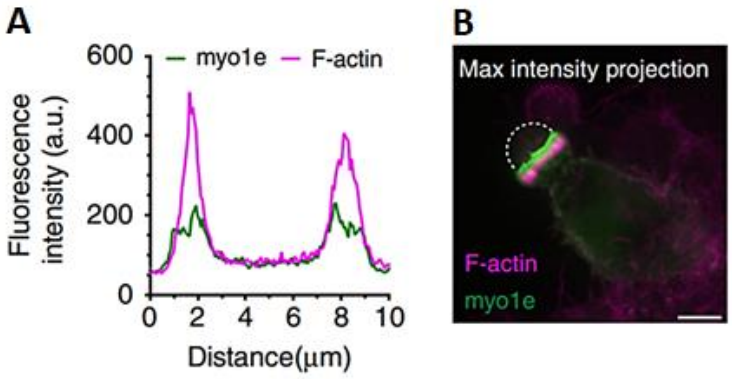

Figure 15. Myo1e is required for efficient phagocytosis. A) Fluorescence intensity of EGFP-myosin1e and F-actin along the line in B of the phagocytic cup. **B)** EGFP-myo1e-transfected RAW264.7 macrophage engulfing a 6 µm IgG-coated bead. F-actin in purple and Myo1e in green. Maximum intensity projection of EGFP-myo1e and F-actin. Dotted circle represents the IgG-coated bead (Adapted from Barger et. al., 2019).

In summary, Myo1e regulates cytoskeletal dynamics, interactions of neutrophils with EC during inflammation, and ensures efficient phagocytosis and antigen presentation in macrophages. However, it remains unknown whether Myo1e is implicated in the regulation of neutrophil effector functions. Therefore, it is important to study whether Myo1e plays a key role in functions such as phagocytosis, respiratory burst, and NET formation.

2. JUSTIFICATION

Myo1e is an ABP that connects membranes to the actin cytoskeleton and plays a role in cell migration. Although the functional domains in the myosin 1e sequence are well known, post-translational modifications that might affect the functions of Myo1e and its recruitment patterns are not well known. Furthermore, myosin 1e is expressed in neutrophils; and its absence reduces actin polymerization, chemotaxis, integrin activation and neutrophil extravasation. However, it is still unknown whether myosin 1e also plays a role in neutrophil effector functions such as phagocytosis and ROS production.

3. HYPOTHESIS

Myo1e deficiency decreases the efficiency of neutrophil effector functions.

4. GENERAL OBJETIVE

To unravel expression, secondary structure, subcellular localization and potential post-translational modifications and interactions that may affect the functions of myosin 1e through an *in-silico* analysis and to analyze the efficiency of phagocytosis and ROS production in Myo1e-deficient neutrophils.

5. SPECIFIC OBJECTIVES

1. To analyze the expression profile, post-translational modifications, interactions, and functions of myosin 1e *in-silico*
2. To investigate phagocytosis of opsonized and non-opsonized beads in WT and Myo1e-deficient neutrophils
3. To compare the production of ROS in WT and Myo1e-deficient neutrophils

6. MATERIALS AND METHODS

6.1. Databases

- The National Center for Biotechnology Information (https://www.ncbi.nlm.nih.gov/gene/4643) and Ensembl (http://www.ensembl.org/) databases were employed for gathering information on genomic regions, transcripts and products using the Gene ID 4643.
- The Myo1e amino acid sequence was obtained from the UniProt knowledge base (https://www.uniprot.org/uniprot/Q12965.fasta) with the accession number Q12965 (MYO1E_HUMAN).
- RaptorX Property server was employed to predict the secondary structure, solvent accessibility and disorder regions of the Myo1e sequence (http://raptorx.uchicago.edu/StructurePropertyPred/myjobs/54965834_610714/); and the COILS program (https://embnet.vital-it.ch/cgi-bin/COILS_form_parser) was employed for the prediction of parallel two-stranded coiled-coil conformations.
- The homology model was obtained from the Swiss-Model protein structure homology-modelling server, accessible via the Expasy web server (https://swissmodel.expasy.org/repository/uniprot/Q12965).
- Physicochemical characterization including the number of amino acids, atomic composition, amino acid composition profile, number of positively charged (Arg + Lys) and negatively charged (Asp + Glu) amino acid residues, molecular weight, estimated half-life, theoretical isoelectric point (pI), extinction coefficient, instability index, aliphatic index and Grand Average of Hydropathicity (GRAVY) value were calculated using the Expasy ProtParam and ProtScale tools (https://web.expasy.org/cgi-bin/protparam/protparam1?Q12965@1-1108@) (https://web.expasy.org/protscale/).
- Post-translational modifications including phosphorylation, acetylation, and ubiquitinylation were obtained from the PhosphoSitePlus database (https://www.phosphosite.org/proteinAction?id=8633&showAllSites=true); and

the NetPhos 3.1 server was employed for the prediction of serine, threonine or tyrosine phosphorylation sites as well as the kinases likely involved in residue phosphorylation (http://www.cbs.dtu.dk/services/NetPhos/). Using the Human Protein Reference Database PhosphoMotif Finder, the presence of potential binding motifs for protein-protein interaction was obtained (http://hprd.org/FAQ/PhosphoMotif_finder).

- Information regarding protein-protein physical and functional interactions was analyzed using the STRING Database (https://string-db.org/cgi/network?taskId=bdZL91Begamn&sessionId=b5EWiWJ5Pvl2&allnodes=1).
- The Human Protein Atlas database was employed to obtain the RNA and protein expression profile in diverse tissues, cell types and organs (https://v19.proteinatlas.org/ENSG00000157483-MYO1E/tissue). RNA expression in hematopoietic cells was obtained from the BloodSpot database (http://servers.binf.ku.dk/bloodspot/?gene=MYO1E&dataset=DMAP).

6.2. Reagents, buffers, and solutions

Table 2. Reagents, buffers, and solutions

Reagents	Trademark	Catalogue number
AlexaFluor™ 488-Phalloidin	Invitrogen™	#A12379
Dihydrorhodamine-1,2,3 (DHR-123)	Sigma-Aldrich®	#D1054
Fetal bovine serum	Biowest®	#S1810
FluoroSpheres™ carboxylate-Modified Microspheres 1.0 µm, red fluorescent (580/605)	Invitrogen™	#F8821
Gelatin	Sigma-Aldrich®	#G1393
Histopaque-1077 (1.077 g/ml)	Sigma-Aldrich®	#10771
Histopaque-1119 (1.119 g/ml)	Sigma-Aldrich®	#11191
LTB_4 (Leukotriene B_4)	Sigma-Aldrich®	#L0517
LPS-EK (Lipopolysaccharide)	Invivogen™	#tlrl-eklps
Murine IL-1β (Interleukin-1β)	PeproTech®	#AF-211-11B
PE anti-mouse Ly-6G/Ly-6C (Gr-1) Antibody	Biolegend®	# 108407
Pentobarbital sodium (100 µL) Pisabental	Pisa Agropecuaria	Q-7833-215
PFA (Paraformaldehyde)	Sigma-Aldrich®	#P6148
PMA (phorbol-12-myristate-13-acetate)	Sigma-Aldrich®	#P8139

ProLong™ Gold Antifade Mountant with DAPI	Invitrogen™	# P36935
Recombinant Human TNF-α (Tumor Necrosis Factor- α)	PeproTech®	#300-01A
RPMI-1640 Medium	SAFC®	#R4130
Trypan Blue	Gibco™	#15250061
Zymosan A *S. cerevisiae* BioParticles™, fluorescein conjugate	Invitrogen™	#Z2841
Buffers and solutions	**Composition**	
1x HBSS	8000 mg/L NaCl 400 mg/L KCl 40 mg/L Na2HPO4 60 mg/L KH2PO4 350 mg/L NaHCO3 1000 mg/L D-glucose pH 7.4	-----
1x PBS	138 mM NaCl 3 mM KCl 8.1 mM Na2HPO4 1.5 mM KH2PO4	-----
1M Hydrochloric acid	HCl	-----
Ethylenediaminetetraacetic acid (EDTA)	5mM EDTA	-----

6.3. Animals

Female Myo1e-KO mice on a C57BL/6J WT background, kindly provided by Dr. Richard Flavell (Yale School of Medicine, New Haven, CT), and C57BL/6J wild-type mice (The Jackson Laboratory, Bar Harbor, Maine, USA), were used in an age range of 8-12 weeks for all experiments. Mice were euthanized by anesthesia over-dose followed by cervical dislocation. Mice were kept under pathogen-free conditions in a barrier-type facility at CINVESTAV-IPN. All animal experiments were approved by the Institutional Animal Care and Use Committee of CINVESTAV (Mexico City, Mexico).

6.4. Neutrophil isolation

For functional assays, bone marrow neutrophils were isolated from the bone marrow of the femurs and tibias of WT and Myo1e-KO mice. This was done by aseptically removing the femurs and tibias and placing them in a sterile Eppendorf tube with 1x PBS (phosphate-buffered saline). The epiphyses were cut, and the bone marrow flushed out

by injecting 5 mL of cold 1x PBS. The cell suspension was filtered through a 40 µm nylon mesh in a falcon tube to remove bone particles or remnants. The remaining cell suspension was centrifugated at 1500 rpm for 5 minutes at 4°C, and the pellet resuspended in 3 mL cold 1x PBS.

To separate neutrophils from the rest of the cell population, the cell suspension was centrifuged in a density gradient using Histopaque 1119 and 1077 (density, 1.119 g/ml, and 1.077 g/ml, respectively; Sigma-Aldrich, Missouri, USA) 3 mL each, at 700 x g for 30 minutes at room temperature (RT) without brakes. Neutrophils were collected from the interphase between Histopaque 1119 and 1077, washed once with 1x PBS and centrifuged again at 1500 rpm for 5 minutes. Finally, the neutrophil pellet was resuspended in 5 mL 1x PBS/10% FBS (fetal bovine serum) and the number of live cells were counted in a Neubauer chamber using trypan blue. To determine the number of cells the following formula was used:

$$\textbf{\textit{cells/ µL}} = (\boldsymbol{Total\ \#\ cells\ in\ 4\ quadrants})(\boldsymbol{Dilution\ factor})(\boldsymbol{Neubauer\ correction\ factor})$$

Cells were immediately used for functional assays.

6.5. Blood collection

Peripheral blood from both WT and Myo1e-KO mice was obtained by cardiac puncture of the right heart ventricle of anaesthetized mice and collected in sterile Eppendorf tubes. To obtain serum, the blood was centrifuged at 10,000 rpm for 15 minutes at 4°C, and the supernatant was transferred into a fresh Eppendorf tube. The serum was used to opsonize zymosan particles.

6.6. Phagocytosis assay of zymosan particles

First, fresh serum obtained by cardiac puncture was used to opsonize 2 x 10^6 zymosan-fluorescein particles (Invitrogen™) per reaction. The particles were incubated with 150 µl serum or 1x PBS for 1 hour at 37°C, with shaking every 20 minutes. After this time, the particles were washed by adding 1 ml 1x PBS and centrifuged at 10,000 rpm for 5 minutes at 4°C and resuspended in 1x PBS. Then, 1x10^6 neutrophils from bone marrow were suspended in 250 µl 1x PBS per reaction in cytometry tubes. Next, 50 µl of opsonized or non-opsonized zymosan particles were added and incubated for 1 hour at

37°C to allow phagocytosis. Neutrophils were washed with cold 1x PBS to stop phagocytosis, centrifuged at 1500 rpm for 5 minutes at 4°C and fixed using 4% PFA for 20 min at RT. Subsequently, neutrophils were washed once again and resuspended in 50 µL of PE anti-mouse Ly-6G/Ly-6C (Gr-1) antibody (1:200) (Biolegend®)/per reaction for 20 minutes on ice in the dark. Finally, neutrophils were washed one more time, resuspended in 150 µl 1x PBS. The presence of zymosan particles within neutrophils was measured using a Cytoflex flow cytometer (Beckman Coulter, USA). The analysis was performed only with cells found in the granulocyte gate identified in the Gr1-PE positive dot-plot and quantifying the zymosan-fluorescein positive cells using the FlowJo Treestar V10 software.

6.7. Oxidative Burst assay

Quantification of ROS production in WT and Myo1e-KO mice over a period of 4 h was measured using DHR-123 (Sigma-Aldrich®). Neutrophils (1.5 x10^5cells/100 µL per reaction) were pre-warmed at 37°C for 10 minutes in a 96-well cell culture plate and then incubated with 1050 ng/µL DHR-123 (in 100 µL for a final concentration of 350 ng/mL) for 20 minutes at 37°C. Next, neutrophils were activated by adding 195 ng/mL PMA (Sigma-Aldrich®) per reaction (in 100 µL for a final concentration of 65 nM) to stimulate ROS production, and incubated at 37°C. After 0, 5, 10, 15, 20, 25, 30, 35, 40, 45, 50 ,55, 60, 90, 120, 150, 180, 210 and 240 minutes of stimulation, the oxidation of DHR-123 to fluorescent rhodamine-123 (R-123) was automatically measured in the microplate reader (TECAN, Switzerland). The analysis was performed with the mean fluorescence intensity minus the autofluorescence signal of untreated cells using the GraphPad PRISM Version 8.0.1 software.

7. RESULTS

7.1. Long-Tailed Myosin 1e is localized in human chromosome 15

Due to the lack of information available on biochemical and physicochemical properties, as well as regulation and modifications of Myo1e, we performed an *in-silico* analysis to gain a better understanding of possible Myo1e functions.

To analyze the gene encoding Myo1e, the National Center for Biotechnology Information and Ensembl databases were employed (**Figure 16**). In humans, this class I myosin is encoded by the *MYO1E* gene, located in the long arm of the 15th chromosome (**Figure 16A**) in the cytogenic band 22.2 (**Figure 16B**). By contrast, mouse Myo1e is encoded by the *myosinIE* gene located on chromosome 9 (**Figure 16D**). The databases yielded that the human *MYO1E* gene is encoded in the reverse strand and composed of 240,438 bases. The *MYO1E* gene contains 27 introns and 28 exons in both mouse and human, that might lead to diverse transcript variants (**Figure 16C**).

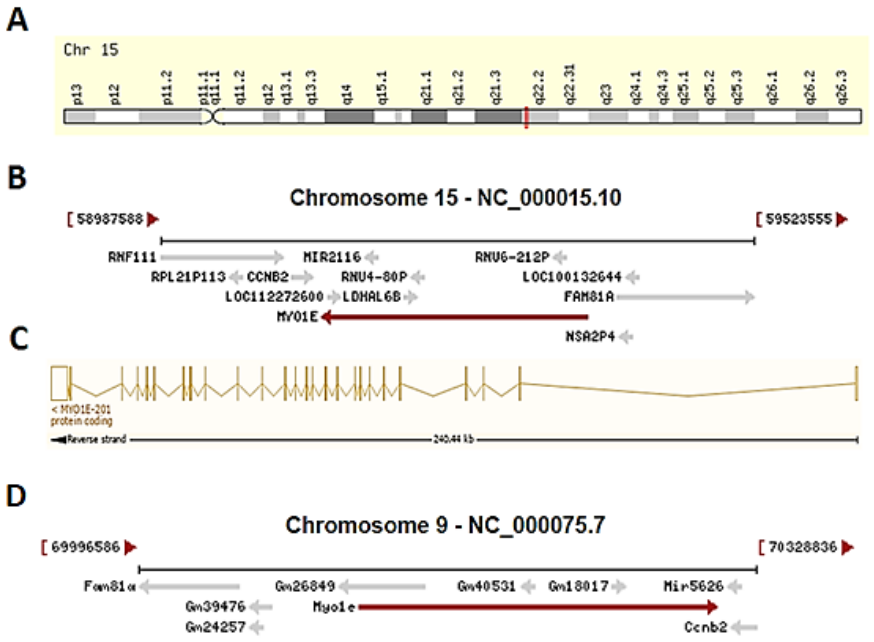

Figure 16. Human and mouse *MYO1E* gene. A) Schematic of human chromosome 15. The red line indicates the location of *MYO1E* (long arm, cytogenic band 22.2). **B)** Schematic of the gene distance range within which *MYO1E* is found. Red arrow pointing to the left represents the reverse strand where *MYO1E* is encoded. Gray arrows represent adjacent genes located either on reverse or forward strands. **C)** *MYO1E* gene. The v-shaped lines represent 27 introns, and the vertical lines represent 28 exons. Wider lines represent two to three exons adject to one another. **D)** Schematic of the gene distance range in mouse chromosome 9 within which the *myosin IE* gene is found. Red arrow pointing to the right represents the

forward strand where *myosinIE* is encoded. This information was obtained from the Ensembl and NCBI databases, http://www.ensembl.org/ and https://www.ncbi.nlm.nih.gov/gene/4643, respectively.

7.2. Myo1e undergoes alternative splicing

Given that *MYO1E* gene has 27 introns, we hypothesized that *MYO1E* may suffer alternative splicing to generate isoforms. The Ensembl database revealed that there are 10 experimentally confirmed splice variants, of which only 5 are protein-coding mRNAs (**Figure 17**). MYO1E-206 encodes for a protein of 276 residues that belong to a section of the motor domain and the complete TH1 domain, with a molecular weight of 31.4 kDa. MYO1E-207 encodes for only 73 amino acids yielding a protein of only 7.7 kDa. MYO1E-208 encodes a section of the motor domain consisting of 187 residues with a molecular weight of 21.6 kDa. MYO1E-210 encodes for 317 residues (37.2 kDa) belonging to a section of the motor domain containing the actin-binding site, and the complete IQ and TH1 domains. Finally, the complete 1,108 amino acid protein is encoded by the MYO1E-201 transcript, leading to the 127 kDa Myo1e protein (**Figure 17**). Unfortunately, using these databases, we could not find additional information on the transcriptional regulation of the *MYO1E* gene in different cell types. However, the Ensembl database showed that other *MYO1E* splice variants exist that, although not protein-coding, might have an impact on the regulation of MYO1E mRNA expression.

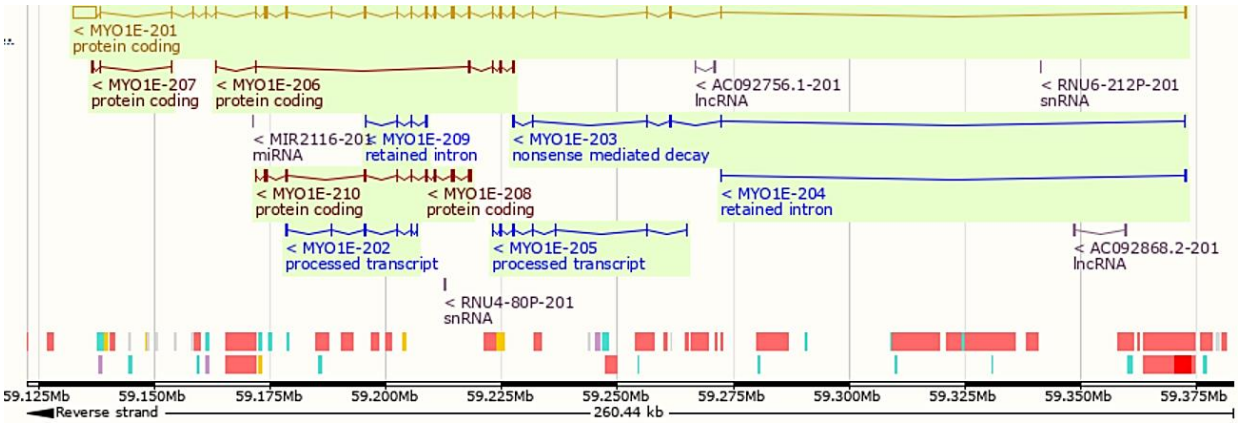

Figure 17. Splice variants of the MYO1E gene. Schematic representation of the different splice variants of *MYO1E*. Protein coding variants MYO1E-207, 206, 210 and 208 are depicted in burgundy. The primary transcript (MYO1E-201) is depicted in yellow. The noncoding RNAs, long non-coding RNAs (lncRNAs), short non-coding RNAs (snRNAs) and micro RNAs (miRNAs) are in dark gray. Other variants are depicted

in dark blue. V-shaped lines represent introns; vertical lines exons. The *MYO1E* gene is encoded by the reverse strand, therefore the order of exons and introns is read from right to left. http://www.ensembl.org/

7.3. Myo1e is a hydrophilic protein predicted to be localized in the cytoplasm, but also at the plasma membrane.

Next, we assessed the physicochemical properties of Myo1e to determine whether this protein localizes to certain subcellular compartments. Using the Expasy ProtParam and ProtScale tools, we performed a physicochemical characterization of Myo1e protein to obtain data on the number of amino acids, amino acid composition, number of positively charged (Arg + Lys) and negatively charged (Asp + Glu) amino acid residues (**Supplementary Table 1**), molecular weight, estimated half-life, theoretical isoelectric point (pI), as well as the Grand Average of Hydropathicity (GRAVY) values (**Table 3**), and Hydrophobic Kyte & Doolitle theoretical scales (**Figure 18**) (**Supplementary information note 5 and 6, respectively**). Myo1e has a higher percentage of basic amino acids (Lys + Arg) and is therefore considered a basic protein (**Table 3**). To confirm this data, we also looked at the theoretical pI, and revealed that at a neutral pH (i.e., common intracellular pH in neutrophils of approximately 7.40, Sachse et. al., 2000), Myo1e indeed has a basic pI ranging from 9.01 to 8.737 (**Supplementary Figure 2**). This suggests that, under neutral pH conditions, Myo1e can bind to acidic molecules. This agrees with the known interaction of Myo1e with actin, which is known to be an acidic protein. We then performed an analysis of the hydrophilic profile of Myo1e using the ProtScale tool. The Hydrophobic scales from Kyte & Doolittle (**Figure 18; Supplementary information note 6**) revealed that when analyzing sets of 9 or 21 residues to reveal hydrophilic and hydrophobic regions, respectively, within the protein structure, the majority of Myo1e residues had negative values, demonstrating that most of the protein has a hydrophilic character, with the majority of residues forming hydrophilic regions within the Myo1e sequence (**Figure 18**). This is in agreement with the GRAVY value of -0.571 (**Table 3**), indicating strong hydrophilicity of Myo1e. These results demonstrate that Myo1e is a hydrophilic protein that theoretically is localized in the cytoplasm and the nucleus where hydrophilicity is higher.

Table 3. *Physiochemical parameters of myosin 1e.*

Analyzed parameter	Result
Number of amino acids	1108
Molecular weight	127061.89
Total number of negatively charged residues (Asp + Glu)	132
Total number of positively charged residues (Arg + Lys)	151
Atomic composition	Carbon C 5686 Hydrogen H 8899 Nitrogen N 1571 Oxygen O 1665 Sulfur S 36
Formula	$C_{5686}H_{8899}N_{1571}O_{1665}S_{36}$
Total number of atoms	17857
Estimated half-life	The N-terminal of the sequence considered is M (Met). The estimated half-life is: 30 hours (mammalian reticulocytes, in vitro). • 20 hours (yeast, in vivo) • 10 hours (Escherichia coli, in vivo)
Instability index	The instability index (II) is computed to be 47.42 This classifies the protein as unstable
Aliphatic index	79.18
Grand average of hydropathicity (GRAVY)	-0.571

Data obtained from the Expasy ProtParam tool. https://web.expasy.org/cgi-bin/protparam/protparam1?Q12965@1-1108@.

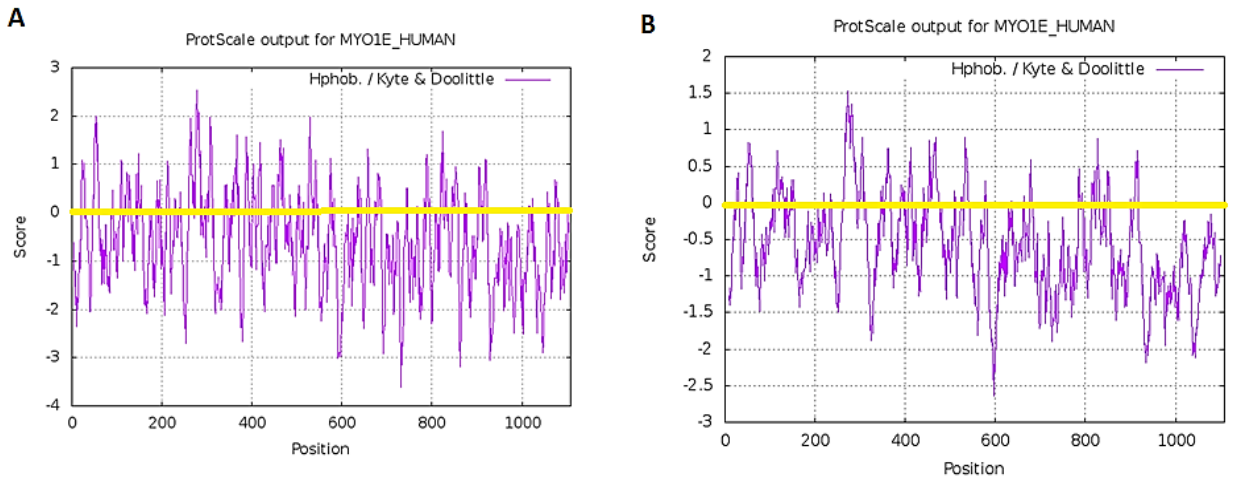

Figure 18. Hydropathic Kyte & Dolittle scales of myosin 1e. Hydrophathic scales with **A)** an interval size of 9 residues to determine hydrophilic regions and **B)** 21 residues to determine hydrophobic regions in the Myo1e sequence. Residues with negative scores (below zero indicated by the yellow line) indicate that they belong to hydrophilic regions in the structure of the protein. Position: indicates the residue analyzed within the total residues of the wild type protein. http://www.cbs.dtu.dk/cgi-bin/webface2.fcgi?jobid=6022DDA800000C1CDE8B55E2&wait=20.

Given that Myo1e has been found to also bind to hydrophobic molecular structures such as the plasma membrane and other phospholipid-rich structures such as intracellular vesicles or granules through its TH1 domain regardless of its hydrophilicity (Yamamoto, 2016), we decided to analyze the secondary structure of Myo1e to determine whether the spatial conformation contributes to its ability to bind hydrophobic structures. A crystallographic structure of human Myo1e has not yet been obtained. Thus, we conducted an *in-silico* analysis using the RaptorX Property server to predict the secondary structure of Myo1e (**Figure 19**). Overall, this server predicted that Myo1e is made up of 33% α-helixes, 16% β-sheets and 50% coiled-coiled secondary structures. Coiled-coiled structures and α-helixes have been reported to be the conformational structures needed for interactions with hydrophobic structures such as the plasma membrane (Truebestein & Leonard, 2016). Most of the coiled-coiled structures make up the tail domain of Myo1e (**Figure 19**), thus confirming that the TH domains allow Myo1e to bind membranes (Feeser et. al., 2010).

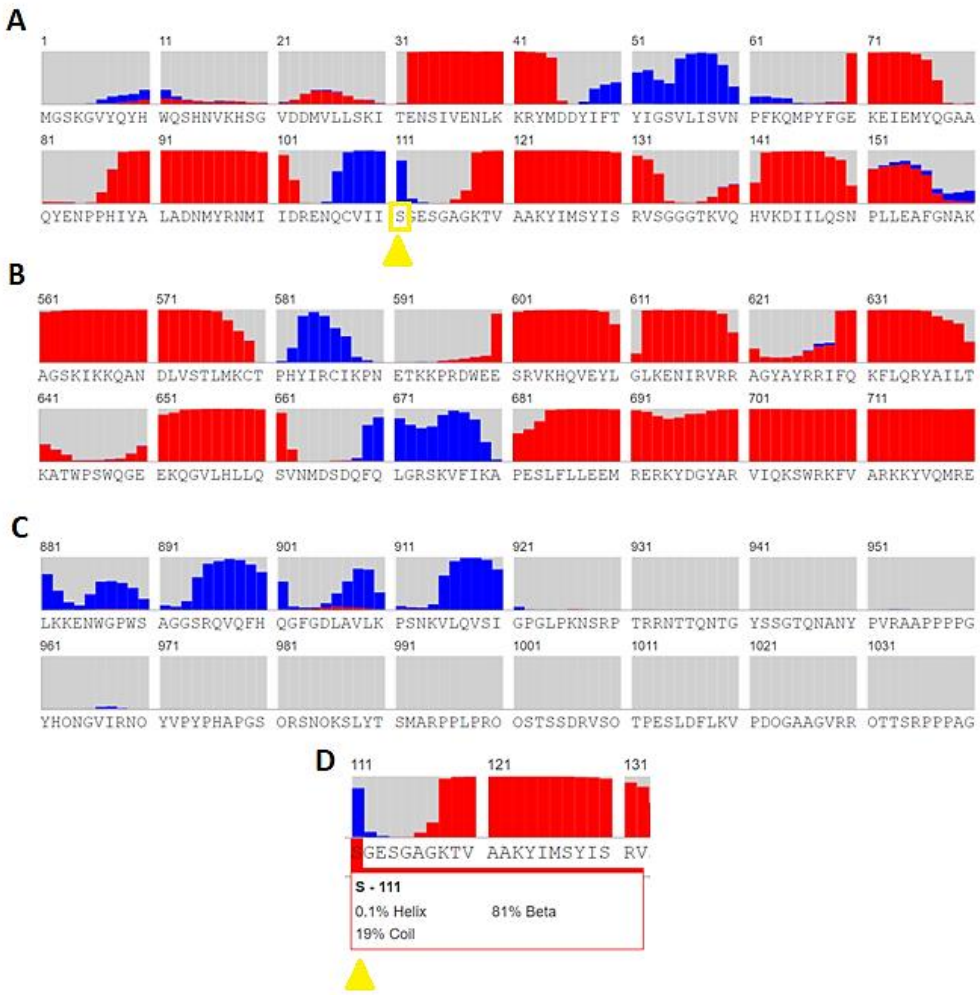

Figure 19. Predicted distribution of the secondary structure of Myo1e. Schematic representation of the predicted distribution for each residue in the Myo1e sequence. Representative residues accounting for the **A)** first section of the motor domain containing the ATP-binding site, **B)** the actin-binding site and IQ-domain and **C)** the TH2-domain. **D)** Example of how the software, by clicking on a residue, displays the predicted distribution percentage for that residue. Example of the display of the residue S111 (yellow box) from A. Arrowheads indicate the residue in the yellow box. The columns represent the percentage of each residue belonging to an α-helix (red), a β-sheet (blue) or a coiled-coiled structure (gray). Overall, myosin 1e is predicted to be comprised of 33% α-helixes, 16% β-sheets and 50% coiled-coiled secondary structures.
http://raptorx.uchicago.edu/StructurePropertyPred/myjobs/54965834_610714/.

7.4. Myosin 1e is highly phosphorylated at the tail region and functions as a scaffold protein.

Having analyzed the theoretical cellular localization of Myo1e, we then asked if modifications of the Myo1e protein could affect its localization or allow for different protein-protein interactions thus determining its localization. Using the PhosphoSitePlus

database, we identified several post-translational modifications of Myo1e including phosphorylations, acetylations, and ubiquitylations (**Figure 20; supplementary note 7**). Myo1e is phosphorylated at serine, threonine, and tyrosine residues predominantly within the TH2 domain of the tail region. The addition of phosphate groups has been reported to introduce additional negative charges to the protein that induce conformational changes, increase protein size, and modify function. According to our physicochemical analyses, the pI of Myo1e drastically drops to 4.68 when it is phosphorylated (**Supplementary Figure 2**), suggesting a change of the localization of Myo1e to compartments where it can bind to basic proteins such as those within or at the plasma membrane.

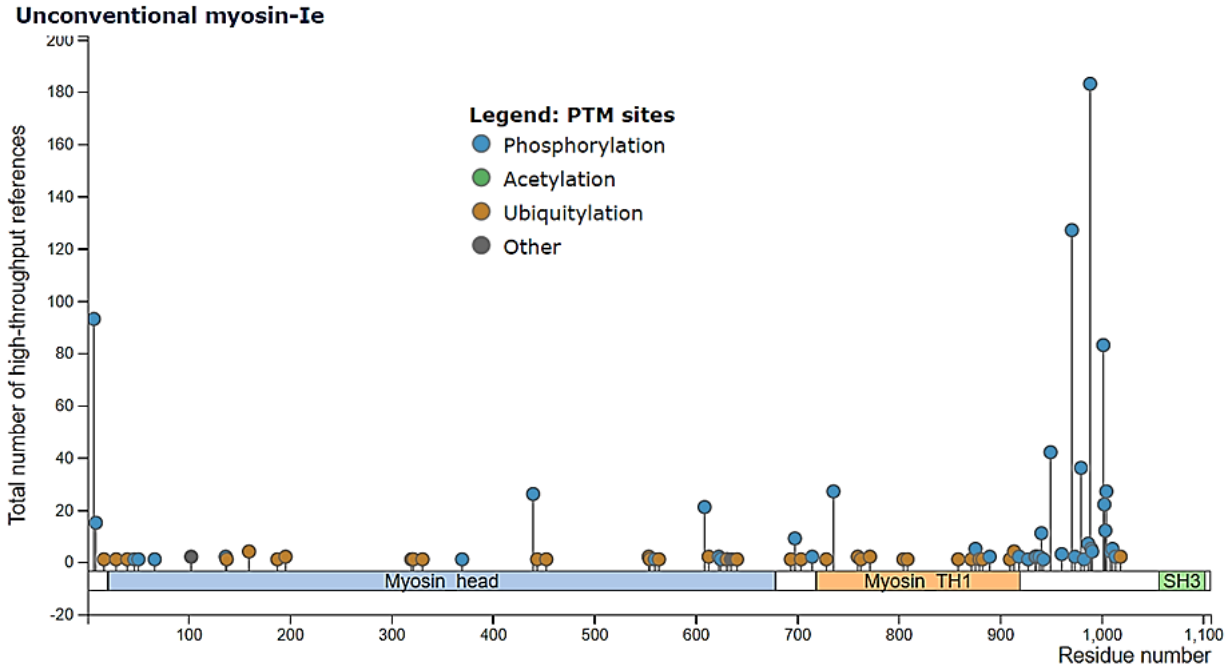

Figure 20. Post-translational modifications of myosin 1e. Graph depicting the total number of experimental references (y-axis) in which the modification sites were determined using mass spectrometry: phosphorylation (blue circles), acetylation (green circles), ubiquitylation (orange circles) and other modifications (gray circles) present in Myo1e sequence. The TH2 domain (between TH1 and SH3 domains, x-axis) contains most phosphorylations. The SH3 domain is not modified. https://www.phosphosite.org/proteinAction?id=8633&showAllSites=true.

Additionally, given that binding to the plasma membrane allows Myo1e to be in closer proximity to membrane-associated proteins, we hypothesized that phosphorylation of its residues creates new binding motifs enabling interaction with these proteins. To

confirm this hypothesis, we employed the Human Protein Reference Database PhosphoMotif Finder to find potential binding motifs within Myo1e. Indeed, we identified several binding motifs within Myo1e that include target residues for phosphorylations. **Figure 21** shows the different motifs containing phosphorylated tyrosine, serine and threonine residues and the corresponding proteins that can potentially bind to these motifs including the adaptor proteins Gab2 and Grb2, and the tyrosine kinases Syk and Btk, and PI3K (Freeman & Grinstein, 2014). These results suggest that the post-translational modifications allow Myo1e to serve as a scaffold protein with potential roles in different signaling pathways.

A

	Position in query protein	Sequence in query protein	Corresponding motif described in the literature (phosphorylated residues in red)	Features of motif described in the literature
1	9 - 12	YHWQ	pYXXQ	STAT3 SH2 domain binding motif
2	82 - 84	YEN	pY[E/M/V][N/V/I]	3BP2 SH2 domain binding motif
3	82 - 84	YEN	pYXN	Grb2 SH2 domain binding motif
4	82 - 85	YENP	pY[A/E/V][Y/F/E/S/N/V][P/F/I/H]	Itk SH2 domain binding motif
5	82 - 85	YENP	pYXXP	Crk SH2 domain binding motif
6	82 - 85	YENP	pYENP	Abl SH2 domain binding motif
7	82 - 85	YENP	pYXXP	RasGAP C-terminal SH2 domain binding motif
8	93 - 96	DNMY	D[N/D]XpY	Cbl PTB domain binding motif
9	96 - 98	YRN	pYXN	Grb2 SH2 domain binding motif
10	96 - 99	YRNM	pYXXM	PI3 Kinase p85 SH2 domain binding motif
11	211 - 216	IFYQLI	[I/V/L/S]XpYXX[L/I]	SHIP2 SH2 domain binding motif
12	235 - 238	YYYL	pY[I/E/Y/L]X[I/L/M]	SHC SH2 domain binding motif
13	237 - 240	YLSL	pY[M/I/L/V]X[M/I/L/V]	GRB2, 3BP2, Csk, Fes, Syk C-terminal SH2 domain binding motif
14	440 - 442	YFN	pYXN	Grb2 SH2 domain binding motif
15	607 - 612	VEYLGL	[I/V/L/S]XpYXX[L/I]	SHIP2 SH2 domain binding motif
16	607 - 612	VEYLGL	[I/V]XpYXX[L/V]	SHP1 SH2 domain binding motif
17	609 - 612	YLGL	pY[I/E/Y/L]X[I/L/M]	SHC SH2 domain binding motif
18	609 - 612	YLGL	pY[M/I/L/V]X[M/I/L/V]	GRB2, 3BP2, Csk, Fes, Syk C-terminal SH2 domain binding motif
19	625 - 628	YRRI	pY[R/K/H/Q/E/D][R/K/H/Q/E/D][I/P]	Src, Fyn, Lck, Fgr, Abl, Crk, Nck SH2 domain binding motif
20	698 - 701	YARV	pY[T/A/S][R/K/Q/N][M/I/V/R]	Csk SH2 domain binding motif
21	715 - 718	YVQM	pYXXM	PI3 Kinase p85 SH2 domain binding motif
22	715 - 718	YVQM	pY[M/I/L/V]X[M/I/L/V]	GRB2, 3BP2, Csk, Fes, Syk C-terminal SH2 domain binding motif
23	745 - 748	YIGM	pYXXM	PI3 Kinase p85 SH2 domain binding motif
24	745 - 748	YIGM	pY[I/E/Y/L]X[I/L/M]	SHC SH2 domain binding motif
25	745 - 748	YIGM	pY[M/I/L/V]X[M/I/L/V]	GRB2, 3BP2, Csk, Fes, Syk C-terminal SH2 domain binding motif
26	773 - 776	YDRR	pY[E/D][P/R][R/P/Q]	STAT1 SH2 domain binding motif

B

	Position in query protein	Sequence in query protein	Corresponding motif described in the literature (phosphorylated residues in red)	Features of motif described in the literature
1	167 - 169	SSR	S[pS/pT]X	MDC1 BRCT domain binding motif
2	167 - 169	SSR	S[pS/pT]X	Plk1 PBD domain binding motif
3	179 - 180	SP	[pS/pT]P	WW domain binding motif
4	436 - 437	TP	[pS/pT]P	WW domain binding motif
5	536 - 538	SSE	S[pS/pT]X	MDC1 BRCT domain binding motif
6	536 - 538	SSE	S[pS/pT]X	Plk1 PBD domain binding motif
7	574 - 576	STL	S[pS/pT]X	MDC1 BRCT domain binding motif
8	574 - 576	STL	S[pS/pT]X	Plk1 PBD domain binding motif
9	580 - 581	TP	[pS/pT]P	WW domain binding motif
10	733 - 736	RRNS	RXXpS	14-3-3 domain binding motif
11	785 - 789	LLTPK	[I/L][I/L/P]pTP[R/K]	CDC4 WD40 domain binding motif
12	787 - 788	TP	[pS/pT]P	WW domain binding motif
13	820 - 823	RILS	RXXpS	14-3-3 domain binding motif
14	827 - 829	STM	S[pS/pT]X	MDC1 BRCT domain binding motif
15	827 - 829	STM	S[pS/pT]X	Plk1 PBD domain binding motif
16	942 - 944	SSG	S[pS/pT]X	MDC1 BRCT domain binding motif
17	942 - 944	SSG	S[pS/pT]X	Plk1 PBD domain binding motif
18	999 - 1002	RQQS	RXXpS	14-3-3 domain binding motif
19	1002 - 1004	STS	S[pS/pT]X	MDC1 BRCT domain binding motif
20	1002 - 1004	STS	S[pS/pT]X	Plk1 PBD domain binding motif
21	1011 - 1012	TP	[pS/pT]P	WW domain binding motif

Figure 21. Motifs generated in myosin 1e upon tyrosine, serine and threonine phosphorylation. A) Corresponding positions of the phosphorylated tyrosine residues in the myosin 1e sequence and potential interaction partners. The yellow box highlights the motif recognized by the GAP involved in the regulation of the small GTPase Ras. Green boxes highlight interactions with adaptor proteins involved in downstream signaling events upon receptor engagement. The red box highlights the motif recognized by PI3K, a kinase involved in small GTPase activation and actin dynamics. **B)** Corresponding positions of phosphorylated serine and threonine residues in the myosin 1e sequence and potential interaction partners. http://hprd.org/FAQ/PhosphoMotif_finder.

Given that the PhosphoMotif Finder only reports the presence of theoretical motifs in the Myo1e sequence upon phosphorylation, we decided to investigate the full interactome of experimentally confirmed Myo1e interactions. To this end, we utilized the STRING Database to recover information regarding physical and functional Myo1e interactions with other proteins (**Figure 22**). As reported before (Foth et. al., 2006), and predicted by the physicochemical analysis (**Table 3**), the STRING interactome corroborated Myo1e interaction with β-actin (ACTB). Also, Myo1e functionally associates with the subunit 4 of the Arp2/3 complex (ARPC4), and the formin FNBP1 involved in WASp/WAVE recruitment, thus further highlighting the importance of Myo1e for actin dynamics. Myo1e was also found to be associated with other motor proteins such as Myosin 5c that regulates actin-based membrane trafficking, and the conventional myosins, MYH9 and MYH11 that regulate cytoskeletal remodeling, lamellipodial retraction and focal adhesions. Surprisingly, Myo1e can also interact with proteins that induce epigenetic transcriptional activation through histone modification (MOV10) and mRNA-mediated gene silencing by RISC (RNF20) via its coiled-coiled structures (**Figure 19**). These results suggest that Myo1e contributes to many cellular processes including motility, scaffolding, signaling and gene expression.

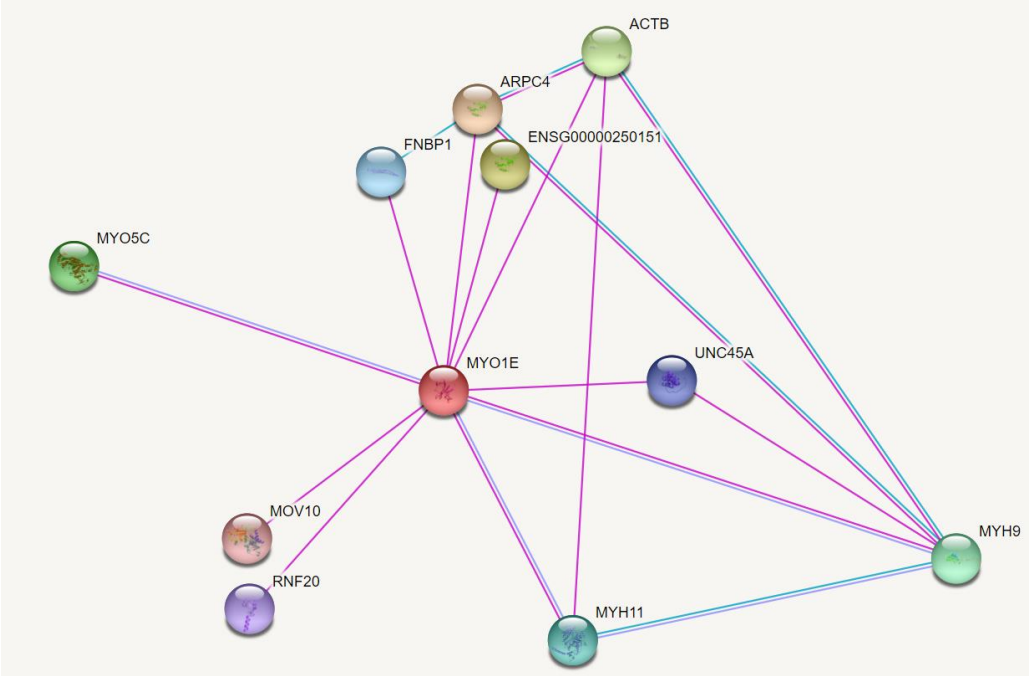

Figure 22. Protein interactions of myosin 1e. Lines represent protein-protein interactions from curated databases (blue) and experimentally confirmed ones (magenta). Colored nodes represent query proteins with direct interactions. Filled nodes include the known or predicted structures of each protein. FNBP1 (Formin-binding protein 1); ARPC4 (Actin-related protein 2/3 complex subunit 4); ACTB (Actin); MYO5C (Unconventional myosin-Vc); MYH9 (Myosin-9); MYH11 (Myosin-11); Putative helicase (MOV-10); E3 ubiquitin-protein ligase BRE1A (RNF20).
https://string-db.org/cgi/network?taskId=bdZL91Begamn&sessionId=b5EWiWJ5Pvl2&allnodes=1.

7.5. *MYO1E* expression in neutrophils increases during inflammatory diseases.

Finally, even though these results suggest that Myo1e has the potential to be involved in several cytoskeleton-related cellular functions, information on how it changes during inflammatory processes is still largely unknown. Given that Myo1e was found to be a critical regulator of neutrophil recruitment *in vivo* (Vadillo, et. al, 2019), we investigated whether Myo1e changes during inflammatory processes in neutrophils. The only data available to be analyzed in this context are those of *MYO1E* gene expression in neutrophils from arthritic mice. Of note, the expression of *MYO1E* increases in neutrophils isolated from the bone marrow and synovial fluid of arthritic mice in comparison to that of resting control neutrophils (**Figure 23**). Thus, Myo1e might be differentially expressed in neutrophils during inflammatory diseases.

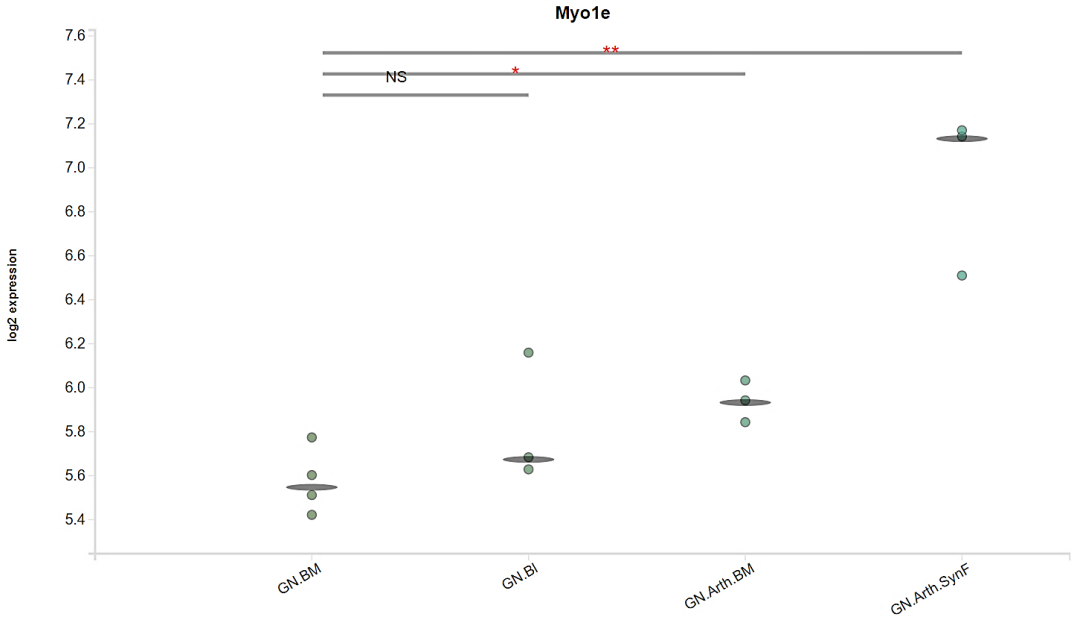

Figure 23. Expression profile of *MYO1E* in activated or resting mouse neutrophils. Expression of *MYO1E* increases in neutrophils from arthritic mice. Graph obtained from the BloodSpot database of the *MYO1E* mRNA expression in a log2 scale. The gray ovals represent the mean expression. Non-significant (NS), *p<0.01, **p< 0.001. GN.BM (bone marrow neutrophils); GN.Bl (Neutrophils from Blood); GN.Arth.BM (bone marrow neutrophils from arthritic mice); GN.Arth.SynF (neutrophils from synovial fluid of arthritic mice).
http://servers.binf.ku.dk/bloodspot/?gene=MYO1E&dataset=DMAP.

7.6. Myosin 1e is required for efficient neutrophil phagocytosis

In addition to its role in neutrophil migration, Myo1e also seems to have a critical role in neutrophils during inflammatory diseases, given that its expression increases during arthritis. Moreover, Myo1e regulates macrophage phagocytosis (Barger, et. al, 2019; Swanson et. al., 1999), but it has not yet been studied in neutrophils, although they are recognized as the most effective phagocytes (Silva & Correoia-Neves, 2012). Thus, we hypothesized that Myo1e might have an important role in neutrophil phagocytosis; and we decided to experimentally compare neutrophil phagocytosis in WT and Myo1e KO neutrophils.

Bone marrow neutrophils from WT and Myo1e-KO mice were incubated with opsonized (Op-Zym) and non-opsonized (NOp-Zym) zymosan particles to assess the efficiency of phagocytosis. To quantify the number of neutrophils that internalized zymosan particles, flow cytometry was performed. The neutrophil population was

selected from the Gr1-Phycoerithrin vs side-scatter (SSC-A) gate to ensure that the data are neutrophil-specific. Then, the percentage of neutrophils that phagocytosed zymosan particles (red fluorescence signal) was identified from the Fluorescein vs. SSC-A gate (**Figure 24A, B**). After 1 h, a mean of 11.65% WT and 10.65 % Myo1e-KO neutrophils were able to phagocytose NOp-Zym particles showing no statistical difference between the efficiency of phagocytosis in the presence or absence of Myo1e (**Figure 24C**).

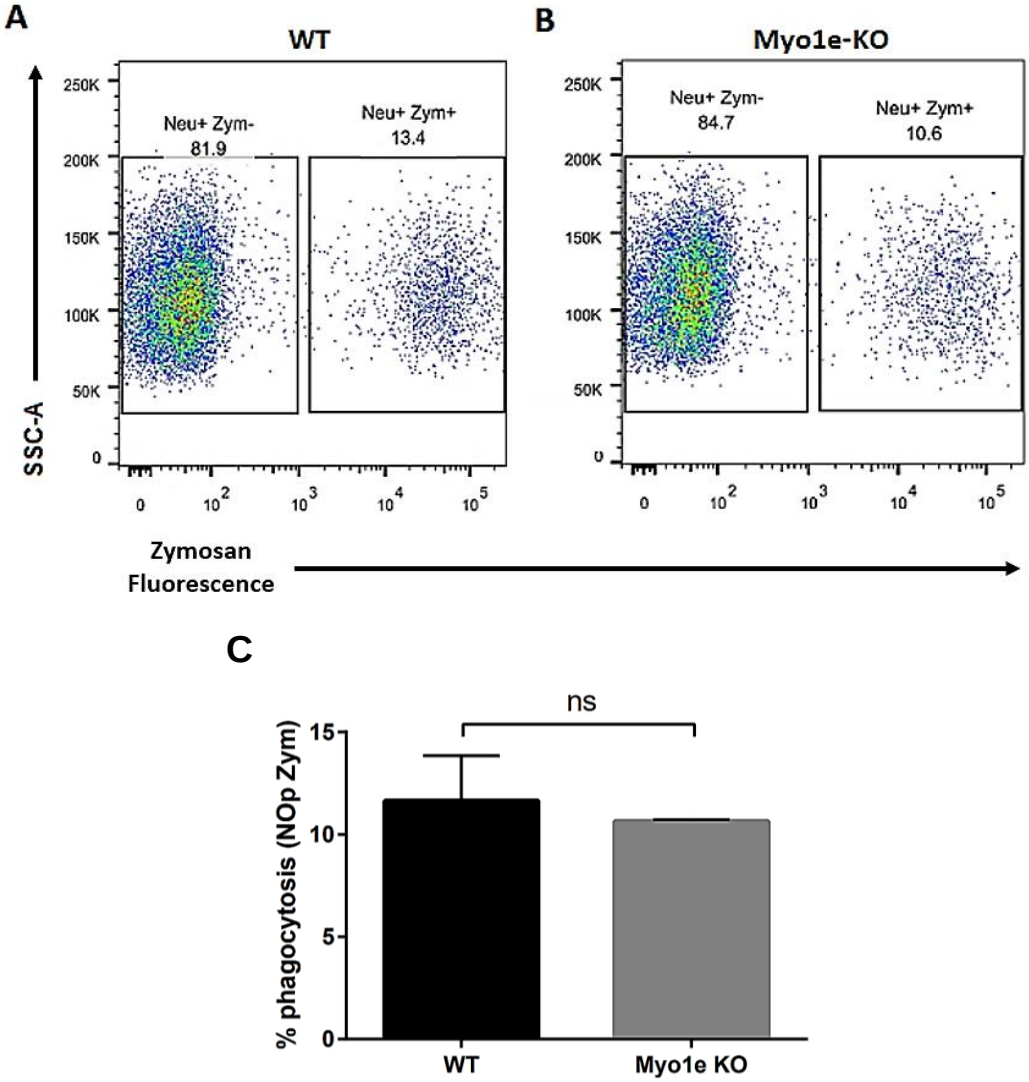

Figure 24. Absence of Myo1e does not affect phagocytosis of non-opsonized zymosan particles. Representative dot-plots of **A)** WT and **B)** Myo1e-KO neutrophils incubated with $2x10^6$ non-opsonized zymosan particles (around 20 zymosan particles per neutrophil) at 37°C for 1 hour to stimulate phagocytosis. The left square shows neutrophils negative for the zymosan particle fluorescein signal (Neu+, Zym-). The right square shows neutrophils that phagocytosed non-opsonized zymosan particles (Neu+, Zym+). **C)** Quantification of the percentage of WT and Myo1e-KO neutrophils that phagocytosed non-opsonized zymosan particles after 1 hour. Data are represented as mean ± SD (WT n= 2 mice in triplicate

and Myo1e-KO n=1 mouse in triplicate), ns, non-significant. Side scatter (SSC-A), Zymosan-Fluorescein signal (Comp-FITC-A), non-opsonized zymosan particles (NOp Zym), myosin 1e deficient neutrophils (Myo1e-KO).

The percentage of phagocytic Myo1e-KO neutrophils significantly increased when co-incubated with Op-Zym in both WT and KO neutrophils. Of note, the percentage of Myo1e-KO neutrophils that phagocytosed Op-Zym in comparison to that of WT neutrophils was significantly lower (**Figure 25A and B**). While 60% of all WT neutrophils phagocytosed Op-Zym particles, only 37% Myo1e-KO neutrophils phagocytosed Op-Zym particles (**Figure 25C**). These data suggest that Myo1e deficiency decreases the efficiency of receptor-dependent phagocytosis in neutrophils.

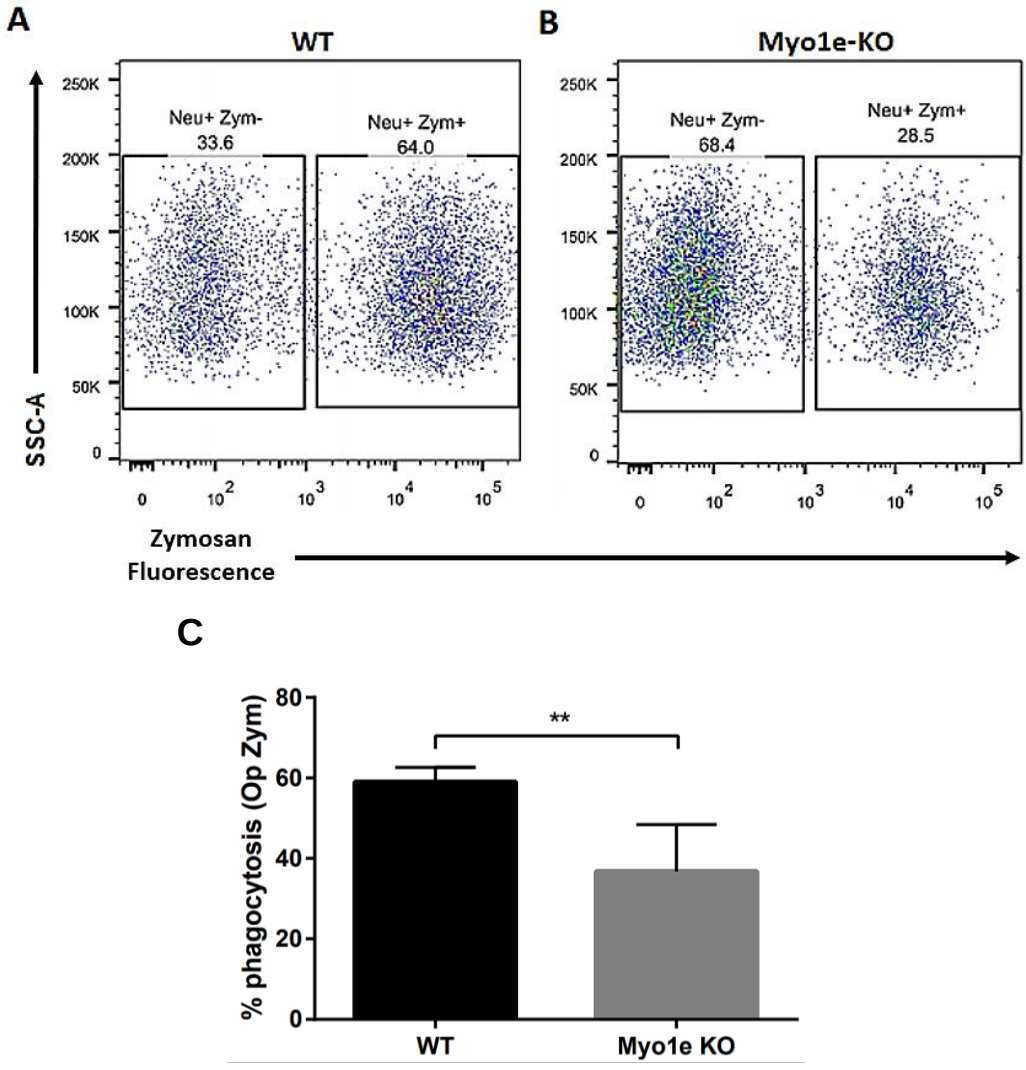

Figure 25. Myo1e is required for efficient neutrophil phagocytosis of opsonized zymosan particles. Representative dot-plots of **A)** WT and **B)** Myo1e-KO neutrophils were incubated with $2x10^6$ non-opsonized zymosan particles (around 20 zymosan particles per neutrophil) at 37°C for 1 hour to stimulate

phagocytosis. The left square shows neutrophils negative for the zymosan particle fluorescein signal (Neu+, Zym-). The right square shows neutrophils that phagocytosed opsonized zymosan particles (Neu+, Zym+). **C)** Quantification of the percentage of WT and Myo1e-KO neutrophils that phagocytosed opsonized zymosan particles after 1 hour. Data are represented as mean ± SD (WT n= 2 mice in triplicate and Myo1e-KO n=1 mouse in triplicate), **p<0.001. Side scatter (SSC-A), Zymosan-Fluorescein signal (Comp-FITC-A), opsonized zymosan particles (Op Zym), myosin-1e-deficient neutrophils (Myo1e-KO).

7.7. Myo1e is required for efficient ROS production during PMA-stimulation

Given that the *in-silico* analysis demonstrated that Myo1e might serve as a scaffold protein for kinases involved in the activation of the NADPH oxidase complex, and the fact that Myo1e is involved in Rac1 activation, an essential component for the function of this complex (Girón-Perez, et. al., 2020), we evaluated whether ROS production is affected in the absence of Myo1e. To assess the production of ROS, bone marrow neutrophils from WT and Myo1e-KO mice were incubated in 96-well plates with the non-fluorescent DHR-123 probe and then activated by the addition of PMA to stimulate ROS production for up to 4 hours. The production of ROS was quantified by measuring the amount of fluorescence intensity emitted by rhodamine (R-123) produced by oxidation of DHR-123 using an automated microplate reader.

We observed similar low basal levels of ROS in both WT and KO neutrophils. Stimulation with PMA induced high fluorescence intensity in WT neutrophils and the absence of Myo1e caused a significant reduction in ROS production (**Figure 26**). ROS production increased significantly over 4 h in WT neutrophils, and the reduction of ROS production in Myo1e KO neutrophils was consistent over time. These results suggest that the absence of Myo1e reduces ROS production in neutrophils stimulated with PMA.

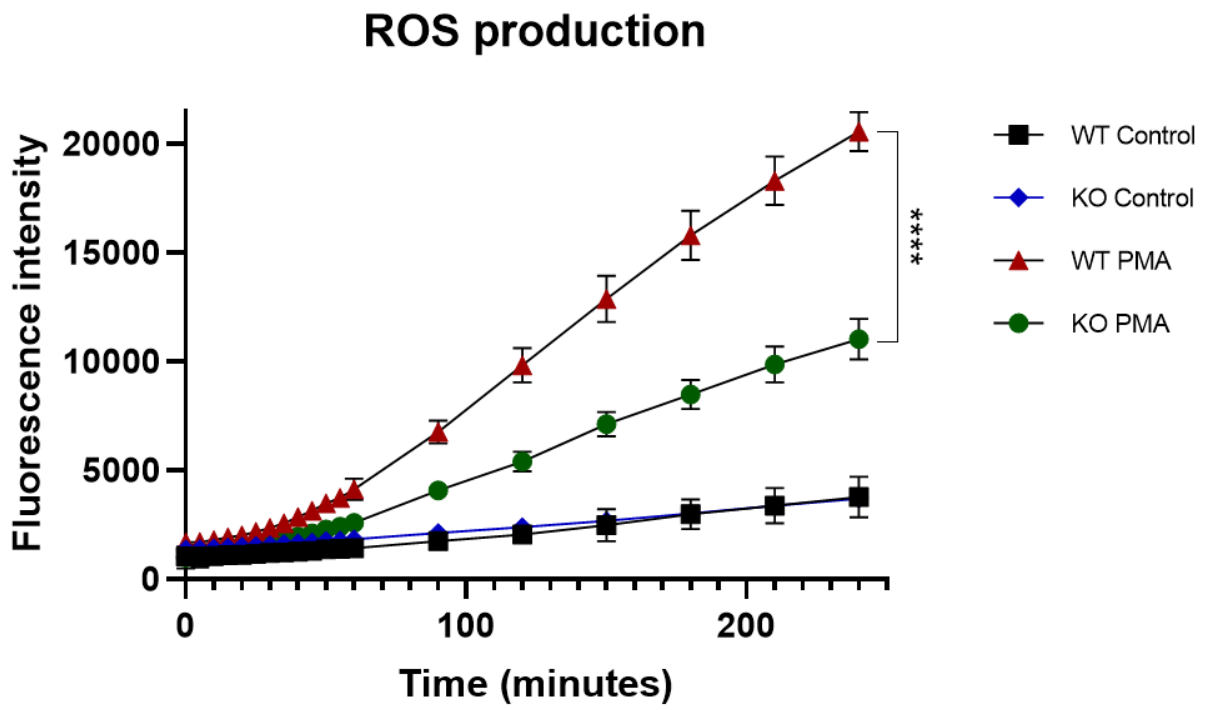

Figure 26. Absence of Myo1e reduces ROS production in neutrophils after PMA stimulation. WT and Myo1e-KO neutrophils were stimulated with 65 ng/ml PMA in 96-well microplates and ROS production was measured in a microplate reader at the indicated times (TECAN). Data represented as mean ± SD (n=1 mouse each in triplicate), ****p < 0.0001.

8. DISCUSSION

In this study, we performed *in-silico* analyses to analyze the physicochemical properties of Myo1e and found that the long-tailed Myo1e motor protein is a hydrophilic protein that can be localized in the cytoplasm, the nucleus, and at the plasma membrane. Depending on the cellular functional requirements, Myo1e gets phosphorylated to create binding motifs for proteins involved in signaling pathways such as MAPKs and small GTPases. Moreover, the expression of the *MYO1E* gene increases during arthritis in neutrophils. Experimental studies revealed that in the absence of Myo1e, the efficiency of opsonic receptor-mediated phagocytosis and ROS production in neutrophils significantly decreases, likely due to its functions as modulator of actin-cytoskeleton dynamics and actin-membrane interactions. Thus, we provide here first evidence that Myo1e is an essential long-tailed class I myosin needed for efficient neutrophil effector functions.

To better understand how Myo1e could affect neutrophil effector functions, we analyzed Myo1e at a physicochemical, biochemical, and functional level. It appears that long-tailed Myo1e is a motor protein mainly localized in the cytoplasm and the nucleus where hydrophilicity is higher (**Figure 18**). This localization is dependent on its basic amino acids, which determine its ability to bind to acidic molecules such as actin in neutral pH environments (Kalhammer & Bähler, 2000). These physicochemical characteristics add to the potential spatial regulation of the mechanochemical functions of Myo1e in a way that the hydrophilicity might regulate the compartmentalized localization in the cytoplasm, in order to establish proximity to actin and allow for efficient actin-cytoskeleton dynamics. Moreover, the nucleus is also a subcellular compartment with high hydrophilicity making it another suitable subcellular compartment for Myo1e localization. This idea is supported by previous reports showing that other unconventional myosins such as myosin-5a, myosin-6, myosin-16 and myosin-1c are present in the nucleus (Cameron et al., 2007; Philimonenko et al., 2004; Pranchevicius et al., 2008; Vreugde et al., 2006; Ye et al., 2008). This potential nuclear localization of Myo1e suggest its role in other cellular functions such as transcriptional regulation.

Other unconventional class-I myosins such as Myo1g and Myo1c have been reported to localize to the plasma membrane (Patino-Lopez et. al., 2010), and Myo1e is no exception despite its hydrophilic properties. It has been demonstrated that the ancient divergent Pleckstrin Homology (PH) domain embedded in the TH1 region helps short-tailed class-I myosins localize to plasma membranes (Lu et. al., 2015; Patino-Lopez et. al., 2010). Long-tailed Myo1e additionally contains two extra tail TH domains composed of coiled-coiled structures and α-helixes. These conformational structures have been reported to be essential for the interaction with hydrophobic structures such as the plasma membrane (Truebestein & Leonard, 2016). Therefore, even though Myo1e is a hydrophilic protein, it can bind membranes through the spatial conformations within its tail domain. This agrees with the finding that in podosomes, Myo1e is enriched at the membrane through interactions with PI(3,4,5)P3 via its TH1 and TH2 domains (Zhang et. al., 2019).

The finding that *MYO1E* has at least 10 different splice variants varying in its domain structure, could potentially be a way for cells to regulate the localization of Myo1e protein isoforms to different subcellular locations, and to regulate different functions of Myo1e depending on the cellular demands. For example, another class-I myosin, Myo1b, is alternatively spliced within its neck region during development in various tissues, yielding proteins with six (myo1b^{a}), five (myo1b^{b}), or four (myo1b^{c}) calmodulin-binding IQ motifs (Laakso et. al., 2010). Given that this region is a key mechanical component during force production as it acts as the lever arm, the difference in lengths of the lever arm was related to the magnitude of tension sensitivity during force-sensing and therefore affecting their motile properties in response to changes in cellular tension (Laakso et. al., 2010). Moreover, a nuclear isoform of myosin 1c that co-localized with RNA polymerase II in an α- amanitin and andactinomycin D sensitive manner, potentially regulates transcription (Pestic-Dragovich et. al, 2000). These studies clearly support the idea that *MYO1E* splice variants could perform crucial yet unknown cellular functions in various types of cells including neutrophils.

Myo1e suffers post-translational modifications as has been shown for other myosins (Heissler & Sellers, 2017). Phosphorylation is one of the most prominent forms of post-

translational modification as it is a covalent but reversible allosteric regulatory mechanism for many proteins. In the case of Myo1e, phosphorylation predominantly occurs at residues within theTH2 and TH1 domains suggesting that these phosphorylations play a role in the binding of Myo1e to the plasma membrane. These phosphorylations might allow Myo1e to come into close proximity with plasma-associated proteins involved in signaling pathways that activate kinases such as FAK and PI3K, that may further modify Myo1e to regulate its functions at the plasma membrane (Heissler & Sellers, 2017). One of the consequences of the introduction of negative charges to the side chain of serine, threonine, and tyrosine residues in Myo1e, is a decrease of its pI and a change in spatial conformation that might lead to changes in the cellular recruitment patterns of Myo1e according to cellular demands. This idea is supported by studies of phosphorylation of TEDS (T:Thr, E:Glu, D:Asp or S:Ser) sites within the myosin motor domain by STE20 family kinases, which are located at the solvent exposed surface-loop near the ATP-binding domain and the highly conserved DALAK sequence (Bement et. al., 1995) that are required for the localization of Myo1 proteins to actin patches at the plasma membrane to regulate endocytosis in fission yeast (Attanapola et. al., 2009). In this case, these phosphorylations increase actin affinity and motor activity. However, even though Myo1e contains a glutamine residue 16 residues above its DALAK sequence corresponding to the TEDS-site (**Supplementary Figure 1**), it does not seem to be phosphorylated at this residue (**Figure 21**), because in vertebrate class-I myosins, where the presence of an already negatively charged amino acid at the TEDS-site has been shown to overcome the requirement of phosphorylation to induce ATPase activity (Bement et. al., 1995). This could also explain why the majority of phosphorylations of Myo1e seem to be restricted to the tail region. Changes in subcellular localization of Myo1e upon post-translational modifications could be possible, as has been the case for Myo5a, where upon phosphorylation of its Ser1650, Myo5a is redistributed to nucleoli during inhibition of transcription (Pranchevicius et. al., 2008). Although, nothing is known about functional or localization changes upon modification of Myo1e, the motifs identified upon residue phosphorylation may shed light on potential signaling pathways in which Myo1e might be involved. For example, proteins involved in the activation of small GTPases can recognize these tyrosine-phosphorylated motifs in Myo1e. Of note, some

of these motifs are recognized by proteins involved in FcR-mediated phagocytosis in macrophages and neutrophils such as the kinases Syk and PI3K, and adapter proteins such as NcK, Gab2, and Grb2 (Freeman & Grinstein, 2014). Moreover, Myo1e carries motifs recognized by Rac1 GEFs that may contribute to actin-cytoskeleton regulation (Spieering & Hodgson, 2011). Thus, phosphorylations of Myo1e are likely important for the scaffolding functions of Myo1e and for Myo1e contributions to signaling pathways activated by surface receptors leading to changes in actin cytoskeleton dynamics important for leukocyte effector functions.

Unfortunately, no information is available about the possible functions of other putative modifications of Myo1e including acetylations and ubiquitinations. However, given the known functional consequences of these modifications from other proteins, i.e. actin affinity regulation in the case of acetylations and proteasomal degradation in the case of ubiquitinations, it is tempting to speculate that actin affinity and cellular protein levels of Myo1e are also regulated by these modifications (Aksnes et. al., 2018).

Further protein-protein interaction analyses corroborated that Myo1e interacts with β-actin. Of note, these analyses also revealed that Myo1e interacts with the subunit 4 (ARPC4) of the Arp2/3 complex and with other actin-related proteins such as the Formin-binding protein 1 (FNBP1). Through these interactions Myo1e may control the formation of Arp2/3-dependent formation of branched actin networks and the reorganization of the actin cytoskeleton during the late stage of clathrin-mediated endocytosis regulated by FNBP1 (Kamioka et. al., 2004). Myo1e also associates with other myosins including Myo5c, Myo9 (MYH9) and Myo11 (MYH11), which are involved in cytokinesis, cell polarization, exocytosis, actin capping, cytoskeletal reorganization during cell spreading, focal adhesions and lamellipodial retraction, and vesicle trafficking (Betapudi V., 2010). These types of interactions between conventional and unconventional myosins have been reported to be required for coordinated actin remodeling during endocytosis (Yu & Bement, 2007). However, the most surprising and hitherto unknown finding was the association of Myo1e with two nucleus-related proteins, the putative helicase MOV-10 and the E3 ubiquitin-protein ligase BRE1A (RNF20). These data further support the possible location of Myo1e in the nucleus, where it associates with MOV-10 and RNF20

through the coiled-coiled structures to regulate monoubiquitination of histone H2B, thereby modulating gene regulation (Zhu et. al., 2005). On the other hand, MOV10, has been reported to be required for miRNA-mediated gene silencing via the RNA-induced silencing complex (RISC) (Kenny et. al., 2014). Thus, Myo1e might be recruited to the nucleus under certain, yet to be identified conditions, to support epigenetic and transcriptional regulation. These findings suggest that Myo1e has more potential functions in addition to regulating actin-cytoskeleton dynamics and membrane-actin interactions.

Our group has recently demonstrated Myo1e expression in neutrophils and its role in neutrophil extravasation (Vadillo et. al. 2019), and together with the observed increased expression of the *MYO1E* gene in neutrophils from arthritic mice, it is tempting to speculate that Myo1e is essential for neutrophil functions during inflammation. TNF-α is one of the most prominent cytokines governing arthritis (Farrugia & Baron, 2016) and neutrophils contribute to RA physiopathology (Cascão et. al., 2010), implicating that the engagement of TNF receptors (TNFR1/TNFR2) on neutrophils drive the increase in *MYO1E* expression. This is true for osteoclasts, in which the expression of *MYO1E* increases upon RANKL binding to the RANK receptor (a TNF family receptor) to trigger osteoclast differentiation (Nakamura et. al., 2020). Whether the inflammatory increase in *MYO1E* gene expression coincides with Myo1e protein levels in neutrophils is still unknown and will be investigated in future studies. Moreover, it will be interesting to analyze if different protein levels during inflammation would depend on transcriptional, translational, or post-translational modifications.

Given that neutrophils are recognized as the most effective phagocytes (Silva & Correoia-Neves, 2012) and the role of Myo1e for phagocytosis and cellular migration has so far only been evaluated in other immune cells such as macrophages (Wenzel et. al., 2015) and B lymphocytes (Girón-Pérez et. al., 2020), respectively, we analyzed whether the role of Myo1e is also crucial for phagocytosis in neutrophils. We found that Myo1e is only essential for receptor-mediated phagocytosis in neutrophils. It is likely that the opsonized zymosan particles might resemble the complement factors (Medicus et. al., 1983), and thus bind to the CR3/Mac-1 receptor, a β2-integrin that is the primary receptor

responsible for the recognition of C3b and iC3b opsonic factors and that is abundantly expressed in neutrophils (Rosetti & Mayadas, 2016). Our results therefore suggest that in the absence of Myo1e, β2 integrin-mediated phagocytosis is affected. Barger and colleagues (2019) did not see a significant reduction in phagocytosis efficiency in the absence of Myo1e, but only when both Myo1f and Myo1e were deleted. However, it is important to highlight that this deficiency was seen during FcR-mediated phagocytosis and not β2-integrin-mediated phagocytosis (Barger, et. al, 2019; Swanson et. al., 1999), which may explain the different results in neutrophils as integrin clustering is also significantly reduced in Myo1e-deficient neutrophils (Vadillo, et al., 2019). This clustering defect may also affect downstream signaling. Integrin clusters have been reported to promote the auto-phosphorylation of FAK (Calalb et. al., 1996); and Myo1e interacts with phosphorylated FAK in activated B-lymphocytes suggesting that Myo1e regulates also integrin-dependent signaling (Girón-Pérez et al., 2020). In addition, PI3K is involved in FAK-mediated signaling and known to contribute to β2-integrin activation in B-lymphocytes (Girón-Pérez et al., 2020) and neutrophils (Gambardella et. al., 2013). Given that phosphorylation of tyrosine residues in Myo1e permit PI3K binding, it is reasonable to think that Myo1e is involved in PI3K-dependent inside-out signaling leading to full integrin activation. Moreover, Myo1e-deficient B cells showed decreased adhesion to ICAM-1, fibronectin, and hyaluronic acid, due to reduced expression of the β2-integrin LFA-1 and the β1-integrin VLA-4 (Girón-Pérez et al., 2020). Thus, integrin functions and integrin-dependent signaling need to be analyzed in more details in Myo1e-KO neutrophils as integrins mediate many critical neutrophil functions.

Finally, following internalization of a phagocytosis target, the phagocytic vacuole becomes a mature phagosome, characterized by the integration of the NADPH oxidase complex into its membrane allowing the neutrophils the production of ROS. Here, we show for the first time that Myo1e is required for effective ROS production. In future studies, we will study the exact mechanisms by which Myo1e supports ROS production. A possibility is that Myo1e might bind PI3K through binding motifs generated upon tyrosine phosphorylation to support PI3K activity during NADPH oxidase activation, as it has been shown that neutrophils treated with PI3K inhibitors fail to produce ROS (Fumagalli et. al.,2013). Another mechanism could be that the absence of Myo1e impairs

the activation of FAK, PI3K, and Rac1/2, which in turn is critical for NADPH oxidase assembly, thus negatively affecting ROS production. One could envision that by directly interacting with FAK and/or PI3K, Myo1e might serve as a scaffold protein to orchestrate the molecular machinery required to activate Rac1 to allow assembly of the NADPH oxidase and effective ROS production in neutrophils.

In summary, we could demonstrate that the absence of Myo1e reduces the efficiency of phagocytosis and PMA-mediated ROS production, suggesting that Myo1e plays an important role in neutrophil effector functions. We will use other stimuli such as TNF-α, LPS and LTB_4 to prove general effects on ROS production in different contexts. It will also be important to analyze whether production of NETs is also reduced in the absence of Myo1e. However, its potential localization in the nucleus suggests possible functions in histone decondensation and NET formation. In the near future, we seek to elucidate the signaling pathways through which Myo1e controls neutrophil effector functions; and whether Myo1e-deficient mice are more susceptible infectious or inflammatory diseases that depend on efficient neutrophil effector functions for inflammation resolution.

9. REFERENCES

1. Abram CL, Lowell CA. (2009). The ins and outs of leukocyte integrin signaling. Annu Rev Immunol. 27: 339–362.
2. Aksnes H, Marie M, Arnesen T, Drazic A. (2018). Actin polymerization and cell motility are affected by NAA80-mediated posttranslational N-terminal acetylation of actin. Commun Integr Biol. 11(4): e1526572.
3. Allen, L. A. and Aderem, A. (1996). Molecular definition of distinct cytoskeletal structures involved in complement- and Fc receptor-mediated phagocytosis in macrophages. J. Exp. Med. 184: 627-637.
4. Attanapola SL, Alexander CJ, Mulvihill DP. (2009). Ste20-kinase-dependent TEDS-site phosphorylation modulates the dynamic localisation and endocytic function of the fission yeast class I myosin, Myo1. J Cell Sci. 122:3856–3861.
5. Barger, S.R.; Reilly, N.S.; Shutova, M.S.; Li, Q.; Maiuri, P.; Heddleston, J.M.; Mooseker, M.S.; Flavell, R.A.; Svitkina, T.; Oakes, P.W.; et al. (2019). Membrane cytoskeletal crosstalk mediated by myosin-I regulates adhesion turnover during phagocytosis. Nat. Commun. 10:1249
6. Batters, C.; Veigel, C. (2016). Mechanics and Activation of Unconventional Myosins. Traffic. 17:860–871.
7. Bear JE, Gertler FB. (2009). Ena/VASP: towards resolving a pointed controversy at the barbed end. J Cell Sci. 122:1947–1953.
8. Bement WM, Mooseker MS. (1995). TEDS rule: a molecular rationale for differential regulation of myosins by phosphorylation of the heavy chain head. Cell Motil Cytoskeleton. 31:87–92.
9. Benarafa C, Simon HU. (2017). Role of granule proteases in the life and death of neutrophils. Biochem Biophys Res Commun. 482: 473–481.
10. Berg, J. S., Powell, B. C., Cheney, R. E. (2001). A millennial myosin census. Mol. Biol. Cell. 12:780–794.
11. Berton, G., Laudanna, C., Sorio, C., and Rossi, F. (1992). Generation of signals activating neutrophil functions by leukocyte integrins: LFA-1 and gp150/95, but not CR3, are able to stimulate the respiratory burst of human neutrophils. *J. Cell Biol.* 116:1007–1017.
12. Betapudi V. (2010). Myosin II motor proteins with different functions determine the fate of lamellipodia extension during cell spreading. PLoS One. 5(1):e8560.
13. Birch, K. A., Ewenstein, B. M., Golan, D. E. & Pober, J. S. (1994). Prolonged peak elevations in cytoplasmic free calcium ions, derived from intracellular stores, correlate with the extent of thrombin-stimulated exocytosis in single human umbilical vein endothelial cells. J. Cell. Physiol. 160: 545–554.
14. Boras, M. et al. (2017). Skap2 is required for β2 integrin-mediated neutrophil recruitment and functions. J. Exp. Med. 214:851–874.

15. Borregaard, N.; Christensen, L.; Bejerrum, O. W.; Birgens, H. S.; Clemmensen, I. (1990). Identification of a highly mobilizable subset of human neutrophil intracellular vesicles that contains tetranectin and latent alkaline phosphatase. J. Clin. Invest. 85: 408–416.
16. Brandau, S. et al. (2010). Tissue-resident mesenchymal stem cells attract peripheral blood neutrophils and enhance their inflammatory activity in response to microbial challenge. J. Leukoc. Biol. 88:1005–1015.
17. Brinkmann V, Reichard U, Goosmann C, Fauler B, Uhlemann Y, et al. (2004). Neutrophil extracellular traps kill bacteria. Science. 303:1532–35.
18. Broermann, A., Winderlich, M., Block, H., Frye, M., Rossaint, J., Zarbock, A., Cagna, G., Linnepe, R., Schulte, D., Nottebaum, A.F., and Vestweber, D. (2011). Dissociation of VE-PTP from VE-cadherin is required for leukocyte extravasation and for VEGF-induced vascular permeability in vivo. J. Exp. Med. 208: 2393–2401.
19. Burns AR, Bowden RA, MacDonell SD, Walker DC, Odebunmi TO, Donnachie EM, Simon SI, Entman ML, and Smith CW. (2000). Analysis of tight junctions during neutrophil transendothelial migration. J Cell Sci 113: 45–57.
20. Burgoyne RD, Morgan A. (2003). Secretory granule exocytosis. Physiol Rev. 83: 581–632.
21. Calalb MB, Zhang X, Polte TR, Hanks SK. (1996). Focal adhesion kinase tyrosine-861 is a major site of phosphorylation by Src. Biochem Biophys Res Commun. 228(3):662-8.
22. Cameron, R.S. et al. (2007). Myosin16b: The COOH-tail region directs localization to the nucleus and overexpression delays S-phase progression. Cell Motil. Cytoskeleton. 64:19–48.
23. Cascão R, Rosário HS, Souto-Carneiro MM, Fonseca JE. (2010). Neutrophils in rheumatoid arthritis: More than simple final effectors. Autoimmun Rev. 9(8):531-5.
24. Chen, L., et. al. (2018). Inflammatory responses and inflammation-associated diseases in organs. Oncotarget. 9(6): 7204-7218.
25. Chen, Y., Junger, W.G. (2012). Measurement of Oxidative Burst in Neutrophils. Methods Mol Biol. 844: 115–124.
26. Choi KY, Chow LN, Mookherjee N. (2012). Cationic host defense peptides: multifaceted role in immune modulation and inflammation. J. Innate Immun. 4:361–70.
27. Clark SR, Ma AC, Tavener SA, McDonald B, Goodarzi Z, Kelly MM., et. al. (2007). Platelet TLR4 activates neutrophil extracellular traps to ensnare bacteria in septic blood. Nat Med.13:463–469.
28. Colucci-Guyon, E., Niedergang, F., Wallar, B. J., Peng, J., Alberts, A. S. and Chavrier, P. (2005). A role for mammalian diaphanous-related formins in complement receptor (CR3)-mediated phagocytosis in macrophages. Curr. Biol. 15:2007-2012.

29. Coluccio, L. M., Mooseker, M. S., Foth, B. J. (2008). The structural and functional diversity of the myosin family of actin-based molecular motors. In Myosins, Springer. 7: 1–34.
30. Costantini, C. et al. (2011). Human neutrophils interact with both 6-sulfo LacNAc+ DC and NK cells to amplify NK-derived IFNγ: role of CD18, ICAM-1, and ICAM-3. Blood. 117: 1677–1686
31. Dambuza, I.M., and Brown, G.D. (2015). C-type lectins in immunity: recent developments. Curr. Opin. Immunol. 32: 21–27.
32. de Bruyn, P. P. H. (1946). The amoeboid movement of the mammalian leukocyte in tissue culture. Anat. Rec. 95:117–192.
33. Davidson, P. M & Cadot, B. (2021). Actin on and around the Nucleus. Trends in Cell Biol. 31(3): 211-223.
34. Dippold HC, NgMM, Farber-Katz SE, Lee SK, KerrML, et al. (2009). GOLPH3 bridges phosphatidylinositol4-phosphate and actomyosin to stretch and shape the Golgi to promote budding. Cell 139:337–51.
35. Duppuy, A. G.; Caron, E. (2008). Integrin-dependent phagocytosis – spreading from microadhesion to new concepts. Jour Cell Scien. 121: 1773-1783.
36. El-Benna, J., Dang, P. M., Gougerot-Pocidalo, M. A., Marie, J. C., and BrautBoucher, F. (2009). p47phox, the phagocyte NADPH oxidase/NOX2 organizer: structure, phosphorylation and implication in diseases. *Exp. Mol. Med*. 41: 217–225
37. El-Benna, J., Hurtado-Nedelec, M., Marzaioli, V., Marie, J. C., Gougerot-Pocidalo, M. A., and Dang, P. M. (2016). Priming of the neutrophil respiratory burst: role in host defense and inflammation. *Immunol. Rev*. 273:180–193.
38. Ethuin, F. et al. (2004). Human neutrophils produce interferon γ upon stimulation by interleukin-12. Lab. Invest. 84: 1363–1371.
39. Falahzadeh, K, Banaei-Esfahani, A, Shahhoseini, M. (2015). The Potential Roles of Actin in The Nucleus. Cell J. 17(1): 7-14.
40. Fan Z., Ley, K. (2015). Leukocyte arrest: Biomechanics and molecular mechanisms of β2 integrin activation. *Biorheology*. 52: 353–377.
41. Fang, F. C. (2004). Antimicrobial reactive oxygen and nitrogen species: concepts and controversies. Nature Reviews Microb. 2(10): 820–832.
42. Farrugia, M., Baron, B. (2016). The role of TNF-α in rheumatoid arthritis: a focus on regulatory T cells. J Clin Transl Res. 2(3): 84–90.
43. Faurschou M, Sorensen OE, Johnsen AH, Askaa J, Borregaard N. (2002). Defensin-rich granules of human neutrophils: characterization of secretory properties. Biochim Biophys Acta. 1591: 29–35).
44. Feeser, E.A.; Ignacio, C.M.G.; Krendel, M.; Ostap, E.M. (2010). Myo1e binds anionic phospholipids with high affinity. Biochemistry, 49: 9353–9360.

45. Felix L.C., Almas S., Lacy P. (2018). Regulatory Mechanisms in Neutrophil Degranulation. In: Riccardi C., Levi-Schaffer F., Tiligada E. (eds) Immunopharmacology and Inflammation. Springer, Cham.
46. Feng, D., Nagy, J. A., Pyne, K., Dvorak, H. F. and Dvorak, A. M. (1998). Neutrophils emigrate from venules by a transendothelial cell pathway in response to FMLP. J. Exp. Med. 187: 903-915.
47. Foth, B.J.; Goedecke, M.C.; Soldati, D. (2006) New insights into myosin evolution and classification. Proc. Natl. Acad. Sci. 103:3681–3686
48. Freeman, S.A.; Grinstein, S. (2014). Phagocytosis: Receptors, signal integration, and the cytoskeleton. Immunol. Rev. 262:193–215.
49. Fuchs T a, Abed U, Goosmann C, Hurwitz R, Schulze I, Wahn V, et al. (2007). Novel cell death program leads to neutrophil extracellular traps. Cell.176(2):231–41.
50. Fumagalli, L., Campa, C. C., Germena, G., Lowell, C. A., Hirsch, E., and Berton, G. (2013). Class I phosphoinositide-3-kinases and SRC kinases play a nonredundant role in regulation of adhesion-independent and -dependent neutrophil reactive oxygen species generation. J. Immunol. 190:3648–3660.
51. Fusté, Berta; Mazzara, Roberto; Escolar, Ginés; Merino, Anna; Ordinas, Antonio; Díaz-Ricart, Maribel (2004). Granulocyte colony-stimulating factor increases expression of adhesion receptors on endothelial cells through activation of p38 MAPK. Haematologica. 89:578-585.
52. Futosi, K., Fodor, S., Mócsai, A. (2013). Neutrophil cell surface receptors and their intracellular signal transduction pathways. *International Immunopharmacology*. 17:638–650.
53. Gambardella L, Anderson KE, Jakus Z, Kovács M, Voigt S, Hawkins PT, Stephens L, Mócsai A, Vermeren S. (2013). Phosphoinositide 3-OH kinase regulates integrin-dependent processes in neutrophils by signaling through its effector ARAP3. J Immunol. 190(1):381-91.
54. Giagulli, C., Ottoboni, L., Caveggion, E., Rossi, B., Lowell, C., Constantin, G., et al. (2006). The Src family kinases Hck and Fgr are dispensable for inside-out chemoattractant-induced signaling regulating β2 integrin affinity and valency in neutrophils but are required for β2 integrin-mediated outside-in signaling involved in sustained adhesion. *J. Immunol.* 177: 604–611.
55. Girón-Pérez, D. A., Vadillo, E., Schnoor, M., Santos-Argumedo, L. (2020). Myo1e modulates the recruitment of activated B cells to inguinal lymph nodes. Journal of Cell Science. 133: 1-12.
56. Golightly, C., McHenry, M., Racanelli, P., Golightly, M. (2015). Neutrophil Oxidative Burst Assay: A Dihydrorhodamine (DHR) based testing of Chronic Granulomatous Disease (CGD) with CytoFlex Flow Cytometer. *Beckman Coulter, Life Sci*.

57. Goley, E.D., Welch, M.D. (2006). The ARP2/3 complex: an actin nucleator comes of age. Nature Reviews. 7:713-726
58. Greenlee-Wacker MC. (2016). Clearance of apoptotic neutrophils and resolution of inflammation. Immunol Rev. 273(1):357-70.
59. Gu, H., Botelho, RJ., Yu, M., Grinstein, S., Neel, BG. (2003). Critical role for scaffolding adapter Gab2 in Fc gamma R-mediated phagocytosis. *J Cell Biol*. 161:1151–1161
60. Guerrero Fonseca, Idaira M. (2018). The role of the actin-binding protein HS1 in effector functions of neutrophils. CINVESTAV. Mexico City. 1-60.
61. Haas A. (2007). The phagosome: Compartment with a license to kill. Vol. 8, Traffic. p. 311–30.
62. Häger M; Cowland JB; Borregaard N. (2010). Neutrophil granules in health and disease. J Intern Med. 268: 25–34.
63. Hall AB, et al. (2006). Requirements for Vav guanine nucleotide exchange factors and Rho GTPases in FcgammaR- and complement-mediated phagocytosis. *Immunity.* 24:305–316.
64. Hartman, M. A., Finan, D., Sivaramakrishnan, S., & Spudich, J. A. (2011). Principles of Unconventional Myosin Function and Targeting. *Annual Review of Cell and Developmental Biology*. 27(1):133–155.
65. Hawkins, P. T., Stephens, L. R., Suire, S., and Wilson, M. (2010). PI3K signaling in neutrophils. *Curr. Top. Microbiol. Immunol.* 346:183–202.
66. Herant M. (2006). Mechanics of neutrophil phagocytosis: experiments and quantitative models. J Cell Sci. 119(9):1903–13.
67. Heissler, S. M., & Sellers, J. R. (2016). *Myosins. Encyclopedia of Cell Biology, 597–607.*
68. Hodge, R. G., and Ridley, A. J. (2016). Regulating Rho GTPases and their regulators. *Nat. Rev. Mol. Cell Biol*. 17:496–510.
69. Hood, J., Cheresh, D. (2002). Role of integrins in cell invasion and migration. *Nat Rev Cancer* 2:91–100.
70. Hurst, James K. (2012). What really happens in the neutrophil phagosome? Free Radic Biol Med. 53(3): 508-520.
71. Hyun, Y.M., Sumagin, R., Sarangi, P.P., Lomakina, E., Overstreet, M.G., Baker, C.M., Fowell, D.J., Waugh, R.E., Sarelius, I.H., and Kim, M. (2012). Uropod elongation is a common final step in leukocyte extravasation through inflamed vessels. J. Exp. Med. 209: 1349–1362.
72. Johnson-Leger C, Aurrand-Lions M, and Imhof BA. (2000) The parting of the endothelium: miracle, or simply a junctional affair? J Cell Sci 113: 921–933).
73. Kalhammer G. & Bähler M (2000). Unconventional myosins. Essays Biochem. 35:33-42.

74. Kamioka Y, Fukuhara S, Sawa H, Nagashima K, Masuda M, Matsuda M, Mochizuki N. (2004.) A novel dynamin-associating molecule, formin-binding protein 17, induces tubular membrane invaginations and participates in endocytosis. J Biol Chem. 279(38):40091-9.
75. Kaplan MJ, Radic M. (2012). Neutrophil Extracellular Traps: Double-Edged Swords of Innate Immunity. J Immunol. 189(6):2689–95.
76. Kim, S. V., Flavell, R. A. (2008). Myosin I: from yeast to human. *Cell. Mol. Life Sci*. 65:2128–2137.
77. Klaas, M.; Crocker, P. R. (2012). Sialoadhesin in recognition of self and non-self. Semin. Immunopathol. 34: 353-364.
78. Kobayashi SD, et. al. (2010). Rapid neutrophil destruction following phagocytosis of Staphylococcus aureus. J Innate Immun. 2(6):560-575.
79. Kolaczkowska E, Kubes P. (2013). Neutrophil recruitment and function in health and inflammation. Nat Rev Immunol.13(3):159–75.
80. Kolárová H., B. Ambruzova, L. Svihalkova Sindlerova, A. Klinke, and L. Kubala, "Modulation of endothelial glycocalyx structure under inflammatory conditions". Mediators of Inflammation. 1-17.
81. Koukouritaki, S. B., E. A. Vardaki, E. A. Papakonstanti, E. Lianos, C. Stournaras, and D. S. Emmanouel. (1999). TNF-a Induces Actin Cytoskeleton Reorganization in Glomerular Epithelial Cells Involving Tyrosine Phosphorylation of Paxillin and Focal Adhesion Kinase. Molecular Medicine. 5: 382-392.
82. Krendel M., et. al. (2009). Disruption of Myosin 1e promotes podocyte injury. *J. Am. Soc. Nephrol.* 20:86-94.
83. Kurochkina, N.; Guha, U. (2013). SH3 domains: Modules of protein–protein interactions. Biophys. Rev., 5: 29–39.
84. Kuwano Y, Spelten O, Zhang H, Ley K, Zarbock A. (2010). Rolling on E- or Pselectin induces the extended but not high affinity conformation ofLFA-1 in neutrophils. Blood.116(4):617–24.
85. Laakso, J. M., et al. (2010). Control of myosin-I force sensing by alternative splicing. PNAS. 107(2):698-702.
86. Lacy, Paige. (2006). Mechanisms of Degranulation in Neutrophils. Allergy, Asthma, and Clinical Immunology. 2(3): 98-108.
87. Lambeth JD. (2004). NOX enzymes and the biology of reactive oxygen. Nat. Rev. Immunol. 4:181–89.
88. Latasiewicz, J. et al. (2017). HS1 deficiency impairs neutrophil recruitment in vivo and activation of the small GTPases Rac1 and Rap1. J. Leukoc. Biol. 101:1133–1142.
89. Ley K, Laudanna C, Cybulsky MI, Nourshargh S. Getting to the site of inflammation: the leukocyte adhesion cascade updated. Nat. Rev. Immunol. 2007; 7:678–89.

90. Lu Q, Li J, Ye F, Zhang M. (2015). Structure of myosin-1c tail bound to calmodulin provides insights into calcium-mediated conformational coupling. Nat Struct Mol Biol. Jan. 22(1):81-8.
91. Mantovani, A.; Cassatella, M. A.; Costantini, C. et. al. (2011). Neutrophils in the activation and regulation of innate and adaptive immunity. Nature Reviews Immunolgy. 11(8): 519–531.
92. Maravillas-Montero, José and Santos-Argumedo, Leopoldo. (2012). The myosin family: unconventional roles of actin-dependent molecular motors in immune cells. J Leu Biol. 91: 35-46.
93. Massena, S.; Christoffersson, G; Hjertström, E.; et al. (2010). A chemotactic gradient sequestered on endothelial heparan sulfate induces directional intraluminal crawling of neutrophils. Blood. 116(11):1924–1931.
94. Mayadas, T. N. (2014). The Multifaceted Functions of Neutrophils. *Annu Rev Pathol, 9*, 181–218.
95. Medicus RG, Melamed J, Arnaout MA. (1983). Role of human factor I and C3b receptor in the cleavage of surface bound C3bi molecules. Eur J Immunol. 13(6):465-70.
96. Meijles, D. N., Fan, L. M., Howlin, B. J., and Li, J. M. (2014). Molecular insights of p47phox phosphorylation dynamics in the regulation of NADPH oxidase activation and superoxide production. *J. Biol. Chem*. 289: 22759–22770
97. Minozzo F., Rassier D.E. (2013). Myosin Family Classification. In: Roberts G.C.K. (eds) Encyclopedia of Biophysics. Springer, Berlin, Heidelberg.
98. Mitchell, T.; Lo, A.; Logan, M.; Lacy, P. (2008). Primary granule exocytosis in human neutrophils is regulated by Rac-dependent actin remodeling. Am J Physiol Cell Physiol. 295(5):C1354-C1365.
99. Mitroulis I, Kambas K, Chrysanthopoulou A, Skendros P, (2011). Neutrophil extracellular trap formation is associated with IL-1beta and autophagy-related signaling in gout. PLoS One. 6(12):e29318.
100. Moore KL, Patel KD, Brehl RE, Johnson DA, Lichenstein HS, Cummings RD, et al. (1995). P-selectin glycoprotein ligand mediates rolling of human neutrophils on Pselectin. J Cell Biol. 128:661-71.
101. Mocsai, A., Zhou, M. J., Meng, F. Y., Tybulewicz, V. L., and Lowell, C. A. (2002). Syk is required for integrin signaling in neutrophils. *Immunity* 16: 547–558.
102. Mueller H; Stadtmann A ;Van Aken H; Hirsch E; Wang D; Ley K, et al. (2010).Tyrosine kinase Btk regulates E-selectin-mediated integrin activation and neutrophil recruitment by controlling phospholipase C (PLC) γ2 and PI3Kγ pathways. Blood. 115(15): 3118–3127.
103. Muller, William A. (2011). Mechanisms of Leukocyte Transendothelial Migration. Annu Rev Payhol. 6: 323-344.

104. Murphy, K., Travers, P., & Walport, M. (2008). Janeway's Immunobiology. 7th ed. McGraw Hill.
105. Nakamura, S., et. al. (2020). SH3P2 suppresses octeoclast differentiation through restricting membrane localization of myosin 1E. Genes to cells. 25(11):707-717.
106. Navinés-Ferrer, A.; Martín, M. (2020). Long-Tailed Unconventional Class I Myosins in Health and Disease. Int. J. Mol. Sci. 21(2555): 1-13.
107. Nguyen, G. T.; Green, E. R.; Mecsas, J. (2017). Neutrophils to the ROScue: Mechanisms of NADPH Oxidase Activation and Bacterial Resistance. Front. Cell. Infect. Microbiol. 373(7): 1-24.
108. Nourshargh, Sussan; Alon, Ronen. (2014). Leukocyte Migration into Inflamed Tissues. Nature Immunity. 41: 694-707.
109. Nourshargh, S., Hordijk, P.L., and Sixt, M. (2010). Breaching multiple barriers: leukocyte motility through venular walls and the interstitium. Nat. Rev. Mol. Cell Biol. 11, 366–378.
110. Papayannopoulos V, Metzler KD, Hakkim A, Zychlinsky A. (2010). Neutrophil elastase and myeloperoxidase regulate the formation of neutrophil extracellular traps. J Cell Biol. 191(3):677–91.Park, H., et al. Tyrosine phosphorylation of Wiskott-Aldrich syndrome protein (WASP) by Hck regulates macrophage function. (2014). *J Biol Chem*. 289:7897–790.
111. Patino-Lopez, G.; Aravind, L.; Dong, X.; Kruhlak, M.J.; Ostap, E.M.; Shaw, S. (2010). Myosin 1G Is an Abundant Class I Myosin in Lymphocytes Whose Localization at the Plasma Membrane Depends on Its Ancient Divergent Pleckstrin Homology (PH) Domain (Myo1PH). J. Biol. Chem. 285: 8675–8686.
112. Patten, D. A., & Shetty, S. (2018). More Than Just a Removal Service: Scavenger Receptors in Leukocyte Trafficking. *Frontiers in immunology*, *9*, 2904.
113. Paul, P.; van den Hoorn, T.; Jongsma, M.L.M.; Bakker, M.J.; Hengeveld, R.; Janssen, L.; Cresswell, P.; Egan, D.A.; van Ham, M.; ten Brinke, A.; et al. (2011). A Genome-wide Multidimensional RNAi Screen Reveals Pathways Controlling MHC Class II Antigen Presentation. Cell. 145:268–283.
114. Perretti, M. & Dalli, J. (2009). Exploiting the Annexin A1 pathway for the development of novel antiinflammatory therapeutics. Br. J. Pharmacol. 158:936–946.
115. Pestic-Dragovich, L. (2000). A Myosin I Isoform in the Nucleus. Science. 290(5490): 337–341.
116. Petrache, I., Birukova, A., Ramierz, S. I., Garcia, J. G. N. & Verin, A. D. (2002). The role of microtubules in tumor necrosis factor-α-induced endothelial cell permeability. Am J. Respir. Cell Mol. Biol. 28:574–581.
117. Philimonenko, V.V. et al. (2004). Nuclear actin and myosin I are required for RNA polymerase I transcription. Nat. Cell Biol. 6:1165–1172.

118. Phillipson M, Heit B, Colarusso P, Liu L, Ballantyne CM, Kubes P (2006). Intraluminal crawling of neutrophils to emigration sites: a molecularly distinct process from adhesion in the recruitment cascade. J Exp Med. 203: 2569-2575).
119. Pillay, J. et al. (2010). In vivo labeling with $^{2}H_{2}O$ reveals a human neutrophil lifespan of 5.4 days. Blood 116:625–627.
120. Pober JS, Gimbrone MA, Lapierre LA, et.al. (1986). Overlapping patterns of of activation of human endothelial cells by interleukin 1, tumor necrosis factor and immune interferon. J Immunol. 1337: 1893.
121. Pranchevicius, M.C. et al. (2008). Myosin Va phosphorylated on Ser1650 is found in nuclear speckles and redistributes to nucleoli upon inhibition of transcription. Cell Motil. Cytoskeleton 65:441–456
122. Prehoda, KE., Scott, JA., Mullins, RD., Lim, WA. (2000). Integration of multiple signals through cooperative regulation of the N-WASP-Arp2/3 complex. *Science*.290:801–806.
123. Rabinovitch M. (1995). Professional and non-professional phagocytes: an introduction. Trends Cell Biol. 5(3):85–7.
124. Rodak, B.; Fritstma, G. A. ; Keohane, E. M. (2014). Hematología: fundamentos y aplicaciones. 4th ed. Mexico: Médica Panamericana.
125. Rosales, C. (2020). Neutrophils at the crossroads of innate and adaptive immunity. JLB. 1-20.
126. Rosetti F, Mayadas TN. (2016). The many faces of Mac-1 in autoimmune disease. Immunol Rev. 269:175–93.
127. Salvermoser, M.; Pick, R.; Weckbach, L.T.; Zehrer, A. et. al. (2018). Myosin 1f is specifically required for neutrophil migration in 3D environments during acute inflammation. Blood. 131:1887–1898.
128. Sangwon. V. K. et al. (2006). Modulation of cell adhesion and motility in the immune system by Myo1f. Science 314:136–139.
129. Schnoor M., et al. (2011). Cortactin deficiency is associated with reduced neutrophil recruitment but increased vascular permeability in vivo. J. Exp. Med. 208:1721–1735.
130. Schnoor, M. A.-B. (2015). Crossing the Vascular Wall: Common and Unique Mechanisms Exploited by Different Leukocyte Subsets during Extravasation. *Mediators of Inflammation*, 1-23.
131. Scott MG, Davidson DJ, Gold MR, Bowdish D, Hancock R. (2002). The human antimicrobial peptide LL-37 is a multifunctional modulator of innate immune responses. J Immunol.169:3883–3891.
132. Sengelov H, Kjeldsen L, Borregaard N. (1993). Control of exocytosis in early neutrophil activation. J Immunol. 150: 1535–1543.
133. Serhan, C. N. (2010). Novel lipid mediators and resolution mechanisms in acute inflammation: to resolve or not?. Am. J. Pathol. 17:1576–1591.

134. Soehnlein, O. & Lindbom, L. (2009). Neutrophil-derived azurocidin alarms the immune system. J. Leukoc. Biol. 85:344–351.
135. Soehnlein, O. et al. (2008). Neutrophil secretion products pave the way for inflammatory monocytes. Blood 112, 1461–1471
136. Sørensen OE, Borregaard N. (2016). Neutrophil extracellular traps - The dark side of neutrophils. Vol. 126, Journal of Clinical Investigation. 1612–1620.
137. Spiering D, Hodgson L. (2011). Dynamics of the Rho-family small GTPases in actin regulation and motility. Cell Adh Migr. 5(2):170-80.
138. Subrahmanyam YV, Newburger PE, Weissman SM. (2001). RNA expression patterns change dramatically in human neutrophils exposed to bacteria. Blood. 97: 2457–2468.
139. Sumagin R, Prizant H, Lomakina E, Waugh RE, Sarelius IH. (2010). LFA-1 and Mac-1 define characteristically different intralumenal crawling and emigration patterns for monocytes and neutrophils in situ. Journal of Immunology. 185(11): 7057–7066.
140. Sundd P, Gutierrez E, Koltsova EK, Kuwano Y, Fukuda S, Pospieszalska MK, et al. (2012). 'Slings' enable neutrophil rolling at high shear. Nature. 488(7411): 399–403.
141. Swanson, J.A., Johnson, M.T., Beningo, K., et. al. (1999). A contractile activity that closes phagosomes in macrophages. J Cell Sci. 112(3): 307-316.
142. Tak, Tamar; Tesselaar, Kiki; Pillay, Janesh; et. al. (2013). What's your age again? Determination of human neutrophil half-lives revisited. JLB. 94: 595- 601.
143. Thiam, H. R. et al. (2020). NETosis proceeds by cytoskeleton and endomembrane disassembly and PAD4-mediated chromatin decondensation and nuclear envelope ruptura. PNAS. 117(13): 7326-7337.
144. Thompson, R.F.; Langford, G.M. (2002). Myosin superfamily evolutionary history. *Anat. Rec*. 268: 276–289.
145. Truebestein L, Leonard TA. (2016). Coiled-coils: The long and short of it. Bioessays.. 38(9):903-16.
146. Uribe-Querol, E.; Rosales, C. (2020). Phagocytosis: Our Current Understanding of a Universal Biological Process. Front. Immunol. 11:1066.
147. Vadillo, E. et. al. (2019). Intermittent rolling is a defect of the extravasation cascade caused by Myosin1e-deficiency in neutrophils. Proc. Natl. Acad. Sci., 116, 26752–26758.
148. van Golen, R. F., van Gulik, T. M., and M. Heger, "Mechanistic overview of reactive species-induced degradation of the endothelial glycocalyx during hepatic ischemia/reperfusion injury," Free Radical Biology and Medicine. 52(8):1382–1402.
149. van Kessel, KPM., Bestebroer J., van Strijp, JAG. (2014). Neutrophil-mediated phagocytosis of *Staphylococcus aureus*. *Front. Immunol.* 5:467.

150. Vale, R. D. (2003). The molecular motor toolbox for intracellular transport. *Cell.* 112:467–480.
151. Vestweber, D. (2012). Relevance of endothelial junctions in leukocyte extravasation and vascular permeability. Annals of the New York Academy of Sciences, 1257(1): 184–192.
152. Vestweber D. (2015). How leukocytes cross the vascular endothelium. Nat Rev Immunol. 15(11):692–704.
153. Vockel, M., and Vestweber, D. (2013). How T cells trigger the dissociation of the endothelial receptor phosphatase VE-PTP from VE-cadherin. Blood 122: 2512–2522.
154. Voisin, M. B., Woodfin, A. & Nourshargh, S. (2009). Monocytes and neutrophils exhibit both distinct and common mechanisms in penetrating the vascular basement membrane in vivo. Arterioscler. Thromb. Vasc. Biol. 29:1193–1199.
155. Volmering, S., Block, H., Boras, M., Lowell, C. A., and Zarbock, A. (2016). The Neutrophil Btk signalosome regulates integrin activation during sterile inflammation. Immunity 44:73–87.
156. Vreugde, S. et al. (2006). Nuclear myosin VI enhances RNA polymerase II-dependent transcription. Mol. Cell. 23:749–755.
157. Wachsstock DH, Schwarz WH, Pollard TD. (1994). Cross-linker dynamics determine the mechanical properties of actin gels. *Biophys J*. 66:801–809.
158. Wang, J. (2018). Neutrophils in tissue injury and repair. *Cell and Tissue Research, 371*, 531-539.
159. Wang, S. et al. (2006). Venular basement membranes contain specific matrix protein low expression regions that act as exit points for emigrating PMN. J. Exp. Med. 203:1519–1532.
160. Wenzel J, Ouderkirk JL, Krendel M, Lang R. (2015). Class I myosin Myo1e regulates TLR4-triggered macrophage spreading, chemokine release, and antigen presentation via MHC class II. Eur J Immunol. Jan;45(1):225-37
161. Wiedemann, A., Patel, J. C., Lim, J., Tsun, A., van Kooyk, Y. and Caron, E. (2006). Two distinct cytoplasmic regions of the beta2 integrin chain regulate RhoA function during phagocytosis. J. Cell Biol. 172:1069-1079.
162. Williams R. (2006). Killing controversy J. Exp. Med. 203:2404.
163. Winterbourn CC, Kettle AJ, Hampton MB. (2016). Reactive oxygen species and neutrophil function. *Annu Rev Biochem*. 85:765-792.
164. Wojciak-Stothard, B., A. Entwistle, R. Garg, and A. J. Ridley. (1998). Regulation of TNF-alpha-induced reorganization of the actin cytoskeleton and cell-cell junctions by Rho, Rac, and Cdc42 in human endothelial cells. J. Cell. Physiol. 176:150–165.
165. Wolenski, J. S. (1995). Regulation of calmodulin-binding myosins. Trends in Cell Biology, 5(8), 310–316.

166. Woodfin, A.; M.-B. Voisin, M. Beyrau et al. (2011). The junctional adhesion molecule JAM-C regulates polarized transendothelial migration of neutrophils in vivo. Nature Immunology. 12(8):761–769.
167. Woolner, S.; Bement, W.M. (2009). Unconventional myosins acting unconventionally. Trends Cell Biol. 19:245–252.
168. Yamamoto, E.; Kalli, A.C.; Yasuoka, K.; Sansom, M.S.P. (2016). Interactions of Pleckstrin Homology Domains with Membranes: Adding Back the Bilayer via HighThroughput Molecular Dynamics. Structure. 24:1421–1431.
169. Ye, J. et al. (2008). Nuclear myosin I acts in concert with polymeric actin to drive RNA polymerase I transcription. Genes Dev. 22, 322– 330.
170. Yipp, B. G. & Kubes, P. (2013). Antibodies against neutrophil LY6G do not inhibit leukocyte recruitment in mice in vivo. Blood 121:241–242.
171. Yoshimura M, Homma K, Saito J, Inoue A, Ikebe R, Ikebe M. (2001). Dual regulation of mammalian myosin VI motor function. J Biol Chem. 276:39600–39607.
172. Yumura, S., Uyeda, T. Q. (2003). Myosins and cell dynamics in cellular slime molds. *Int. Rev. Cytol*. 224:173–225.
173. Zhang, Q. et al. (2010). Circulating mitochondrial DAMPs cause inflammatory responses to injury. Nature. 464:104–107.
174. Zhang X, Ding L, and Sandford A.J. (2004). Gene expression in mature neutrophils: early responses to inflammatory stimuli. Jo Leuk Biol. 75: 358–372.
175. Zhang, Y., et. al. (2019). Tail domains of myosin-1e regulate phosphatidylinositol signaling and F-actin polymerization at the ventral layer of podosomes. Mol Bio Cell. 30(5): 622-635.

10. SUPPLEMENTARY INFORMATION

```
MGSKGVYQYH WQSHNVKHSG VDDMVLLSKI TENSIVENLK KRYMDDYIFT YIGSVLISVN   60
PFKQMPYFGE KEIEMYQGAA QYENPPHIYA LADNMYRNMI IDRENQCVII SGESGAGKTV  120
AAKYIMSYIS RVSGGGTKVQ HVKDIILQSN PLLEAFGNAK TVRNNNSSRF GKYFEIQFSP  180
GGEPDGGKIS NFLLEKSRVV MRNPGERSFH IFYQLIEGAS AEQKHSLGIT SMDYYYYLSL  240
SGSYKVDDID DRREFQETLH AMNVIGIFAE EQTLVLQIVA GILHLGNISF KEVGNYAAVE  300
SEEFLAFPAY LLGINQDRLK EKLTSRQMDS KWGGKSESIH VTLNVEQACY TRDALAKALH  360
ARVFDFLVDS INKAMEKDHE EYNIGVLDIY GFEIFQKNGF EQFCINFVNE KLQQIFIELT  420
LKAEQEEYVQ EGIRWTPIEY FNNKIVCDLI ENKVNPPGIM SILDDVCATM HAVGEGADQT  480
LLQKLQMQIG SHEHFNSWNQ GFIIHHYAGK VSYDMDGFCE RNRDVLFMDL IELMQSSELP  540
FIKSLFPENL QADKKGRPTT AGSKIKKQAN DLVSTLMKCT PHYIRCIKPN ETKKPRDWEE  600
SRVKHQVEYL GLKENIRVRR AGYAYRRIFQ KFLQRYAILT KATWPSWQGE EKQGVLHLLQ  660
SVNMDSDQFQ LGRSKVFIKA PESLFLLEEM RERKYDGYAR VIQKSWRKFV ARKKYVQMRE  720
EASDLLLNKK ERRRNSINRN FIGDYIGMEE HPELQQFVGK REKIDFADTV TKYDRRFKGV  780
KRDLLLTPKC LYLIGREKVK QGPDKGLVKE VLKRKIEIER ILSVSLSTMQ DDIFILHEQE  840
YDSLLESVFK TEFLSLLAKR YEEKTQKQLP LKFSNTLELK LKKENWGPWS AGGSRQVQFH  900
QGFGDLAVLK PSNKVLQVSI GPGLPKNSRP TRRNTTQNTG YSSGTQNANY PVRAAPPPPG  960
YHQNGVIRNQ YVPYPHAPGS QRSNQKSLYT SMARPPLPRQ QSTSSDRVSQ TPESLDFLKV 1020
PDQGAAGVRR QTTSRPPPAG GRPKPQPKPK PQVPQCKALY AYDAQDTDEL SFNANDIIDI 1080
IKEDPSGWWT GRLRGKQGLF PNNYVTKI                                    1108
```

Supplementary Figure 1. Myosin 1e primary structure. Sequence was obtained in a FASTA format from the Uniprot data base, with the accession number Q12965. Highlighted in yellow is the DALAK sequence and in blue the TEDS site. https://www.uniprot.org/uniprot/Q12965.fasta.

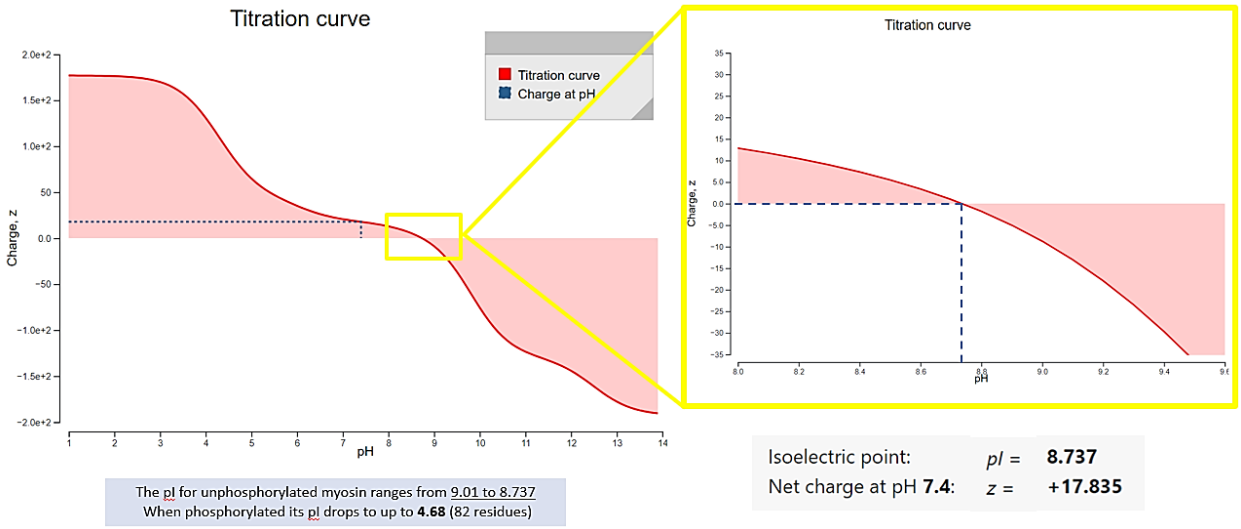

Supplementary Figure 2. Theoretical titration curve of the isoelectric point of Myo1e*. The graph shows the myosin 1e pH charge of 0. The yellow box highlights the pI area of myosin 1e. The pI ranges from 9.01 to 8.737 (according to the database).* https://www.protpi.ch/Calculator/ProteinTool/#Results.

Supplementary Table 1. *Amino acid composition of myosin 1e*.

Amino acid		Percentage (%)	Amino acid		Percentage (%)
Ala (A)	56	5.1	Lys (K)	88	7.9
Arg (R)	63	5.7	Met (M)	26	2.3
Asn (N)	56	5.1	Phe (F)	49	4.4
Asp (D)	54	4.9	Pro (P)	53	4.8
Cys (C)	10	0.9	Ser (S)	76	6.9
Gln (Q)	68	6.1	Thr (T)	42	3.8
Glu (E)	78	7.0	Trp (W)	12	1.1
Gly (G)	75	6.8	Tyr (Y)	50	4.5
His (H)	25	2.3	Val (V)	64	5.8
Ile (I)	71	6.4	Lys (K)	88	7.9
Leu (L)	92	8.3			

Red boxes represent acidic amino acids. Blue boxes represent basic amino acids.
https://web.expasy.org/cgi-bin/protparam/protparam1?Q12965@1-1108@.

Bioinformatic tools

ProtParam Tool

ProtParam Tool is a software that allows the user to compute various physical and chemical parameters for a given protein sequence. The computed parameters include the molecular weight, theoretical pI (isoelectric point), amino acid composition, atomic composition, extinction coefficient, estimated half-life, instability index, aliphatic index and grand average of hydropathicity (GRAVY).

- **Note 1: Extinction coefficient.** It is estimated from the amino acid composition of the protein. The software uses the equation:

  E(Prot) = Numb(Tyr) × Ext(Tyr) + Numb(Trp) × Ext(Trp) + Numb(Cystine) × Ext(Cystine)

  The absorbance (optical density) can be calculated using the following formula:

  Absorb(Prot) = E(Prot)/Molecular_weight

  The conditions at which these equations are valid are: pH 6.5, 6.0 M guanidium hydrochloride, 0.02 M phosphate buffer.

- **Note 2: Protein pI.** It is calculated using pK values of amino acids, which were defined by examining polypeptide migration between pH 4.5 and 7.3 in an immobilized pH gradient gel environment with 9.2 M and 9.8 M urea at 15°C or 25°C.
- **Note 3: In vivo half-life**. The half-life is a prediction of the time it takes for half of the amount of protein in a cell to disappear after its synthesis in the cell. The prediction is given for three organisms (human, yeast, and E. coli), but it is possible to extrapolate the result to similar organisms. ProtParam estimates the half-life by looking at the N-terminal amino acid of the sequence under investigation.
- **Note 4: Instability Index.** The instability index provides an estimate of the stability of a protein in a test tube. It is predicted based on a statistical analysis of 12 unstable and 32 stable proteins that revealed that there are certain dipeptides, the occurrence of which is significantly different in the unstable proteins compared with those in the stable ones. A weight value of instability was assigned to each of the 400 different dipeptides (DIWV). Using these weight values, it is possible to compute an instability index (II), which is defined as:

  $$II = \frac{10}{L} \times \sum_{i=1}^{i=L-1} DIWV(x[i]x[i+1])$$

  A protein whose instability index is smaller than 40 is predicted as stable; a value above 40 predicts that the protein may be unstable.

- **Note 5: Grand Average of Hydropathy.** The grand average of hydropathy (GRAVY) value for a peptide or protein is calculated as the sum of hydropathy

values of all the amino acids, divided by the number of residues in the sequence. Negative values indicate hydrophilicity and positive values hydrophobicity.

ProtScale Tool

ProtScale allows computation and representation (in the form of a 2-D plot) of the profile produced by any amino acid scale on a selected protein. The most frequently used scales are hydrophobicity scales, most of which were derived from experimental studies on partitioning of peptides in apolar and polar solvents, with the goal of predicting membrane-spanning segments that are highly hydrophobic, and secondary structure conformational parameter scales. In addition, many other scales exist, based on different chemical and physical properties of the amino acids.

ProtScale can be used with 50 predefined scales entered from the literature. The scale values for the 20 amino acids, as well as a literature reference, are provided on ExPASy for each of these scales. To generate data for a plot, the protein sequence is scanned with a sliding window of a given size. At each position, the mean scale value of the amino acids within the window is calculated, and that value is plotted for the midpoint of the window.

- **Note 6: Window Size in the Kyte-Doolittle scale.** The window size is the length of the interval to use for the profile computation, i.e., the number of amino acids examined at a time to determine a point of hydrophobic character. When computing the score for a given residue i, the amino acids in an interval of the chosen length, centered around residue i, are considered. In other words, for a window size n, the i–(n-1)/2 neighboring residues on each side of residue i, is used to compute the score for residue i. The score for residue i is the sum of the scale values for these amino acids, optionally weighted according to their position in the window. A window was chosen according to the expected size of the structural motif under investigation: A window size of 5 to 7 is appropriate for finding hydrophilic regions that are likely to be exposed on the surface and may potentially be antigenic. Window sizes of 19 or 21 will make hydrophobic, membrane-spanning domains stand out rather clearly (typically >1.6 on the Kyte-Doolittle scale).

PhosphoSitePlus database

PhosphoSitePlus (PSP) database is an open, dynamic, continuously curated, and highly interactive systems biology resource for studying experimentally observed post-translational modifications in the regulation of biological processes. PhosphoSite® includes coverage of commonly studied PTMs including phosphorylation, acetylation, methylation, ubiquitination, and O-glycosylation.

- **Note 7: Post-translational modification data source.** This database integrates both low- and high-throughput (LTP and HTP) data sources into a single reliable and comprehensive resource. Nearly 10,000 journal articles, including both LTP and HTP reports, have been manually curated. The three journals most represented in PSP are the Journal of Biological Chemistry, Molecular and Cellular Biology, and Oncogene. HTP sites, discovered using mass spectrometry (MS2), are not only derived from published literature but also from previously unpublished data.

PhosphoMotif Finder

PhosphoMotif Finder contains known kinase/phosphatase substrates as well as binding motifs that are curated from the published literature. It reports the presence of any literature-derived motif in the query sequence.